On the biological behavior of barrier membranes: implications for Guided Bone Regeneration

Clinical and experimental studies

Alberto Turri

Department of Biomaterials
Institute of Clinical Sciences
Sahlgrenska Academy, University of Gothenburg

UNIVERSITY OF GOTHENBURG

Gothenburg 2022

Cover illustration: Schematic drawing illustrating a dual texture e-PTFE membrane isolating a bone defect from the overlying soft tissue compartment

On the biological behavior of barrier membranes: implications for Guided Bone Regeneration. Clinical and experimental studies

alberto.turri@gu.se

ISBN 978-91-8009-596-9 (PRINT)
ISBN 978-91-8009-597-6 (PDF)

Printed in Borås, Sweden 2022
Printed by Stema Specialtryck AB

To my family,

with endless love and gratitude

On the biological behavior of barrier membranes: implications for Guided Bone Regeneration

Clinical and experimental studies

Alberto Turri

Department of Biomaterials, Institute of Clinical Sciences
Sahlgrenska Academy, University of Gothenburg
Gothenburg, Sweden

ABSTRACT

There is a continuous development of bone augmentation solutions to meet the rising demand for effective dental implant rehabilitations. One of the most used techniques is Guided Bone Regeneration (GBR). Although successful in the clinic, there is still scarce knowledge of the biological mechanisms behind bone regeneration, which therefore, turns out to be the appropriate aim of this project. The clinical **Study** I was a retrospective investigation on the long-term outcome of single implant treatment in the anterior maxilla, in conjunction with or immediately after Guided Bone Regeneration (GBR). The study on 74 included patients indicated the presence of factors negatively influencing marginal bone level, such as small defects, simultaneous GBR-implant placement, short healing time and onset of early and late complications. In **Studies II and IV**, resorbable and nonresorbable barrier membranes with different topographical features, were used to protect bone defects created in the rat femur and were compared with untreated sham defects. After different time points, samples were collected and processed for qPCR, histology, histomorphometry, electron microscopy, Western blot, and immunohistochemistry. In both studies, the protective role of the membranes as "physical barriers" was confirmed by the absence of soft tissue ingrowth inside the defects. Additionally, the membranes held an active role in wound healing dynamics. In Study II, the extracellular matrix-derived collagen membrane showed direct bone regenerative effects on the strength of attracting cells that release signals linked to bone formation and bone remodeling (BMP-2, FGF-2, TGF-β, ALP, CatK). In Study IV, the effect of two types of PTFE membranes in promoting favorable healing in the underlying bone defects was verified. The qPCR findings demonstrated comparable bone formation for the

two barriers applied, and a superior "bioactive role" of the dual e-PTFE in the soft tissue compartment as revealed by high expression of tissue regeneration (FGF-2, FOXO1, COLL1A1) and vascularization (VEGF) genes as well as a downregulation of pro-inflammatory cytokines (IL-6 and TNF-α). Finally, **Study III** was conducted to develop a methodological clinical platform to advance our scientific knowledge of the early bacterial colonization of barrier membranes. By employing CLSM imaging, it was shown that a dual expanded configuration of PTFE membrane resulted in less biofilm accumulation compared to solid dense PTFE.

In conclusion, the present thesis provides a first line of information on molecular and cellular pathways, as well as microbiological response, triggered during GBR by different membranes, featuring a plausible active role in would healing dynamics along with the traditional barrier effect.

Keywords: Guided bone regeneration, Resorbable membrane, Nonresorbable membrane, Gene expression, Histomorphometry, Soft tissue regeneration, Biofilm.

ISBN 978-91-629-596-9 (PRINT)
ISBN 978-91-629-597-6 (PDF)

SAMMANFATTNING PÅ SVENSKA

Det finns ett stadigt ökande behov av benförbättrande tekniker för att möjliggöra behandling med dentala implantat då den sistnämnda kräver en viss volym av käkben för att kunna utföra behandlingen. Guided Bone Regeneration (GBR) är en av de mest dokumenterade och använda teknikerna i klinisk praxis sedan länge. Dock är de bakomliggande biologiska mekanismerna för denna princip inte fullständigt klarlagda vilket är det huvudsakliga syftet för denna avhandling. I **Studie I**, som är en klinisk retrospektiv studie, identifierades patienter som genomgått behandling med implantat för singeltandsförlust i kombination med benuppbyggnad (GBR). Totalt 74 patienter analyserades. Resultaten visade på ett samband mellan bendefektens storlek (små defekter), kort läkningstid samt tidiga o sena komplikationer och marginal benförlust kring implantaten. **Studie II** och **IV** utvärderade både resorberbara och icke resorbebara membran i en experimentell modell med avseende på regenerativ förmåga. Analyser utfördes vid olika tidpunkter med qPCR, histologi, histomorfometri, elektron mikroksopi, Western Blot och immunhistokemi. I båda studierna kunde vi bekräfta "barriär funktionen" hos membranen vilket förhindare inväxt av mjukvävnad i bendefekter vilket resulterade i optimal benläkning. Vidare kunde det påvisas att membranen förutom sin barriärfunktion, spelade en aktiv roll i läkningsprocessen. I Studie II kunde vi demonstrera en direkt påväxt av ny benvävnad på det resorberbara kollagemembranet bestående av extra cellulärt kollagen matrix (ECM). Detta membran attraherade celler som signalerade för faktorer kopplade till bennybildning (BMP-2, FGF-2, TGF-β, ALP, CatK). I studie IV studerades två typer av icke resorberbara membran. ett mer homogent membran (d-PTFE) och ett membran bestående av olika fibernätverk (dual e-PTFE). Båda membranen visade på god benläkning men e-PTFE membranen visade på en överlägsen "bioaktiv roll" avseende mjukvävnadsläkning via uppregulering av vävnadsregeneration (FGF-2, FOXO1, COLL1A1) och kärlnybildning (VEGF). Vidare noterade för detta membrane en nedregulering av pro-inflammatoriska cytokiner (IL-6 och TNF-a). Slutligen så utvecklades i **Studie III** en klinisk plattform för att studera och utöka kunskapen om tidig bakteriepåväxt (biofilm) på olika typer av membran. Det visade sig att fiberorienterade e-PTFE mebranen uppvisade signifikant mindre biofilm jämfört med det mer solida d-PTFE membranet. Sammanfattningsvis ger resultaten från denna avhandling viktig information om de molekulära och cellulära och mikrobiella events som sker i samband med GBR behandling. Resultaten visar också att detta är kopplat till membranets struktur och dess påverkan såsom koordinator i samband med sårläkningen.

LIST OF PAPERS

This thesis is based on the following studies, referred to in the text by their Roman numerals.

I. Turri A, Dahlin C.

Long-term outcomes of single dental implants placed in Guided Bone Regeneration-reconstructed bone in the anterior regions of upper jaws: A single center retrospective clinical study. *Manuscript submitted*

II. Turri A, Elgali I, Vazirisani F, Johansson A, Emanuelsson L, Dahlin C, Thomsen P, Omar O.

Guided bone regeneration is promoted by the molecular events in the membrane compartment. *Biomaterials* 2016; 84: 167-183.

III. Turri A, Čirgić E, Shah FA, Hoffman M, Omar O, Dahlin C, Trobos M.

Early plaque formation on PTFE membranes with expanded or dense surface structures applied in the oral cavity of human volunteers. *Clin Exp Dent Res.* 2021; 7(2): 137-146.

IV. Turri A, Omar O, Trobos M, Thomsen P, Dahlin C.

Bioactive role of expanded and dense nonresorbable membranes during guided bone regeneration. *Manuscript submitted*

CONTENT

ABBREVIATIONS

ALP	Alkaline phosphatase
BMPs	Bone morphogenetic proteins
BMU	Basic Multicellular Unit
BSP	Bone sialoprotein
C(T)R	Calcitonin receptor
CatK	Cathepsin K
CFU	Colony-forming unit
CLSM	Confocal laser scanning microscopy
COL1A1	Collagen type I, alpha 1
CTR	Calcitonin receptor
CXCR4	Chemokine receptor type 4
d-PTFE	Dense polytetrafluoroethylene
DMP1	Dentin matrix protein 1
DNA	Deoxyribonucleic acid
e-PTFE	Expanded polytetrafluoroethylene
FBGC	Foreign body giant cell
FGF-2	Fibroblast growth factor 2
FOXO-1	Forkhead box protein O1
GBR	Guided bone regeneration
GTR	Guided tissue regeneration

HIF-α	Hypoxia-inducible factor-1 alpha
IGFs	Insulin growth factors
IL-1	Interleukin-1
IL-1β	Interleukin-1β
IL-4	Interleukin-4
IL-6	Interleukin-6
IL-8	Interleukin-8
IL-10	Interleukin-10
IL-11	Interleukin-11
IL-18	Interleukin-18
M-CSF	Macrophage colony-stimulating factor
M1	Macrophages type 1
M2	Macrophages type 2
MCP-1	Monocyte chemoattractant protein 1
MMP-9	Matrix metalloproteinase 9
MSCs	Mesenchymal stem cells
OC	Osteocalcin
OPG	Osteoprotegerin
OSCAR	Osteoclast-associated immunoglobulin-like receptor
Osx	Osterix
PDGF	Platelet-derived growth factor

PMNs	Polymorphonuclear neutrophils
PTH	Parathyroid hormone
qPCR	Quantitative real-time polymerase chain reaction
RANK	Receptor activator of nuclear factor kB
RANKL	Receptor activator of nuclear factor-kB ligand
RNA	Ribonucleic acid
ROI	Region of interest
Runx2	Runt-related transcription factor 2
SEM	Scanning electron microscopy
Sema 4D	Semaphorin 4D
Sema3A	Semaphorin 3A
TGF-β	Transforming growth factor-β
TNF-α	Tumor necrosis factor-α
TRAP	Tartrate-resistant acid phosphatase
VEGF	Vascular endothelial growth factor
Wnt	Wingless-related integration site

1 INTRODUCTION

1.1 INTRODUCTORY REMARKS

Bone regeneration is an exceptional synergy of biology and biomechanics that occurs in distinct temporal events, fine-tuned by a rich vascular cascade. The ultimate target of this highly complex process is the restoration of form and function of the original tissue type, which represents a significant medical challenge depending on the extent of bone insufficiency. In dentistry, such an insufficiency is often the result of tooth loss and is the major hindrance for traditional implant strategies. Several surgical procedures have been developed to contrast the bone loss and to secure the outcome of implant rehabilitation.

Among these, Guided Bone Regeneration (GBR) requires the use of a membrane that is inserted between the bone defect and the soft tissue, and that was originally conceived [3-5] to serve as a physical barrier in the attempt to prevent the migration and proliferation of epithelial and connective tissue cells into the bone compartment, thus allowing to harness the intrinsic regenerative capacity of bone.

Although GBR is one of the most successful techniques for local augmentation and defect restitution [6,7], no covering membrane and biomaterial modifications have proved to serve all requirements to ensure a predictable and stable bone healing. Hence, it is of utmost importance to better understand the biological pathways of GBR by assessing how individual events interact within and across the different scales (cellular, molecular, microbiological) as well as anatomical compartments.

1.2 BONE

Bone is a sophisticated mineralized connective tissue that exerts essential mechanical and metabolic functions [8,9]. The general architecture of bone consists of a central marrow space surrounded by cancellous and cortical bone, and periosteum. Cortical (compact) bone is the dense outer surface that provides maximum resistance to bending and torsion, allowing bone to withstand compressive forces. Cancellous bone is the meshwork of spongy tissue that is responsible for a high rate of metabolic activity, remodeling and gives bone allowance of deformation and absorption of loads [10]. The periosteum is a bilayered membrane found on the external surface of bone that possesses osteogenic potential and contributes to the bone blood supply [11].

1.2.1 CELLULAR COMPONENTS OF BONE

Bone exhibits four types of cells that arise from two cell lines: osteoblasts, osteocytes and bone lining cells that derive from osteoprogenitor cells from mesenchymal stem cell lineage, and osteoclasts which are of hematopoietic origin [8]. All together these cells form the basic multicellular unit (BMU) [12,13].

Osteoblasts are specialized bone-forming cells with the capacity to produce organic bone matrix. The activation of osteoblast differentiation from osteoprogenitor lineage is coordinated by the expression of distinct genes and synthesis of specific factors: Runt-related transcription factor 2 (Runx2), osterix (Osx), bone morphogenetic proteins (BMPs), and members of the Wingless (Wnt) pathways [14-17]. When the subsequent proliferation phase begins, osteoblast progenitors display alkaline phosphatase (ALP) activity, and are therefore regarded as preosteoblasts [14]. The maturation into osteoblasts is regulated by various molecular events such as increased Osx expression and production of osteocalcin (OCN), bone sialoprotein (BSP), and collagen type I [9].

Osteoclasts are large, multinucleated bone-resorptive cells of hematopoietic origin. The major osteoclastogenic signals are the receptor activator of nuclear factor-kB ligand (RANKL), secreted by osteoblasts, osteocytes and stromal cells [18] and the macrophage colony-stimulating factor (M-CSF), derived from osteoprogenitor mesenchymal cells and osteoblasts [19]. More specifically, RANKL is essential for osteoclastogenesis. When it binds to its receptor RANK on the surface of osteoclast precursor, osteoclast formation is initiated [20,21]. Conversely, several cells such as osteoblasts, stromal cells, and gingival fibroblasts secrete an inhibitory protein known as osteoprotegerin (OPG) that

binds to RANKL, hindering the RANK/RANKL interaction and thus preventing osteoclast differentiation and activation [22,23].

Osteocytes, which comprise 90-95% of all present cells in bone [24], originate from mesenchymal stem cells via osteoblast differentiation. The osteocytes represent another cell-line of terminally differentiated osteoblasts that develop a dendritic morphology and become embedded in the mineralized bone matrix [25,26]. During osteoblast/osteocyte transition, several osteoblastic markers such as OCN, ALP and collagen type I display a low rate of expression whereas osteocyte markers including dentin matrix protein 1 (DMP1) and sclerostin are upregulated [27-29]. Once surrounded by matrix, the osteocytes develop cytoplasmic processes (up to 50 per each cell) that are connected to adjacent osteocytes as well as osteoblasts and bone lining cells. The result of this intricate network is the osteocyte lacunocanalicular system, responsible for intercellular transport of signaling molecules among bone cells and capable to identify mechanical strains and microdamage, hereby allowing bone adjustment in response to functional loading. The mechanosensitive behavior of osteocytes is thought to be essential to initiate the bone remodeling process by converting mechanical stimuli to biochemical signals [9].

Bone lining cells are flattened "dormant" osteoblasts present on the bone surfaces when the bone multicellular unit is not synthetizing bone [30]. Despite their roles are not fully elucidated, it has been found that bone lining cells participate in osteoclast differentiation secreting OPG and RANKL and impede unfavorable bone resorption preventing the direct intercommunication between the bone matrix and osteoclasts [9,12].

1.2.2 BONE HEALING

Bone healing is a complex biological process, characterized by shift in the expression of thousands of genes [31], and it generally involves the partial overlapping of three stages: inflammation, repair and remodeling [32]. Immediately following a bone injury, the vasculature inside and surrounding the fracture site is damaged. Subsequently, endothelial cells, fibroblasts, tissue macrophages and dendritic cells identify invading microorganisms or tissue injury byproducts, and secrete a variety of cytokines and growth factors that promote the recruitment of polymorphonuclear neutrophils (PMNs), monocytes/macrophages and lymphocytes [33]. Hence, the formation of a blood clot (hematoma) is the *primum movens* for the initiation of the inflammatory cascade since it acts as a frame for the recruitment of inflammatory cells and

secretion of cytokines. The acute inflammation is most pronounced during the first 24-48 hours and usually resolves after 7 days. The initial pro-inflammatory response is portrayed by the presence of tumor necrosis factor-α (TNF-α), interleukin-1β (IL-1β), IL-6, IL-11, and IL-18 [34] by the early-recruited monocytes/macrophages and PMNs. These cytokines are instrumental for the activation of the immune cells and the promotion of angiogenesis. More specifically, it has been shown that TNF-α can act as a chemotactic agent to recruit nearby responsive cells [35], and can induce osteogenic differentiation of mesenchymal stem cells (MSCs) [36]. IL-6 on the other hand, is responsible for the differentiation of osteoblasts and osteoclasts [31], angiogenesis stimulation , and vascular endothelial growth factor (VEGF) production. Furthermore, leukocytes secrete also anti-inflammatory cytokines, such as IL-10 that is believed to be essential in preventing damage to the host tissue since it can hinder the production of the pro-inflammatory cytokines IL-1, IL-6, IL-8 and TNF-α [37]. To initiate osteogenesis, MSCs must be recruited, proliferate, and differentiate into osteogenic cells. It has been suggested that BMPs and stromal cell-derived factor-1 (SDF-1) are key regulators in recruiting specific MSCs to the site of injury [31]. In fracture healing, callus is produced during the repair phase via a vascular network forming a connecting bridge across the bone fracture where the collagen matrix is laid down. The process of callus formation can occur directly at the periosteum (intramembranous ossification) or as a transition from soft to hard callus when it occurs at the endosteum and bone marrow (endochondral ossification) [33]. At the end of the repair phase, a less organized immature bone (woven bone), with an irregular pattern of the collagen fibers, increased number of cells and a reduced mineral content is formed. At the late stage of healing, woven bone is replaced, and bone is restituted to its original anatomy by remodeling. Bone remodeling is a lifelong phenomenon, first described by Frost [13], where osteoclasts and osteoblasts closely collaborate within temporary anatomical BMU to remove old bone or repair damaged bone. Bone resorption in a BMU takes approximately 3 weeks, while bone formation 3 to 4 months, for a process that replaces 5-10% of the adult human skeleton each year [38]. The remodeling cycle consists of five different stages: activation, resorption, reversal, formation, and termination (*Figure 1*):

Activation phase: to initiate a remodeling cycle it has been suggested that osteocytes are triggered by mechanical loading, bone injury on a microscopic scale, or systemic factors such as parathyroid hormone (PTH) [2,39]. The subsequent recruitment of hematopoietic precursors for osteoclast formation is promoted by osteoclastogenic factors including M-CSF, RANKL, vascular endothelial growth factor (VEGF) and nitric oxide, which are secreted by osteoblast lineage cells and endothelial cells [38]. Importantly, RANKL interacts

with the RANK receptor on osteoclast precursor modulating the activity of hematopoietic cells of osteoclast lineage that can initiate the resorption process.

Resorption phase: polarization of osteoclast through its cytoskeleton reorganization in contact with the bone matrix implies the formation of a sealing zone that is an isolated microenvironment defined by the ruffled border appearance of an area of the osteoclast membrane. This structure is essential since it enables the dissolution of hydroxyapatite crystals through acidification and following degradation of the organic matrix by the synergistic activity of several enzymes. Consequently, tartrate-resistant acid phosphatase (TRAP), cathepsin K (CatK), and matrix metalloproteinase-9 (MMP-9) are moved into the Howship lacuna compartment [9]. Additionally, it has been reported that the osteoclasts express a signaling glycoprotein called semaphorin 4D (Sema 4D) that binds to osteoblasts inhibiting osteoblast differentitation and therefore suppressing bone formation during the resorption phase [40]. Conversely, another member of the semaphorin family (Sema3A) is believed to stimulate osteoblasts, suppressing bone resorption prior to bone formation [41]. Further, the effects of RANKL on osteoclasts are blocked by OPG [42], that inhibits their final activation by inducing apoptosis and hence regulating bone resorption.

Reversal phase: after the completion of osteoclastic resorption, "reversal" cells from an osteoblastic lineage[43] clear-away unmineralized collagen fibrils, and add a "cement line" of non-collagenous mineralized matrix to favor the adhesion of osteoblasts [39]. It has been shown that bone-matrix derived factors, such as insulin-growth factors (IGFs), transforming growth factor (TGF-β), BMPs, fibroblast growth factor (FGF) and platelet-derived growth factor (PDGF) are released from the reversal cells during bone resorption [44]. The transition between resorption and formation is the result of communication mechanisms among bone cells. Recent evidence suggests the presence of other factors that are associated with the coupling phenomenon [45]. For example, the molecule ephrinB2 is secreted by mature osteoclasts and can link to ephrinB4, which is expressed in the osteoblast plasma membrane. The ephrinB2/ephrinB4 signaling resulted in enhanced bone formation whereas the reverse signaling ephrinB4/ephrinB2 inhibited osteoclastogenesis [46].

Formation phase: initially, the osteoblasts synthesize and produce dominantly type I collagen proteins, proteoglycans and noncollagen proteins including OCN, osteonectin, and osteopontin that contribute to the development of an organic network to fill the pits left behind by the osteoclasts [39]. Consequently, mineralization of bone matrix occurs when membrane-bound matrix vesicles

rupture due to a supersaturation of calcium and phosphate ions. Hence, hydroxyapatite crystals are released and deposited amongst collagen fibrils [9].

Termination phase: when the amount of newly formed bone at each BMU is equal to the amount of the resorbed bone, the remodeling is completed. Osteocytes secrete TGF-β and sclerostin that impede further osteoclastogenesis and bone formation induced by Wnt signaling in osteoblasts [45]. At this point, osteoblasts can encounter apoptosis or revert to osteocytes or bone-lining cells that cover the bone surface [47].

Taken together all the events occurring during bone remodeling, it is clear that a complex network of fine-tuned cell communication exists at each BMU, with accumulating evidence confirming the presence of several "coupling factors" that act as signals between osteoblast and osteoclast lineage cells both ways [38,45].

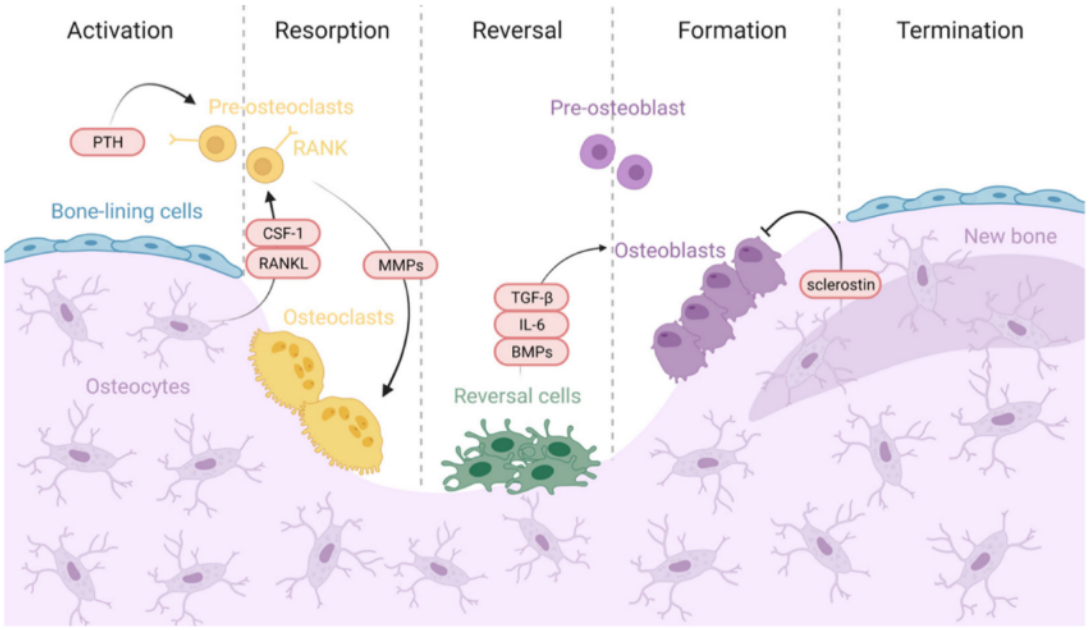

Figure 1. Bone remodeling process is characterized by a critical interplay between bone and bone forming cells within the bone multicellular unit (BMI) – from Pedrero et al. (Materials 2021, 14, 4896) – published by permission from Materials [2]

1.3 INFLAMMATION, IMMUNE RESPONSE AND BIOMATERIAL-MEDIATED TISSUE HEALING

Despite bone tissue retains the ability to self-heal, the presence of large defects may necessitate the use of different biomaterials to facilitate the bone regeneration process.

Immediately after implantation, biomaterials induce a complex host reaction that starts with protein adsorption to the material surface, provisional matrix formation (blood clot) and inflammatory process. It has been reported that the types, amount, and structure of the adsorbed proteins are decisive for the tissue response to the implanted biomaterials [48]. On the other hand, it has also been shown that the surface properties of the biomaterials (topography, chemistry, energy, and roughness) affect the types, concentrations, and conformations of the adsorbed proteins (i.e., albumin, fibrinogen, fibronectin, vitronectin, complement) which can subsequently regulate host inflammatory interactions [49-51]. For example, fibrinogen and complement are largely related to the activation of the cellular component of inflammation, whereas fibronectin and vitronectin may trigger cell adhesion, and promote macrophage fusion [52]. Following the initial blood protein deposition and blood clot formation, the inflammatory responses occur within a few minutes to hours after implantation, inducing the recruitment and adhesion of monocytes that are then differentiated into macrophages. Macrophages are crucial in inflammation and host defense and play multiple roles in the bone healing process. Classically activated macrophages, also known as M1 macrophages, are intimately related to the initial phase of wound healing according to their ability to produce pro-inflammatory cytokines such as IL-6, IL-1β, and TNF-α, chemokines, and enzymes [53,54]. Importantly, the release of TNF-α and IL-6 triggers the recruitment of leucocytes, monocytes, and other macrophages, thus inducing an amplification of the inflammatory response. Moreover, TNF-α and IL-6 are traditionally recognized to activate the process of osteoclastogenesis since IL-6 is known to induce the expression of RANKL and to participate in the TNF-α and IL-1 induced osteoclast formation [55]. Adherent macrophages undergo cytoskeleton changes in the attempt to stretch over the material surface, and merge to form foreign body giant cells (FBGCs). The formation of FBGCs may be viewed as an attempt to increase the phagocytic process of macrophages and degrade large implants. Although the detailed mechanisms behind FBGCs formation have not been fully clarified, it has been claimed that

the physicochemical properties of the materials are very important for macrophage plasticity and fusion [56,57]. Following human monocyte culturing on polystyrene using various protein substrates, it was observed that macrophage response, in terms of adhesion and fusion, was strongly influenced by the presence of vitronectin, thus suggesting that material characteristics that promote its retention may also foster the formation of FBGC [58]. The prolonged presence of M1 (more than 3-4 days) may generate a severe foreign body reaction through the formation of a barrier between the tissue and the material, leading to implant deterioration and/or loss [59,60]. Similar to the wound healing cascade [61], adherent macrophages ultimately shift to "alternatively activated" M2 phenotypes [62]. The M2 macrophages are vital at the late stages of tissue repair and are mainly responsible for an anti-inflammatory activity, as shown by the secretion of high levels of IL-10. In addition, M2 macrophages promote tissue remodeling response since they induce migration and proliferation of fibroblasts improving the integration of the biomaterial with the surrounding tissue [63]. The contribution to regeneration of M2 macrophages arise through a crosstalk with regulatory T-cells that are very important in tissue immune homeostasis [52]. Concisely, prolonged presence of M1 macrophages may result in the intensification of the inflammatory response with subsequent negative effect on normal tissue/bone healing and formation of a fibrocapsule at the biomaterial interface. By contrast, an effective switch to M2 macrophages may produce a successful resolution of the inflammation, resulting in an osteogenesis-enhancing cytokine release pattern with subsequent formation of new bone tissue.

Biomaterials properties (biological, chemical, physical) have shown the ability to modulate immune cells, thus tuning innate and adaptive immune responses at implantation sites, including bone tissue. It is well-established that material properties can affect cellular function. Topographical features have been recognized as important regulators of cell adhesion, proliferation and differentiation, macrophage fusion and cytokine secretion [64]. It has been shown that surface nanostructure may induce conformational changes of adsorbed proteins, which in turn may explain different patterns of cell adhesion and activation on flat versus rough surfaces [65-67]. Furthermore, a decreased macrophage response, which leads to FBGC formation, was noticed on a polymeric surface with more pronounced topography in contrast to observations on more flattened controls [68]. When microroughness of titanium substrates was investigated, it was seen an increase in the TGF-β/BMP osteogenic signaling from osteoblast culturing, and a polarization of macrophages into M2 phenotype with following upregulation of IL-4 and IL-10 cytokines, which are important for osteoblast maturation [69,70]. The use of porous materials can also be critical in clinical settings due to their ability to

foster biological molecules. Recent evidence has shown that scaffold architecture with interconnected pores favored the ingrowth of vasculature with the resultant delivery of osteoprogenitor cells and more bone formation compared with materials with closed or non-existent pores [71]. Further, it was found that porous collagen scaffolds influenced the course of bone healing by promoting revascularization at injury sites via high expression of M2 markers and the secretion of PDGF and MMP-9 [72]. Hence, the distribution and diameter of the pores may perform as topographical "actors" for osteoimmunomodulation, although the ideal pore size for optimal osteoblast behavior is still disputable [73]. It is common knowledge that biomaterial hydrophilicity enhances the ability of cells to provoke an immune response [74]. For example, research has provided evidence for a downregulation of several pro-inflammatory cytokines when human macrophages interacted with hydrophilic modified titanium surfaces [75]. An increase in hydrophilicity may also decrease osteoclast activity, as demonstrated in an *in vitro* study where osteoclastic markers, such as TRAP and osteoclast-associated immunoglobulin-like receptor (OSCAR), were downregulated on hydrophilic sandblasted/acid etched titanium [76]. Moreover, the addition of hydrophilicity to a biomaterial can influence the macrophage response. It was found that a chemically modified hydrophilic surface of microrough titanium implants with subsequent increased surface energy and wettability resulted in a reduced secretion of pro-inflammatory cytokines (IL-1 α, IL-1β, TNF-α), thus suggesting potential enhanced bone wound healing and osseointegration [77]. Surface charge represents another relevant element in the modulation of the immune response, despite contradictory results are reported in the literature [64].

Noteworthy, the current challenge is the development of biomaterials with improved physicochemical properties that could be able to modulate the immune system and the inflammatory response, seen as decisive gateways in bone regeneration.

1.4 GUIDED BONE REGENERATION

Barrier membranes to restore bone deficiencies, prior to or in conjunction with dental implants, were developed according to the osteopromotion principle [3-5,78], based on the soft-tissue exclusion assumption that the creation of a secluded bone compartment may allow undisturbed migration, differentiation and activation of cells with osteogenic potential, thus triggering, protecting and guiding bone regeneration (GBR).

The sequence of bone regeneration in membrane-covered defects was well described in a histologic study in the canine mandible [79]. After 2 and 4 months of healing, test sites covered with non-resorbable expanded polytetrafluoroethylene (e-PTFE) membranes were compared with control sites without membranes. Placement of the barrier membranes promoted the creation of a microenvironment conducive to intramembranous ossification, where an undisturbed blood clot together with a protected solid base for bone deposition promoted better bone healing than that observed in control defects. Interestingly, bone formation started on the surfaces bordering the walls of the defect and subsequently spread towards the middle and top portion of the defect. In a considerable number of histological studies, using different experimental models, this membrane technique has proven effective and reproducible [80]. On this matter, another early investigation explored the bone regenerative potential of ten different membranes in critical size mandibular defects in a rat model [81]. The histological evaluation after 6 weeks of healing revealed varying degrees of bone-promoting capacity depending on the membrane type, with comparable performance between e-PTFE non-resorbable membranes and certain types of resorbable membranes. Afterwards, several synthetic and naturally derived materials have been developed trying to fulfill and optimize a set of basic requirements [82,83]: biocompatibility, occlusive properties, space-making ability, attachment to or integration with the surrounding tissues, adequate mechanical and physical properties, and clinical manageability. A single material that serves all properties has not been found yet, and the current GBR membranes can be classified as synthetic polymers (PTFE, aliphatic polymer based such as polylactic acid PLA, polyglycolic acid PGA, poly ε-caprolactone PCL), natural polymers (collagen, chitosan, alginate based), metals (titanium, titanium alloy cobalt-chromium alloy), and inorganic compounds (calcium sulfate, calcium phosphate) [84]. Furthermore, they can be classified as resorbable and non-resorbable (*Table 1*).

Table 1. Membranes for GBR, presented according to resorbability, material and commercial name (modified from Omar et al. 2019 [83])

Type	Material	Description	Examples of commercial membranes
NON-RESORBABLE	Polytetrafluoroethylene	Expanded	Gore-Tex®
		Dense	Cytoplast™ TXT-200
		Dual textured expanded	NeoGen®
		Titanium-reinforced	Gore-Tex-Ti
			Cytoplast™ Ti-250
			NeoGen® Ti-Reinforced
	Titanium	Titanium mesh	Frios® BoneShields
			Ridge-Form Mesh™
RESORBABLE, naturally derived	Non-cross-linked collagen	Type I collagen	CollaTape®
			Tutodent®
		Type I and III collagen	BioGide®
			Botiss Jason®
		Type I, III, IV, VI collagen and other proteins	DynaMatrix®
		Collagen with intermingled elastin	Creos Xenoprotect™
	Cross-linked collagen	Cross-linked type I collagen	BioMend®
			OSSIX® plus
			OsseoGuard®
		Cross-linked type I and III	OsseoGuard Flex®
			MatrixDerm™ EXT
RESORBABLE synthetic	Aliphatic polyesters	Poly-D, L-lactide-co-glycolide	Resolut adapt®
		D, D-L, L polylactic acid	Epi-Guide®
		Poly-D, L-lactide and poly-L-lactide blended with acetyl tri-n-butyl citrate	Guidor®
		Polyglycolide, poly-D, L-lactide-co-glycosides, poly-L-lactide	BioMesh®-S

1.4.1 NONRESORBABLE MEMBRANES

Expanded PTFE membranes constituted the first generation of clinically successful and well-documented barrier membranes in GBR [5,79]. PTFE is a highly crystalline, stable and hydrophobic synthetic polymer that does not provoke immunological reactions and resists enzymatic breakdown by host tissues and microorganisms [85]. Despite the excellent structural integrity and tissue-exclusion behavior, early research called attention to failure of GBR procedures due to the collapse of PTFE membranes under the external soft tissue pressure [86-88]. Hence, to strengthen the mechanical stability, a titanium reinforcement was introduced inside the membrane structure [89]. Previous research showed successful bone regeneration when e-PTFE membranes were used alone [90,91], and the subsequent wide application of this material has made it as the gold standard for GBR. The technique was then modified by including a bone grafting material underneath the membrane [92], not only for mechanical purposes since it could support the membrane to maintain the created space, but also because bone grafts may help accelerating bone regeneration by their osteoconductive and possibly osteoinductive properties [93]. In general, the decision regarding the clinical use of nonresorbable and resorbable membranes is based on the defect morphology and the volume stability provided by the adjacent bone walls of the region to be augmented. Thus, in the presence of large peri-implant dehiscences, reduced ridge width and/or height, nonresorbable PTFE membranes and bone substitutes are recommended [93] and have proven to be successful in many investigations [94,95], especially with regard to vertical bone deficiencies [96,97], although recent evidence showed promising results also with resorbable membranes [98]. A 6-year double-blind randomized clinical trial was performed on twenty-two patients to study the outcome of two procedures for vertical ridge augmentation in combination with simultaneous implant placement [99]. In the test group autogenous bone graft was covered with a biodegradable collagen membrane fixed to titanium plates, while the controls consisted of autogenous bone graft and a nonresorbable titanium-reinforced e-PTFE membrane. Despite no differences between treatments could be observed, the test group revealed 0.58mm mean bone loss from baseline to 6 years, and the control group lost 0.49mm of peri-implant bone, thus demonstrating good stability of the interproximal vertically regenerated bone. Nevertheless, it has been claimed that the stiffness of the PTFE material together with a highly sensitive surgical management ("PASS principle": primary wound closure, angiogenesis, space and stability of the clot [100]) may enhance the risk of early wound dehiscence and membrane exposure through the soft tissue [101,102]. It was recently reported that when membrane exposure was avoided the horizontal bone gain was 74% higher than at sites showing membrane exposure [103]. Prior research demonstrated a negative

correlation between the number of bacteria found on the surface of the membranes at the time of removal and the clinical attachment gain achieved after guided tissue regeneration (GTR) [104-106]. The *in vivo* behavior of exposed nonresorbable membranes unveiled an unsuccessful protective role against bacterial invasion as early as 4 weeks [107]. These findings agreed with studies reporting on periodontal and implant clinical outcomes where the exposed e-PTFE barrier membranes were removed 4-6 weeks after the surgical interventions [108,109] to still allow for an adequate bone regeneration as long as the acute infection could be prevented [110]. On this matter, high-density PTFE barriers seemed to offer an interesting alternative since it has been argued that they would contribute with a better protection to bacterial penetration due to a much smaller pore size (< 0.3 μm) compared to e-PTFE (0.5 – 30 μm) [94,103]. Socket preservation studies on intentionally exposed d-PTFE barriers reported satisfactory outcomes regarding bone regeneration and absence of infection [111-113]. A prospective randomized controlled trial on 23 patients requiring vertical bone augmentation in atrophic posterior mandibles didn't reveal neither clinical nor histological differences in bone gain at implants treated with GBR procedures where e-PTFE or d-PTFE membranes [97] were used.

1.4.2 RESORBABLE MEMBRANES

Among the variety of resorbable membranes evaluated for GBR purposes over the years, those made of native collagen are the most used [84,93], considering several intrinsic compelling features such as low immunogenicity, good tissue integration most likely due to its chemotactic effect on fibroblasts and osteoblasts, fast vascularization and good dimensional stability [114]. Collagen membranes may present with different architecture and thickness depending on the source (bovine and porcine tissues, human skin), extraction method and technique used to manufacture the membrane [84]. From a clinical perspective, the main advantages in using collagen membranes for GBR procedures in comparison to nonresorbable PTFE barriers, are represented by an easy manipulation and a decreased patient morbidity since there is no need for an additional surgical intervention to remove the membrane and the fixation devices. Contrarily, the unfavorable mechanical properties of collagen membranes represent the major drawbacks. The lack of rigidity together with the biodegradation process implies a peculiar difficulty of this material in maintaining the barrier function for the duration required to achieve optimal tissue regeneration, which has been previously reported to range between 4 and 6 weeks depending, however, on individual patients' conditions such as age, systemic diseases and morphology of the bone defect [115-117]. Currently, it is

known that soft tissue complications after GBR may occur at a similar frequency with nonresorbable (17.6%) and resorbable membranes (18.3%), as shown in a recent systematic review [118]. Although a spontaneous healing in the presence of mucosal dehiscences is expected when collagen membranes are used, the membrane contamination during or after surgery may accelerate the degradation process up to 80% [119], thus explaining the unpredictable clinical results that are sometimes obtained by resorbable membranes. Nevertheless, collagen barriers may account on a widely successful short- and long-term clinical employment [93,114]. For example, an early split-mouth prospective study evaluated the outcome of GBR procedures for the treatment of 84 implant dehiscences that were filled with deproteinized bovine bone and protected either with a biodegradable collagen membrane or a nonresorbable PTFE [120]. After 4-6 months of healing, the regenerated bone was assessed during the re-entry procedure. The mean percentage of defect reduction was 92% for the resorbable-treated sites and 78% for the nonresorbable-treated defects, and a higher complication rate in terms of membrane dehiscence was observed in the e-PTFE group. Further, in a long-term trial reporting on 58 patients, resorbable collagen membranes and nonresorbable e-PTFE demonstrated comparable outcomes regarding implant survival rate, interproximal marginal bone level and clinical soft tissue parameters [98].

1.5 ANALYTICAL TECHNIQUES TO EVALUATE GBR

The histological and histomorphometrical evaluations of bone tissue and cells present in membrane-treated defects have been the traditional "gold" standard methods for evaluating the bone structure [121,122] and the formation of bone in GBR [4,5,79,88,123]. The newly formed bone, which is defined as the percentage of new bone tissue calculated in relation to the total defect space (i.e., area or volume) is generally the main parameter of interest. The calvarial critical-size defect is the classical model for the study of GBR in small and large animals and is defined as the one that would not heal spontaneously [124,125]. However, it has been argued that even a very small size of induced defect could be regarded "of critical size", depending on the duration of the experiment [126]. Overall, conventional histology and histomorphometry are based on a two-dimensional assessment of tissue sections, and therefore can provide only a snapshot view of a dynamic process such as bone regeneration. Several histological studies in different experimental models have been important as proof of concept, demonstrating the influence of various types of barrier membranes in promoting bone regeneration in the defect compartment [127-130]. Nevertheless, they have not been of any help to elucidate the exact role of the membranes, regarding the cellular and molecular events that foster the overlapping stages of bone healing (inflammation, bone repair, and bone remodeling).

Gene expression profiling has become a valuable tool in medicine to study the molecular changes that underlie physiological processes and pathological conditions. Gene expression is a tightly regulated course of events in which cells convert the information present in their DNA into instructions for making proteins, that are ultimately responsible for the prompt response of cells to a changing environment. Hence, gene expression can be seen as an "on/off switch" to regulate protein synthesis and also as a "volume control" that is capable to increase or decrease the number of proteins synthesized. More specifically about GBR, gene expression related to inflammation, osteogenesis and osteoclastogenesis that occur in the bone, at the bone-material interface and in the soft tissue compartment could be investigated by quantitative real-time polymerase chain reaction (qPCR) analysis. This is a quantitative technique used to amplify and simultaneously quantify the amount of DNA and therefore to measure gene expression [131]. A recent narrative review analyzed the existing evidence that employed cellular and molecular techniques to decode the biological basis of GBR [83]. It was concluded that there is evolving knowledge whereby barrier membranes might exert bioactive bone promotive functions. However, the current literature is still scarce on this

matter and a potential active role of the membranes in GBR needs to be further assessed in their physicochemical properties, bioactivity, and antibacterial effect.

2 AIM

The main objective of this thesis was to investigate the biological processes, including microbiological events that underlie the *in vivo* behavior of barrier membranes used for GBR.

The specific aims were:

1. To report on the long-term effects of clinical applicability of GBR procedures prior to or in conjunction with single implant rehabilitation in the anterior maxilla.

2. To assess *in vivo* whether a resorbable collagen-based membrane used for GBR could actively stimulate the osseous healing in experimental bone defects, thus supporting a new role besides its established barrier effect.

3. To evaluate and compare *in vivo* the potential bioactive involvement of two types of nonresorbable PTFE membranes in the regenerative healing events taking place not only in the osseous defect below the membranes, but also within the membranes and in the overlying soft tissue compartment.

4. To develop a methodological platform for studying *in vivo* the early biofilm formation on different types of nonresorbable PTFE membranes directly exposed to the oral cavity

3 MATERIALS AND METHODS

The present thesis is based on two human clinical trials (Studies I & III) and on two experimental studies (Studies II & IV).

Study I is a retrospective clinical, radiographic study that describes the outcomes of single implant treatment after applying the GBR technique, whereas Study III is a short-term trial that focuses on the *in vivo* microbiological behavior of barrier membranes when exposed to biofilm formation in the oral cavity.

Studies II and IV consist of experimental *in vivo* models that investigate the mechanisms of GBR, providing histological and histomorphometrical assessments as well as quantitative measurements of gene expression through qPCR technology at three structural levels of rat femur experimental defects: in the bone underneath a barrier membrane, in the membrane itself (Studies II and IV) and in the overlying soft tissue compartment (Study IV).

3.1 BARRIER MEMBRANES

The membranes used in Studies I and II were naturally derived collagen-based membranes, while in Studies III and IV, synthetic PTFE, which is nonresorbable, was used.

Study I: The great majority of bone deficiencies, prior to or in conjunction with implant placement, were treated by a combination of bone grafting materials and the bilayered collagen membrane BioGide® (Geistlich Pharma, Wolhusen, Switzerland) (*Figure 2a*).

Study II: An extracellular matrix membrane extracted from the porcine small intestinal submucosa was utilized (DynaMatrix®; Keystone Dental, Boston, USA) (*Figure 2b*).

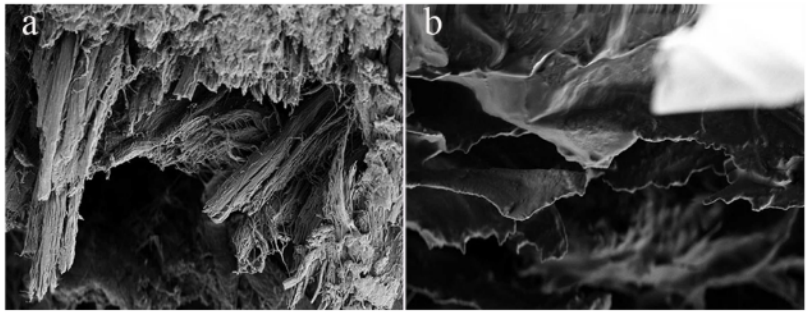

Figure 2. Scanning electron microscopy (SEM) micrographs showing (a) BioGide® membrane and (b) Dynamatrix® extracellular matrix membrane – (courtesy of Prof. Dahlin)

Studies III & IV: Two types of PTFE membranes were used (*Figure 3*). The test membrane was dual-layered expanded PTFE (NeoGen™, Neoss Ltd.; Harrogate, UK) with two different degrees of expansion. The top side of the e-PTFE—facing the soft tissue in Study IV—was characterized by a semi-closed structure, whereas the bottom side—facing the bone defect in Study IV—was biaxially expanded with a similar expansion ratio and an open structure. The control membrane was solid dense PTFE (Cytoplast™ TXT-200, Osteogenics Biomedical, Inc., TX, USA).

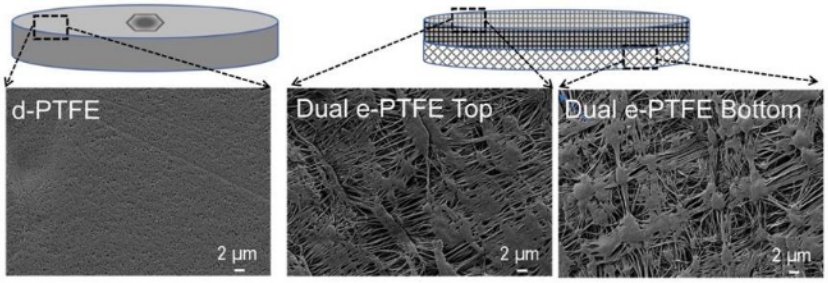

Figure 3. Schematic drawing and corresponding SEM micrographs of solid dense PTFE (d-PTFE) and dual-layered expanded PTFE (e-PTFE) with two different degrees of expansion on the two sides of the membrane: the top (soft tissue) side was biaxially expanded with a dissimilar expansion ratio and a semi-closed structure, while thee bottom (bone) side was biaxially expanded with a similar expansion ratio and an open structure (from Turri et al. – submitted manuscript)

3.2 CLINICAL STUDIES

3.2.1 STUDY DESIGN

Retrospective study (Study I)

The sample population was selected from consecutively treated patients referred to the Brånemark Clinic in Gothenburg (Sweden) from December 2002 to November 2011. The participants were provided with a single implant-supported prosthesis for the replacement of one anterior upper tooth in the presence of inadequate alveolar bone volume. The inclusion criterion for the patient sample was at least 5 years of follow-up. The treatment protocol included bone augmentation and implant placement either using a simultaneous approach or a delayed strategy (*Figure 4*), where the bone defect was first augmented and, after an adequate healing time, the implant was inserted to restore the partial edentulous situation. The two different surgical protocols were chosen based on the bone defect morphology and on the individual surgeon's preference. The GBR technique consisted of the selection of resorbable membranes with the additional use of graft material, either autogenous bone and/or deproteinized bovine bone.

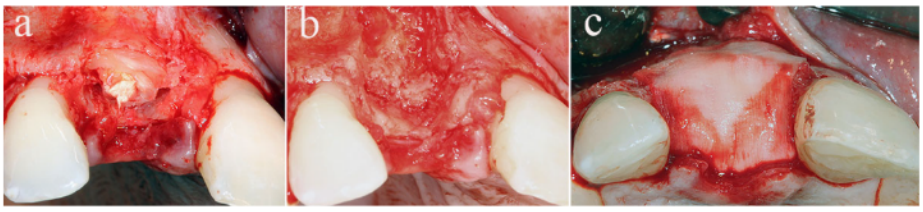

Figure 4. Clinical case to illustrate a staged treatment protocol. Following the surgical extraction of tooth 11 (a), the buccal bone plate (b) was reconstructed with deproteinized bovine bone and a collagen bilayered membrane (c), and implant placement was performed after an appropriate healing time.

After completion of the treatment with the placement of the prostheses, all patients were invited to participate in a follow-up according to a standardized protocol[132]. Clinical examinations, which included radiologic investigations, were scheduled at prosthesis placement, after one year, after three and five years, and then for individual check-ups whenever the patients experienced a problem.

In vivo short-term study (Study III)

The study subjects were enrolled as healthy volunteers and were selected based on good oral health and an absence of mouth breathing and parafunctional habits. None of the participants used chlorhexidine mouth rinses or had taken antibiotics in the 6 months preceding the study.

On each subject, the natural surface of ten teeth was used to apply round membrane specimens (4 mm diameter and 0.25 mm thickness) that were divided into test and control groups (*Figure 5*). The location (cuspid to molar region) of the test and control membranes was assigned at random on the right or left side of the twelve included volunteers according to two experimental protocols that were created to assign an equal number of specimens to the respective quantitative (n = 12) and qualitative (n = 6) analyses. The membranes were bonded using a moisture tolerant light cure bonding system (SmartBond®, Gestenco International AB, Sweden).

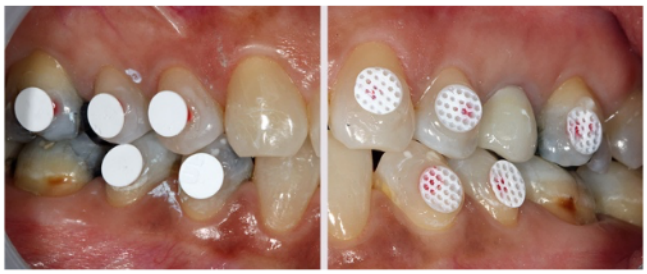

Figure 5. Test membranes (e-PTFE) on the left side and control membranes (d-PTFE) on the right side at baseline – from Turri et al. 2021 [1]

The subjects were asked to cease oral hygiene procedures during a 24-hour period. After 4 h and 24 h, all participants were recalled to retrieve the biofilm-covered membrane discs for a total of four or six specimens at each time point according to the corresponding experimental protocol. Additionally, supragingival plaque samples were collected from the buccolingual surfaces of a lower cuspid before bonding the membrane discs and again before membrane retrieval at 4 h and 24 h. Professional mechanical tooth cleaning was performed at the end of the study.

3.2.2 METHODS

Clinical data collection *(Study I)*

Data were retrospectively retrieved from the included patient files related to implant treatment and the GBR procedure, such as age, general health, smoking habits, reasons for tooth loss, type of bone defect, GBR materials, implant characteristics, and time of implant placement in relation to the bone surgical reconstruction. All recorded biological and technical complications were also collected, and they were divided into three groups according to the time of occurrence: postoperative complications such as wound dehiscence, membrane and graft exposure, infection, and loss of graft [6,118]; "early-stage" complications occurring within the first year of functional loading, such as implant failure, presence of early signs of peri-implant inflammation [133,134] and technical complications [135]; and "late-stage" complications such as loss of osseointegration, peri-implant mucositis, periimplantitis [136-138] and technical complications [135].

Radiographic data collection *(Study I)*

All available intraoral radiographs were analyzed by one examiner (AT), and the distance was calculated between a reference point (fixture-abutment junction) and the nearest thread where the bone level was detected at the interproximal sites of each implant. From the mesial and distal values, the largest was recorded and used in the statistical analysis. If one of the sites was unreadable, the other site was chosen. The change in marginal bone level at different examinations was calculated as the thread difference between the measurements and expressed in mm.

Microbiological sampling and CFU *(Study III)*

One test and one control membrane were retrieved per subject and time point (4 h and 24 h) to measure the bacterial colony-forming unit counts (n = 12). To provide a proper control for microbiological analysis in each patient, the viability counting method was also used to determine the number of bacterial cells detected on the surface of the natural teeth at different time points, including the baseline, immediately before bonding the membrane discs.

CFU counting was performed as described in previous research [139]. At each time point and for each membrane and supragingival sample, an ESwab tube (Copan Italia S.p.A., Brescia, Italy) containing 1 ml transport medium was used. To dislodge the adherent bacteria and break up any aggregates, the tube was vortexed for 30 s at maximum speed (3200 rpm), followed by 5 min of sonication at 40 kHz and additional vortexing for 30 s. Tenfold serial dilutions until 10^{-4} were made in 0.9% saline. A volume of 100 μl from each of the four dilutions was spread on duplicate agar plates and incubated at 37 °C under aerobic conditions for 2 days and anaerobically for 5 days before quantification of viable colony forming units. The presence and number of staphylococci were also determined on duplicate agar plates, and the strains were further identified using CHROMagar™ Staph aureus.

Microbiological sampling and CLSM *(Study III)*

One test and one control membrane were retrieved per subject and time point (4 h and 24 h) for confocal laser scanning microscopy analysis (n = 12).

Briefly, the membranes were covered with 200 ml of staining solution of the FilmTracer™LIVE/DEAD® Biofilm Viability Kit to distinguish live (green) and dead (red) bacteria. Thereafter, the stain was removed, and the membranes were immersed in saline for *in situ* visualization of the biofilms using the C2plus confocal microscopy system (Nikon, Japan). The biofilm images were processed and quantified using Comstat2 software (Lyngby, Denmark) to determine [140]: (1) biofilm biomass ($\mu m^3/\mu m^2$), (2) average thickness of the biofilm, (3) area occupied (%) by the first biofilm layer, and (4) surface-to-volume ratio ($\mu m^2/\mu m^3$).

Microbiological sampling and SEM *(Study III)*

One test and one control membrane were retrieved per subject and time point (4 h and 24 h) for scanning electron microscopy analysis (n = 6).

The membrane samples were first rinsed in saline and then fixed in modified Karnovsky's fixative for 2 hours at 4 °C. After additional rinsing and staining, they were dehydrated in a graded ethanol series and allowed to air-dry overnight. The samples were then mounted on aluminum stubs using conductive silver paint and sputter-coated Au (~15 nm) for scanning electron

microscopy (SEM) (Ultra 55 FEG SEM, Leo Electron Microscopy Ltd., UK) operated in secondary electron mode at an accelerating voltage of 5 kV and a working distance of ~5 mm.

3.2.3 STATISTICS

All statistical tests had a significance level fixed at 5% and were performed using SPSS software (IBM SPSS Statistics, Armonk, NY) for study I and GraphPad Prism version 8.1.0 (GraphPad Software, La Jolla, California, USA) for Study III.

Pitman's test was used in Study I to identify significant correlations between population characteristics at baseline and marginal bone level changes from baseline to follow-ups.

The Wilcoxon matched pairs signed ranked test was used in study III to compare test with control membranes as well as test or control membranes with plaque samples from teeth. Additionally, the Friedman test was used to compare the different time points within the three different groups (baseline, 4 h and 24 h).

3.2.4 ETHICAL APPROVAL

All studies were approved by the Local Ethics Committee at the University of Gothenburg, Sweden: Study I (Dnr 197-12) and Study III (Dnr 379-14).

3.3 EXPERIMENTAL STUDIES

3.3.1 STUDY DESIGN

Male Sprague–Dawley rats were used: 52 in Study II and 60 in Study IV. Bilateral defects were created in the femoral epiphyseal bone of each animal. One site was left to heal without a membrane (sham), while the other site was covered with a membrane, with one collagen resorbable membrane in Study II and one of the two nonresorbable PTFE membranes in Study IV.

The assignment of femoral defects to experimental (test) and control groups was chosen by a predesigned placement schedule to secure rotation (right/left side) and to guarantee that the two groups in Study II and the three groups in Study IV provided an equal number of specimens to the different analytical techniques (*Figure 6*).

Figure 6. Schematic drawing of the experimental defects in the rat femur

Animal sacrifice was performed at 3 d, 6 d and 28 d (16 rats at each time point) in Study II and at 6 d and 28 d (30 rats at each time point) in Study IV (*Table 2*).

Table 2. Outline of the experimental studies and the analytical techniques employed

		STUDY II			STUDY IV		
	Time points	3 d	6 d	28 d	6 d		28 d
	Number of rats	16	16	16	30		30
Analytical techniques	Histology		+	+	+		+
	Histomorphometry		+	+	+		+
	Immunohistochemistry	+	+				
	Western blot	+	+	+			
	qPCR	defect	membrane		defect	membrane	soft tissue

3.3.2 SURGICAL PROCEDURES

In brief, the surgical protocol follows the regimen described in previous experiments from our research group [141]. The surgeries were performed under general anesthesia induced by isoflurane inhalation (4.1% with an air flow of 650 mL/min) in a Univentor 400 anesthesia unit and maintained by the continuous administration of isoflurane via a mask. The recipient leg was shaved and cleaned with 5 mg/ml chlorhexidine and 70% ethanol. After infiltration with a local anesthetic solution (1 ml lidocaine with epinephrine; 10 mg/ml + 5 µg/ml), the distal aspect of the femur was exposed through a skin incision, muscle reflection and periosteal elevation. Under profuse saline irrigation, bone defects were prepared in each femoral epiphysis using a trephine with a 2.3 mm internal diameter and 3.0 mm penetration depth. One defect was covered with a membrane, either resorbable (Study II) or nonresorbable (Study IV), and the other was left uncovered. The barrier membranes were not secured with titanium mini pins on the surrounding bone. The flap was closed in layers subcutaneously using resorbable polyglactin sutures (Vicryl 4-0; Ethicon), whereas the skin was closed with transcutaneous

resorbable poliglecaprone sutures (Monocryl 4-0; Ethicon). The rats received pre- and post-operative buprenorphine analgesic (Temgesic 0.03 mg/kg) subcutaneously and were housed in groups with food and water *ad libitum*. At the indicated times of the retrieval procedure, the animals were euthanized using an overdose of sodium pentobarbital (pentobarbital sodium vet; APL 60 mg/ml).

3.3.3 METHODS

Quantitative Polymerase Chain Reaction (qPCR) *(Study II & IV)*

In the different compartments of the experimental sites, qPCR was performed to analyze the expression of several genes of interest as a measure of the healing state and of the functional activation of cells in relation to the presence or absence of barrier membranes.

In study II, 24 rats were allocated for qPCR (8 at each time point) resulting in n = 8 for each group, whereas in study IV, 30 rats were allocated for qPCR (15 at each time point), resulting in n = 10 for each group.

Special care and precautions were taken for the isolation and preservation of RNA biomolecules, which are unstable due to the ubiquitous presence of enzymes (RNases) in tissues, blood and most bacteria and fungi in the environment [142]. Briefly, total RNA from the homogenized defect sites (Studies II & IV) and soft tissue (Study IV) was extracted using an RNeasy® Mini kit (Qiagen GmbH, Hilden, Germany), while the total RNA from the homogenized membrane-adherent cells was extracted using a NucleoSpin RNA/protein isolation kit (Macherey-Nagel, Germany) in Study II and an RNeasy® Micro kit (Qiagen GmbH, Hilden, Germany) in Study IV. The RNA quality was evaluated with a Nano 6000 RNA kit in a Bioanalyzer 2100 Electrophoresis System (Agilent Technologies; Santa Clara, CA, USA), and the RNA concentration was measured with a Nanophotometer P-36 (Implen GmbH, Munich, Germany). Reverse transcription of RNA into cDNA was carried out using a GrandScript cDNA Synthesis kit (TATAA Biocenter AB, Gothenburg, Sweden) in Study II and an iScript cDNA Synthesis kit (Bio-Rad, Hercules, CA, USA) in Study IV. Before qPCR, predesigned validated assays for the genes of interest were purchased from TATAA Biocenter AB (Gothenburg, Sweden). The selected panels targeted different genes in the three GBR compartments (*Table 3*). Additionally, another panel of genes was screened in different samples from the retrieved tissues as well as from the retrieved membranes at all time points to select the most stable reference genes

for normalization. The expression profiles of the screened reference genes were evaluated using geNorm [143] and Normfinder [144] software. The most stable gene expression was achieved by HPRT1, GAPDH and ACTB, which were selected as reference genes for study II, whereas in study IV, a combination of HPRT and ACTB was designated, and their mean was used for normalization. More specifically, the quantities of the genes were normalized to the expression of the chosen reference gene and were calculated using the delta-delta C_q method and 90% PCR efficiency ($k*1.9^{\Delta\Delta cq}$) [145].

Table 3. List of the genes included in the experimental studies

Gene description (symbol)	**Biological processes**	**Analyzed compartment** (corresponding studies)		
Alkaline phosphatase (ALP)	Bone formation	Membrane (IV)	-	Bone defect (II & IV)
Bone morphogenetic protein 2 (BMP-2)	Bone formation	Membrane (II & IV)	Soft tissue (IV)	Bone defect (IV)
Calcitonin receptor (CTR)	Bone resorption	-	-	Bone defect (II & IV)
Cathepsin K (CatK)	Bone resorption	-	-	Bone defect (II & IV)
Chemokine receptor type 4 (CXCR4)	Cell migration and recruitment	-	-	Bone defect (II)
Collagen, type I, alpha 1 (COL1A1)	Collagen and extracellular matrix organization	Membrane (IV)	Soft tissue (IV)	-
Fibroblast growth factor 2 (FGF-2)	Cell migration and recruitment, Angiogenesis	Membrane (II & IV)	Soft tissue (IV)	-

Forkhead box protein O1 (FOXO-1)	Apoptosis	Membrane (IV)	Soft tissue (IV)	-
Hypoxia-inducible factor 1-alpha (HIF-1α)	Angiogenesis	-	-	Bone defect (IV)
Interleukin-6 (IL-6)	Inflammation	Membrane (IV)	Soft tissue (IV)	Bone defect (II & IV)
Monocyte chemoattractant protein 1 (MCP-1)	Cell migration and recruitment	-	-	Bone defect (II)
Osteocalcin (OC)	Bone formation	Membrane (IV)	-	Bone defect (II & IV)
Osteoprotegerin (OPG)	Bone remodeling	-	-	Bone defect (II)
Receptor activator of NF-kappa B (RANK)	Bone remodeling	-	-	Bone defect (II)
Receptor activator of NF-kappa ligand (RANKL)	Bone remodeling	-	-	Bone defect (II)
Transforming growth factor-beta (TGF-β)	Inflammation, bone remodeling	Membrane (IV)	-	
Transforming growth factor-beta 1 (TGF-β1)	Inflammation, bone remodeling	-	-	Bone defect (II)
Tumor necrosis factor-alpha (TNF-α)	Inflammation	Membrane (IV)	Soft tissue (IV)	Bone defect (II & IV)
Vascular endothelial growth factor (VEGF)	Angiogenesis	Membrane (II & IV)	Soft tissue (IV)	-

Histology and Histomorphometry *(Study II & IV)*

Nondecalcified histology of the experimental sites was conducted in both studies to investigate the structure and morphology of the sham and membrane-covered defects, and comparisons were made among the different groups.

In Study II, eight (n = 8) bone defect sites at 6 and 28 days were allocated for histology and histomorphometry, whereas in Study IV, a total of 30 rats (15 at each time point) were assigned to these analytical techniques, resulting in n = 10 for each group.

In brief, the bone defect sites with and without the overlying membrane were harvested *en bloc*, fixed in formalin, dehydrated in ascending ethanol, and embedded in acrylic resin (LR White; London Resin Company Ltd., Berkshire, UK). Thin sections of approximately 10-20 µm were obtained following the cutting-grinding protocol previously described [146] using an Exakt System (EXAKT Apparatebau GmbH & Co, Norderstedt, Germany). All sections were stained with 1% toluidine blue and subsequently coded and evaluated blindly for histology and histomorphometry using an optical light microscope (Nikon Eclipse E600; Nikon Ltd., Tokyo, Japan) equipped with imaging and analytical software (NIS-Elements; Nikon). In Study IV, a total of ten samples were excluded from the analyses due to large artifacts, resulting in n = 8 for each group at 6 d, n = 10 for the e-PTFE group and n =8 for both the sham and d-PTFE groups at 28 d.

Histomorphometry was performed on each section using a 10× objective and a software grid projected on the defect where each grid square measured 0.8 × 0.8 mm (*Figure 7*).

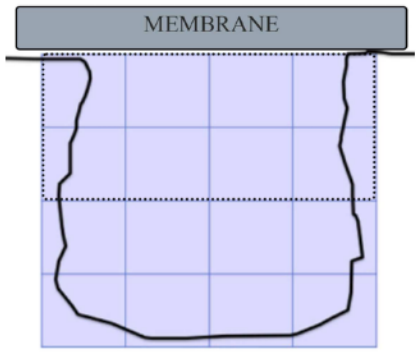

Figure 7. Schematic drawing of the experimental defect. The dotted line represents the region of interest (ROI) in Study IV, whereas the entire grid represents the ROI in Study II.

In Study II, the analysis was conducted on the total defect by dividing the defect area into different regions of interest (ROIs): top, middle, and bottom or central and peripheral regions. In Study IV, the ROIs were represented by the two upper zones of the grid. The area of newly formed bone was analyzed separately in every zone, and the area percentage of bone (%) was then calculated with respect to the total defect area or to the area of the respective ROI.

Immunohistochemistry *(Study II)*

Paraffin-embedded 3-5 µm thick sections were obtained, mounted on poly-L-lysine slides (Menzel GmbH and Co. KG, Braunschweig, Germany) and incubated with antibodies against cellular/molecular markers of interest, either primary rabbit anti-rat BMP-2 polyclonal antibody (18933-1-AP, Proteintech Group, Inc., USA) or primary rabbit anti-rat FGF-2 polyclonal antibody (ABIN1582147, antibodies-online GmbH, Germany). Negative controls were prepared by omission of the primary antibody and incubated with 1% BSA in PBS. The immunoreactivity of BMP-2 and FGF-2 was detected and visualized using goat anti-rabbit IgG secondary antibody with horseradish peroxidase (sc-2004, Santa Cruz Biotechnology, USA). All slides were evaluated qualitatively under light microscopy (Nikon Eclipse E600) using 20× and 40× objectives.

Western blot *(Study II)*

To detect specific protein molecules from the native and retrieved extracellular matrix membranes, the total protein concentration was first assessed using a BCA protein assay kit (Pierce, Thermo Scientific, USA), and then 50 µg from the protein extract of the membrane samples was prepared in Laemmli sample buffer (Bio–Rad Laboratories, Inc., California, USA). The protein molecules from the samples were separated according to their sizes using gel electrophoresis, and the separated protein bands were transferred from the gel to a blotting membrane (Bio-Rad Laboratories, Inc., California, USA). After blocking the nonspecific binding sites by rinsing the nitrocellulose membrane with Tris-buffered saline-Tween (TBST), the following primary antibodies were used to probe the blots: rabbit polyclonal anti-BMP-2 (18933-1-AP, Proteintech Group, Inc., USA) and rabbit polyclonal anti-FGF-2 (antibodies-online GmbH, Germany). After blot incubation and antibody dilution, band detection was performed using the Chemiluminescence with Clarity TM

Western ECL Substrate Detection kit (Bio-Rad Laboratories, Inc., California, USA), and the ChemiDoc XRS + system with Image Lab Software (Bio-Rad Laboratories, Inc., California, USA) was used for digital visualization.

3.3.4 STATISTICS

Statistical comparisons of the gene expression and histomorphometry results were performed using nonparametric tests. In Study II, Wilcoxon's signed-rank test was used to identify differences between the sham and membrane groups in a paired analysis. The Kruskal–Wallis and Mann–Whitney tests were used to determine statistically significant differences between the different groups at each time point (Study IV) as well as between the different time points for each experimental group (Studies II and IV).

Furthermore, Spearman's correlation analysis was applied in Study II between the expression of different genes in the defect, with and without membrane, as well as in the membrane and on the genes in the membrane versus the genes in the defect samples after 3 d, 6 d and 28 d (study II). In Study IV, Spearman's correlation analysis was performed between the molecular activities at the three structural levels of the experimental defect (soft tissue, membrane, and bone defect) with data pooled for the different groups and time points. Power calculation was performed for each method to obtain a minimum number of specimens for statistical analysis.

All statistical tests were conducted with SPSS software (SPSS, Inc., New York, USA). The significance level was set at 0.05 for the comparative analyses and at 0.01 for the correlative analyses.

3.3.5 ETHICAL APPROVAL

Both animal studies were approved by the Local Ethics Committee for Laboratory Animals at the University of Gothenburg (Dnr 279/2011).

4 RESULTS

4.1 CLINICAL STUDIES

4.1.1 STUDY I

The objective of this retrospective study was to evaluate the clinical and radiographical outcomes of GBR at single implants in the anterior upper jaw by measuring marginal bone levels from available periapical radiographs taken at different follow-ups and by assessing the inserted implants in terms of survival/success criteria and registered complications.

Overall, 74 patients were enrolled in the study and were followed for an average of 6.3 years. In 53% of the cases bone augmentation was performed together with implant placement (combined approach) whereas in the remaining 47% of the cases implant placement was planned few months after the regenerative procedure (staged approach). The staged approach was particularly chosen when large bone defects were present (*Figure 8*).

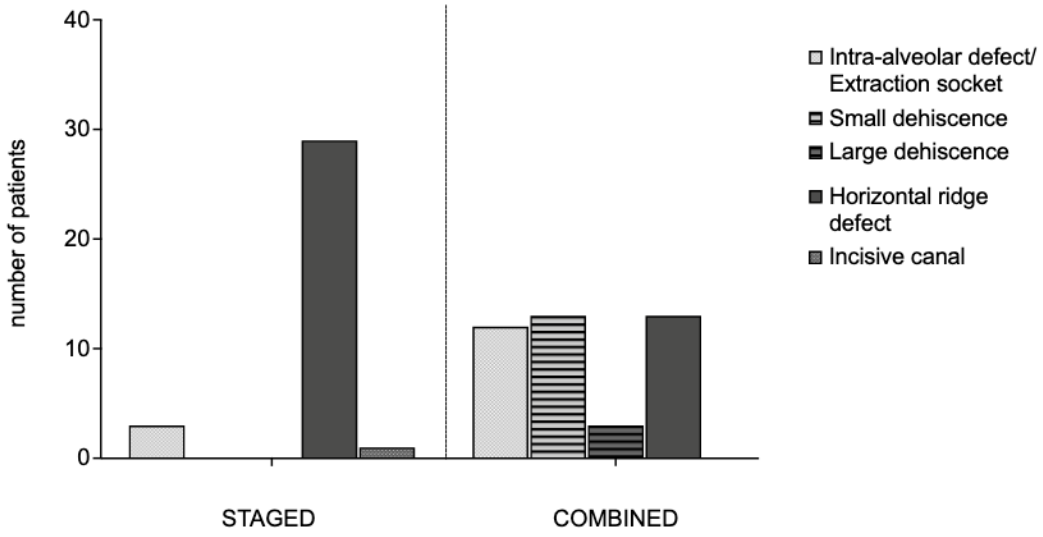

Figure 8. Number of patients treated with a combined or a staged approach in relation to the type of bone defects

None of the implants (98.6% Nobel Biocare™) were lost, and most of the cases revealed a marginal bone level in close relation to the first thread. Successful implants in regenerated bone imply a lack of clinical signs of pathology and stable marginal bone levels over the years to come. In the present sample population, biological and technical complications were registered in relation to the time of onset (*Figure 9*), and several implants showed marginal bone loss (≥ 3 threads) that disqualified them from being successful.

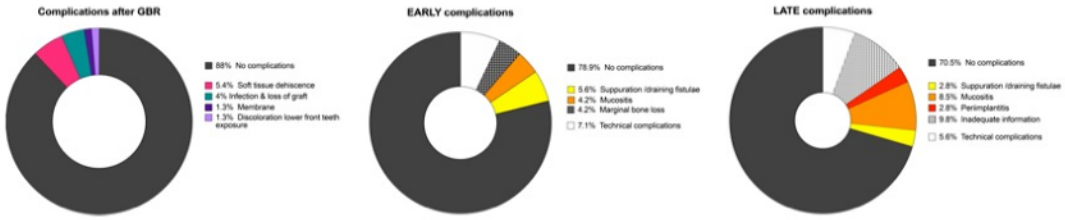

Figure 9. Percentage of single implants/patients with complications at different time points: immediately after GBR procedure, during the 1st year of functional loading (early complications), and at a later stage after the 1st year of function

Univariable statistical analysis revealed a significant association ($p < 0.05$) in marginal bone level changes at different time points for five of the fifteen tested variables: (1) type of bone defect, notably in relation to small peri-implant dehiscence, (2) combined approach GBR-implant placement, (3) short healing time between GBR and implant placement, and (4) early and (5) late complications.

4.1.2 STUDY III

Colony-Forming Units (CFU) counting

Biofilm formation on natural dentition and membranes revealed an increase in viable bacteria counts over time with no difference between test and control membranes between the early (4 h) and later (24 h) time points. While the

amount of viable aerobes and anaerobes was higher on the control tooth in contrast to the membrane groups at both 4 h and 24 h, the number of staphylococci showed a different type of growth: it was reduced on the tooth surfaces, and it increased on both test and control barriers over time displaying a significant difference ($p < 0.05$) in contrast to the tooth surfaces at 4 h for both membranes and 24 h for the test membranes (*Figure 10*).

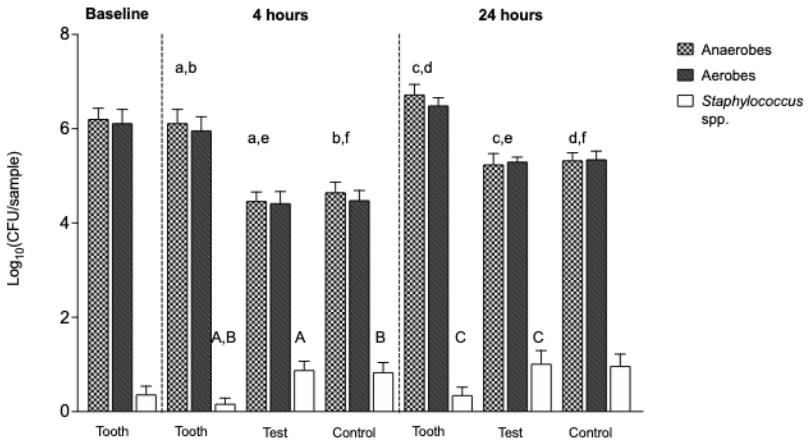

Figure 10. Colony-forming unit (CFU) counting on natural dentition, e-PTFE (test), and d-PTFE (control) membranes at baseline, 4 h and 24 h. Data represent means ± SEM. Bars that share the same letters are significantly different (p < 0.05).

Confocal Laser Scanning Microscopy (CLSM)

Quantitative image analysis of biofilm samples demonstrated that the amount of live and dead biomass and the average thickness were higher at 4 h on the control than on the test membranes ($p < 0.05$), whereas no difference was found at 24 h between the two membrane groups. Regarding the area occupied by bacterial cells at the first biofilm layer, there was no difference between the test and controls, while between the early (4 h) and late (24 h) time points, the amount of live biomass increased on the test membranes ($p < 0.05$), and the amount of dead biomass decreased on both membrane groups ($p < 0.05$). Finally, the surface area of live biomass was greater on the test membranes than on the control membranes at both time points ($p < 0.05$), but no differences could be detected for the dead biomass, despite an increase from 4 h to 24 h for both membrane groups (*Figure 11*).

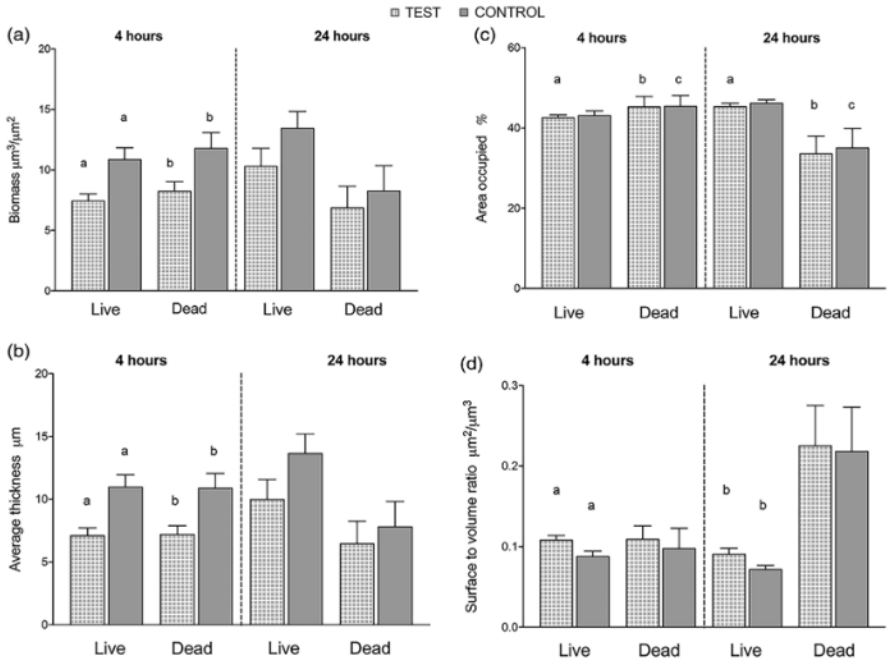

Figure 11. (a-d) Quantification of biofilm formation by CLSM by analyzing the following parameters: (a) biofilm biomass ($\mu m^3/\mu m^2$), average thickness (µm), (c) area occupied by the first biofilm layer (%) and (d) surface to volume ratio ($\mu m^2/\mu m^3$). Data represent means ± SEM. Bars that share the same letters are significantly different ($p < 0.05$)

(with permission from Wiley publ.)

Scanning Electron Microscopy (SEM)

Qualitative evaluation of dental plaque formation on PTFE membranes disclosed typical heterogeneous distributions of biofilms, initially (4 h) in sparsely populated monolayers and subsequently (24 h) in multilayered arrangements with no obvious differences between the test and controls. The most prevalent bacterial cell morphology was cocci, followed by bacilli and coccobacilli. Extracellular polymeric substances (EPSs) were also detected. Further interesting observations were represented by the absence of membrane damage due to the bonding system in areas where the surface was visible and

traces of mechanical manipulation during membrane retrieval and sample preparation (*Figure 12*).

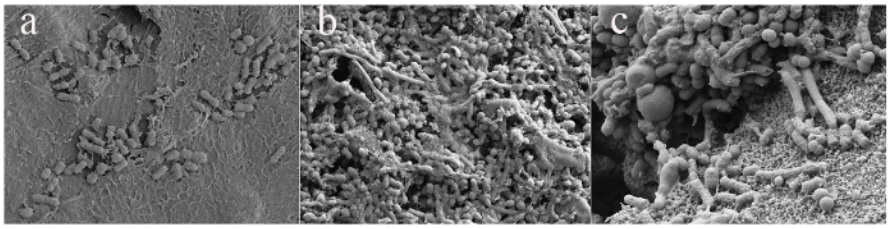

Figure 12. SEM images: (a) at 4 h, oral bacteria colonized the d-PTFE membrane in sparsely populated monolayers, leaving large areas of the membrane surface visible; (b) at 24 h, e-PTFE membranes were densely colonized; and (c) different bacterial cell morphologies were observed

(with permission from Wiley publ.)

4.2 EXPERIMENTAL STUDIES

4.2.1 STUDY II

Gene expression results and correlation analyses

The genetic expression profiles in the bone defect sites were linked to different biological processes: inflammation and cell recruitment, bone formation and resorption and coupling of bone remodeling:

1) TNF-α (*Figure 13A*): in the membrane defect, an upregulation of TNF-α from baseline to 3 days was followed by a significant reduction after 6 days and no major change afterward; the corresponding gene expression pattern in the sham defect was characterized by the absence of variation over time. Moreover, the expression level of this inflammatory marker was significantly higher in the membrane group than in the sham group at 3 days, while the opposite trend was observed at 6 days, and no difference between groups was detected at 28 days.
2) IL-6 (*Figure 13B*): in both membrane and sham defects, IL-6 was upregulated after 3 and 6 days and significantly downregulated from 6 to 28 days. A 10-fold increase in IL-6 was observed for both groups at 6 days compared to baseline, and a 2-fold significant upregulation was found in the membrane defect group than in the sham group at 28 days.
3) MCP-1 (*Figure 13C*): a substantial increase in MCP-1, a cell recruitment factor, was seen in the sham defect group (6-fold) and in the membrane defect group (14.5-fold) in comparison to baseline. Despite a downregulation in the membrane group compared to baseline, the MCP-1 expression levels stayed high at 6 days, followed by a decrease at 28 days for both groups. However, the expression of MCP-1 in the membrane group at 28 days was significantly higher than in the sham group.
4) CXCR4 (*Figure 13D*): compared to baseline, a significant downregulation of CXCR4 was detected at 3 and 6 days for both groups, followed by an upregulation, especially regarding the membrane group. When we compared the membrane and sham groups, the CXCR4 expression level

was significantly higher at 3 and 28 days, whereas no difference was observed at 6 days.

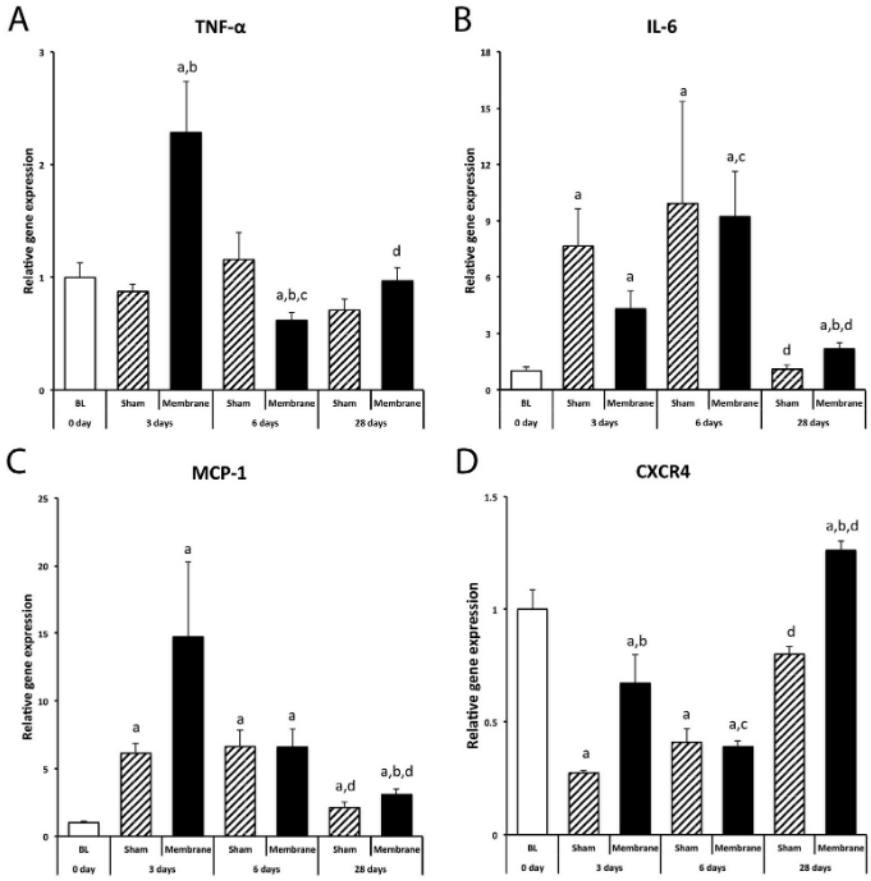

Figure 13. Gene expression of pro-inflammatory cytokines and cell recruitment chemokines. The results are presented as means ± SEM. Statistically significant differences are indicated by small letters: a indicates the significant difference with baseline (BL); b indicates the significant difference with sham; c indicates the significant difference between 3 d and 6 d; and d indicates the significant difference between 6 d and 28 d.

(with permission from Wiley publ.)

5) ALP (*Figure 14A*): for both defects, the expression of alkaline phosphatase was downregulated at 3 and 28 days and upregulated at 6 days in comparison to baseline values; no significant differences between sham and membrane groups could be detected at the three time points.
6) OC (*Figure 14B*): compared to baseline, the expression of osteocalcin was downregulated at 3 and 6 days for both types of defects and at 28 days only for the sham defect group, whereas a statistically significant upregulation was observed after 28 days in the membrane group. Furthermore, the expression of this bone formation marker was significantly higher in the membrane group than in the sham group at 3 and 28 days.
7) CR (*Figure 14C*): in the sham defect, the temporal expression level of calcitonin receptor remained lower than baseline values, whereas the corresponding pattern in the membrane defect was comparable to baseline. The comparative analysis at 3 days revealed higher expression levels of the osteoclastic surface marker in the membrane group than in the sham defect group.
8) CatK (*Figure 14D*): the temporal profile of the osteoclastic activity marker was characterized by lower levels for both groups at 3 days compared with the baseline, followed by an upregulation that reached statistical significance after 28 days in the membrane group. When comparing the sham and membrane groups, the CatK expression levels followed the same pattern as for CR, namely, a significant increase in the membrane group compared with the sham group, but only after 3 days.

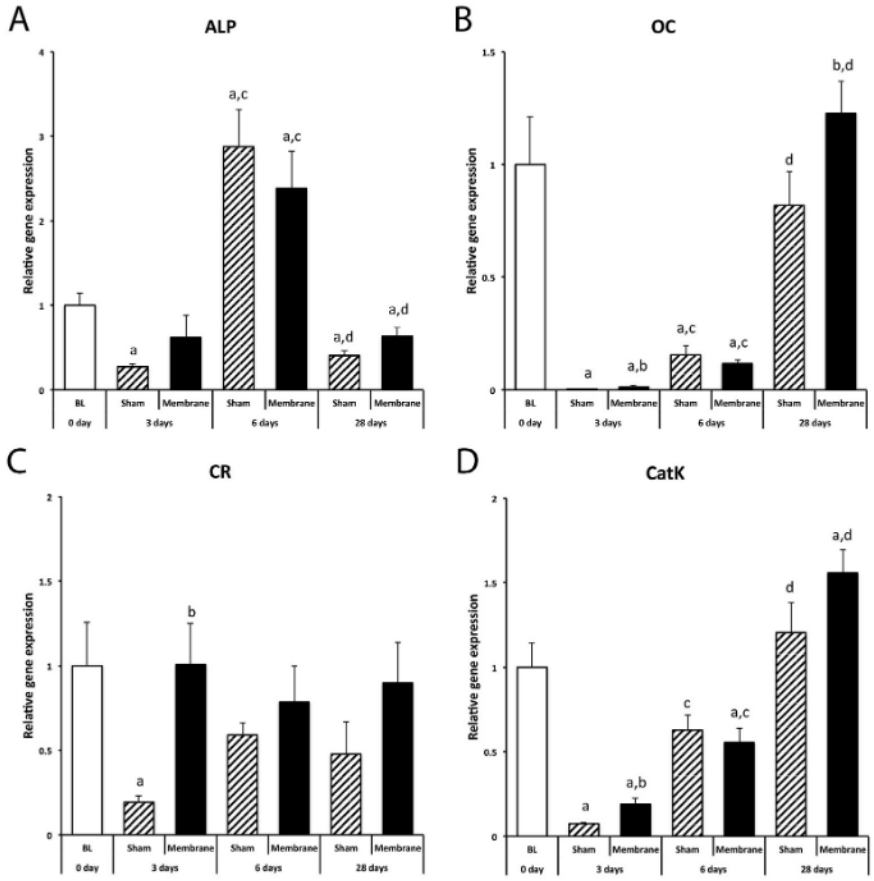

Figure 14. Gene expression of bone formation and resorption factors. The results are presented as means ± SEM. Statistically significant differences are indicated by small letters.: a indicates a significant difference with baseline (BL); b indicates a significant difference with sham; c indicates a significant difference between 3 d and 6 d; and d indicates a significant difference between 6 d and 28 d.

(with permission from Wiley publ.)

9) RANKL (*Figure 15A*): the temporal pattern of RANKL expression levels, compared to baseline, revealed a significant reduction in the sham group at 3 days, followed by a significant increase in both groups at 6 days. At 28 days, a downregulation to levels comparable to the baseline was observed for both the sham and membrane groups. When comparing the two groups, the RANKL profile was significantly higher in the membrane-treated defect group than in the sham group after 3 days. However, the opposite trend was found at 6 days, and at 28 days, no major differences were detected between groups.
10) RANK (*Figure 15B*): the expression of RANK was upregulated at 6 days and downregulated at 28 days compared to the baseline. The comparative analysis at 6 days revealed a significantly higher expression of RANK in the sham defect group than in the membrane-treated defect group. No major differences were found between the groups at 3 and 28 days.
11) OPG (*Figure 15C*): the expression profile of OPG at each time point and its temporal expression were similar to that observed for RANKL
12) RANKL/OPG (*Figure 15D*): no major temporal variations were detected for the RANKL/OPG expression ratio, and there were no major differences between the groups at any time point.

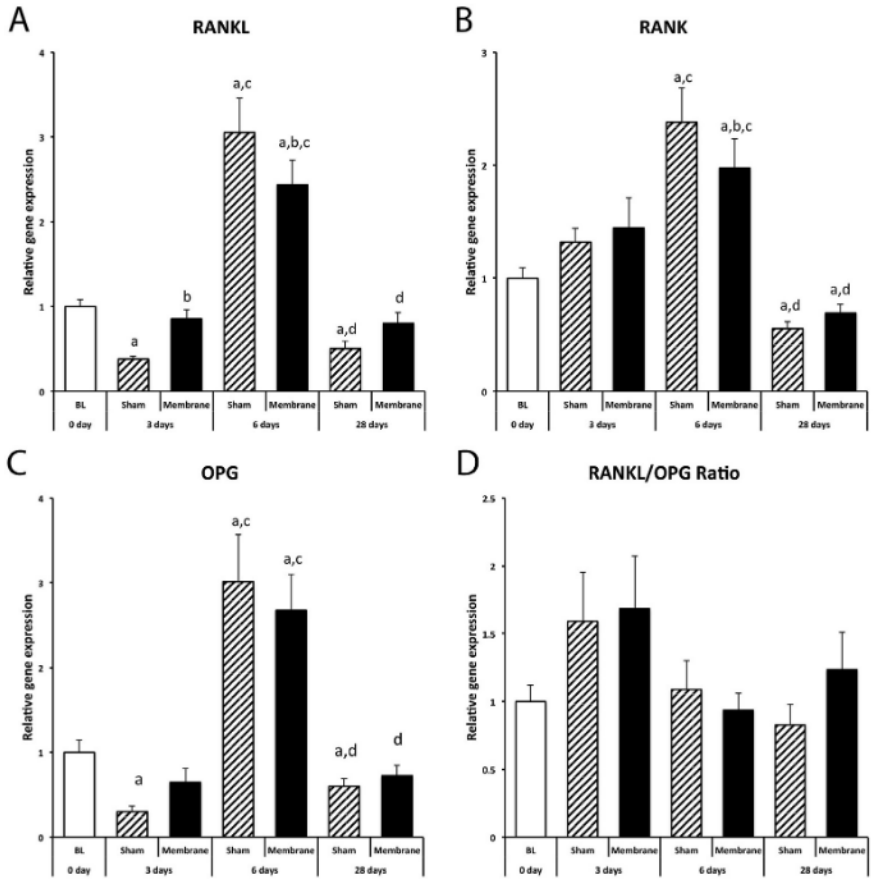

Figure 15. Gene expression of bone remodeling coupling factors. The results are presented as means ± SEM. Statistically significant differences are indicated by small letters: a indicates a significant difference with baseline (BL); b indicates a significant difference with sham; c indicates a significant difference between 3 d and 6 d; d indicates a significant difference between 6 d and 28 d.

(with permission from Wiley publ.)

The genetic expression profiles were also analyzed in the retrieved membrane at the different time points of the experiment but for fewer growth factors than those described in the bone defect (*Figure 16*):

1) BMP-2: At 3, 6 and 28 days, there was an increase in the expression levels of this growth factor in the collagen membrane without statistically significant differences between different time points.
2) FGF-2: The temporal expression was similar to that observed for BMP-2 but with statistically significant differences between different time points.
3) TGF-β1: The temporal expression was similar to that observed for BMP-2 and FGF-2 but with statistically significant differences between different time points.
4) VEGF: The highest expression profile was detected in the membrane at 3 days; thereafter, there was a steady and significant decrease at 6 and 28 days.

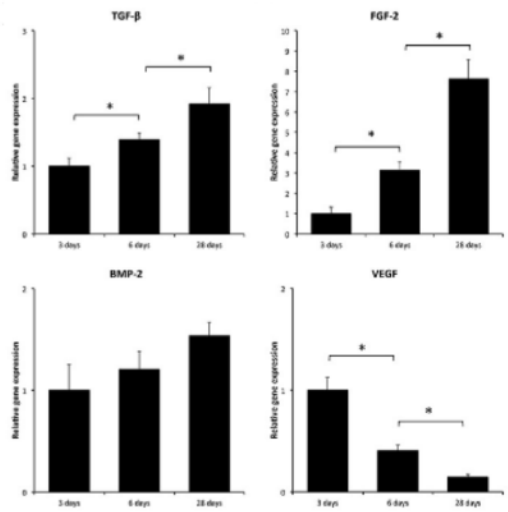

Figure 16. Gene expression of selected growth factors in the retrieved membrane after 3 d, 6 d and 28 d of healing. The results are presented as means ± SEM. Statistically significant differences between time points are indicated by asterisks.

(with permission from Wiley publ.)

Correlation analyses were performed for the different genes in the defect with and without the membrane (*Table 4*) and for the genes expressed in the membrane as well as between the genes in the membrane and in the underlying defects (*Table 5*). More specifically, among several positive correlations detected in the defect, it was observed that, at an early time-point of healing (3 d), the pro-inflammatory cytokine TNF-α was positively associated with the expression of the osteoclastic receptor gene CR, whereas at 28 days, the osteoblastic genes ALP and OC were found to have positive relationships both with one another and with the osteoclastic gene CatK. Additionally, the membrane compartment showed a significantly positive correlation between three out of four growth factors (TGF-β1, FGF-2 and BMP-2) and OC and CatK in the defect. In contrast, VEGF expressed in the membrane was negatively correlated with the same genes OC and CatK in the defect.

Table 4. Correlation analysis of genes expressed in the defect with and without the membrane. The data show genes that revealed significant correlations separately for each time period. Spearman correlation coefficients (r) and level of significance (p values) are presented. At 6 d, no significant correlations were detected, except for one positive correlation of ALP $_{defect}$/OPG $_{defect}$ (r = 0.73; p = 0.003) - (with permission from Wiley publ.)

3 days			**28 days**		
Genes	(r)	(p)	**Genes**	(r)	(p)
MCP-1$_{defect}$/ TNF-α$_{defect}$	0.86	0.007	CXCR4 $_{defect}$/OC $_{defect}$	0.80	0.001
MCP-1$_{defect}$/ CR $_{defect}$	0.88	0.004	CXCR4 $_{defect}$/CatK $_{defect}$	0.73	0.01
MCP-1$_{defect}$/ OPG $_{defect}$	0.93	0.001	CXCR4 $_{defect}$/RANKL $_{defect}$	0.75	0.002
CXCR4 $_{defect}$/OC $_{defect}$	0.86	0.007	ALP $_{defect}$/OC $_{defect}$	0.67	0.009
CXCR4 $_{defect}$/CatK $_{defect}$	0.83	0.01	ALP $_{defect}$/CatK $_{defect}$	0.75	0.002
TNF-α$_{defect}$/CR $_{defect}$	0.93	0.001	OC $_{defect}$/CatK $_{defect}$	0.70	0.005
OC $_{defect}$/ CatK $_{defect}$	0.88	0.004	OC $_{defect}$/RANKL $_{defect}$	0.74	0.003

			OC $_{defect}$/RANK $_{defect}$	0.80	0.0003
			CatK $_{defect}$/RANKL $_{defect}$	0.80	0.001
			CatK $_{defect}$/OPG $_{defect}$	0.80	0.001

Table 5. Correlation analysis of genes expressed in the retrieved membranes and the equivalent defect samples. The data show genes that revealed significant correlations by pooling the expression levels for all healing time periods (3 d, 6 d, 28 d). Spearman correlation coefficients (r) and level of significance (p values) are presented. - (with permission from Wiley publ.)

Correlations between genes in the membrane			**Correlation between genes in the membrane with genes in the equivalent defects**		
Genes	(r)	(p)	**Genes**	(r)	(p)
TGF-$\beta_{membrane}$/FGF-2 $_{membrane}$	0.80	0.00002	TGF-$\beta_{membrane}$/MCP-1$_{defect}$	-0.68	0.001
TGF-$\beta_{membrane}$/VEGF $_{membrane}$	-0.80	0.00008	TGF-$\beta_{membrane}$/OC $_{defect}$	0.83	0.00001
FGF-2$_{membrane}$/VEGF $_{membrane}$	-0.87	0.000002	TGF-$\beta_{membrane}$/CatK $_{defect}$	0.81	0.00002
			FGF-2$_{membrane}$/OC $_{defect}$	0.78	0.00009
			FGF-2$_{membrane}$/CatK $_{defect}$	0.77	0.00001
			VEGF $_{membrane}$/OC $_{defect}$	-0.80	0.00004
			VEGF $_{membrane}$/CatK $_{defect}$	-0.73	0.0004
			BMP-2 $_{membrane}$/OC $_{defect}$	0.76	0.0001
			BMP-2 $_{membrane}$/CatK $_{defect}$	0.59	0.008

Histology and Histomorphometry

On the light microscopy images of histological slides at 28 days, a "more scattered" less organized morphology of mature bone was detected in the sham defect group than in the membrane group, where a higher degree of restitution with sharp contour of newly formed bone at the top of the defect was also recognizable. In contrast, the sham group was characterized macroscopically (*Figure 17*) and histologically by soft tissue ingrowth inside the defect.

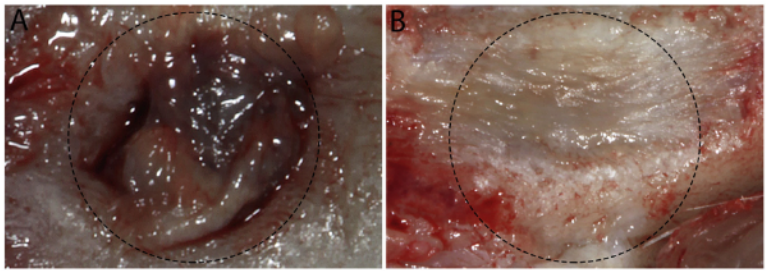

Figure 17. Macroscopic observations after 28 d of healing: (A) sham defect and (B) membrane defect - (with permission from Wiley publ.)

Histomorphometrical values of the defects were similar between groups at 6 days. In contrast, at 28 days, the percentage of total bone area and the volume of novel bone formation at the top and middle levels of the membrane-treated defects were significantly higher than those of the sham defects (*Figure 18*).

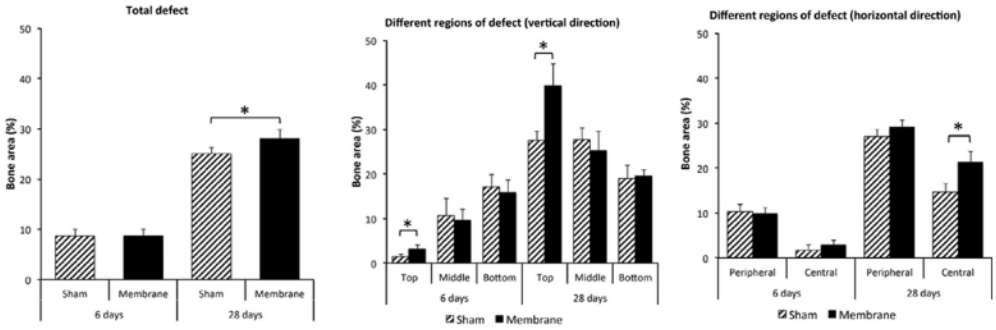

Figure 18. Histomorphometry analysis of bone formed in defects with and without the membrane. The column graphs show the bone area percentages after 6 d and 28 d. The results are presented as means ± SEM. Statistically significant differences are indicated by asterisks. – (with permission from Wiley publ.)

Regarding the main histological findings from the retrieved membrane (*Figure 19*), it was observed that, at 6 days, the collagen fibers of the membrane seemed to be more intact than at 28 days and were characterized by infiltrations with cells from different phenotypes, especially polymorphonuclear and monocyte-/macrophage-like cells. After 28 days of healing, monocyte or macrophage-like cells were observed. In addition, many osteoclast-like cells were observed in connection with resorption areas on the bone side at the boundary between the membrane and the newly formed bone.

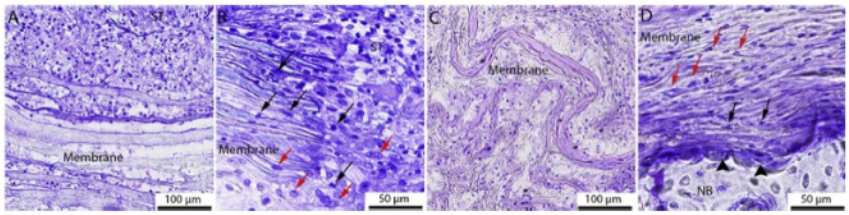

Figure 19. Ground sections of the membrane in place after 6 d (A and B) and 28 d (C and D) of healing. Cells with hematopoietic origin (monocyte-/macrophage-like cells) as well as with a mesenchymal origin are indicated by black and red arrows, respectively, at both 6 d and 28 d. – (with permission from Wiley publ.)

Immunohistochemistry and Western blotting

The presence of the selected growth factor proteins BMP-2 and FGF-2 was analyzed in the membrane compartment by Western blotting and immunohistochemistry, which were performed at all different stages of healing. Further, the presence of these proteins in the native membrane was analyzed.

Immunohistochemistry revealed the presence of both growth factors by demonstrating immunoreactivity inside the retrieved membrane at 3 and 6 days. Additionally, the blot revealed BMP-2 and FGF-2 bands from the retrieved membranes at 3, 6 and 28 days (*Figure 20*). FGF-2, but not BMP-2 protein was detected when Western Blot was applied on the native collagen membrane.

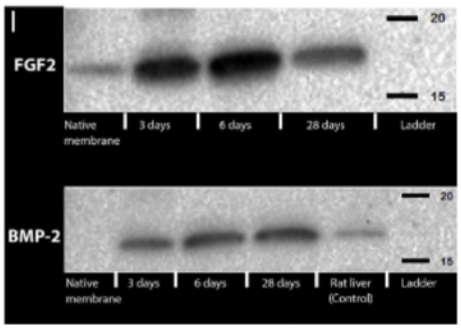

Figure 20. Western blot images showing the bands of FGF-2 and BMP-2 proteins detected on native (FGF-2) and retrieved membranes (FGF-2 and BMP-2). – (with permission from Wiley publ.)

4.2.2 STUDY IV

Gene expression results and correlation analysis

The genetic expression profiles linked to different biological healing phases were analyzed at the three structural levels of the experimental sites:

A. BONE DEFECT:

1) TNF-α (*Figure 21-a*): at the 6-day observation, no significant differences were observed among the three groups. After 28 days of healing, a pattern of downregulation of proinflammatory cytokines was detected, and the temporal expression was statistically significant from 6 d to 28 d for the two membrane-treated defects but not for the sham defects.
2) IL-6 (*Figure 21-b)*: at the 6-day observation, the sham group revealed a significant upregulation of IL-6 compared to the e-PTFE group, but no differences were detected at 28 days among the three groups. The temporal expression of IL-6 was characterized by a downregulation that was statistically significant from 6 d to 28 d for all three experimental groups.
3) BMP-2 (*Figure 21-c*): no major differences among groups and over time were found in the expression profile of BMP-2.
4) OC (*Figure 21-d*): the expression of this bone formation marker was found to be similar in the d-PTFE, e-PTFE, and sham groups at both time points. However, a significant downregulation of OC was detected from 6 d to 28 d for all three experimental groups.
5) CTR (*Figure 21-e*): the expression profile of this bone remodeling gene at both time points and its temporal expression over time were found to be highly similar to that observed for OC.
6) HIF-1*α* (*Figure 21-f*): the transcription factor HIF-1*α* was significantly upregulated in the sham defect at 6 d compared to the membrane groups; thereafter, at 28 d, no differences were observed among groups, and a pattern of downregulation over time was common for all experimental groups.

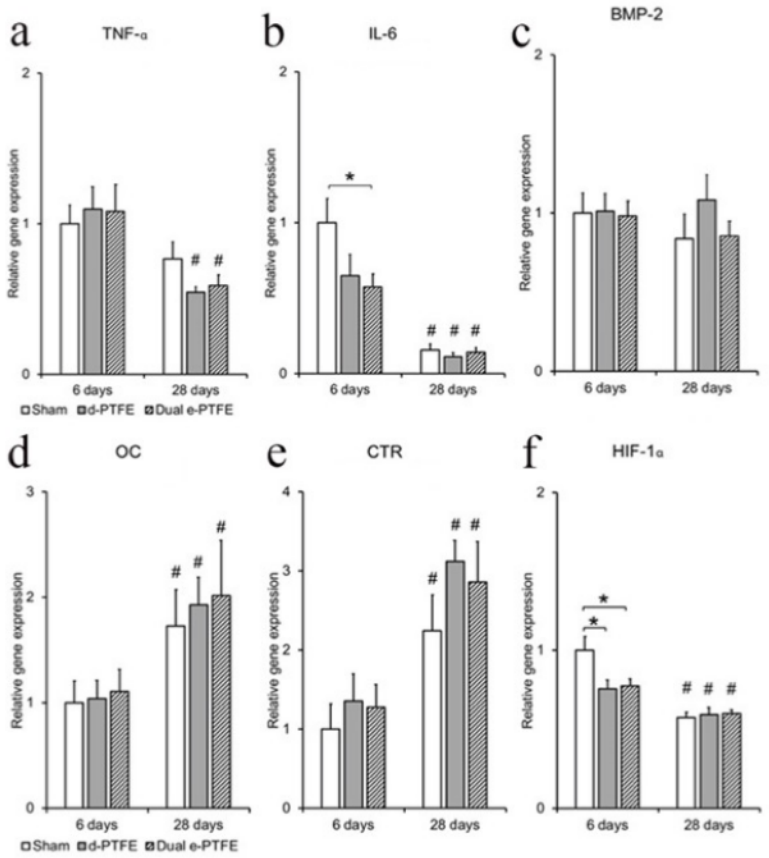

Figure 21. Gene expression profiles of the selected genes in the bone defect. The columns in the graphs show the mean and the standard error of the mean. Statistically significant differences ($p < 0.05$) are indicated by bars and asterisks (*) for differences between the experimental groups or hash signs (#) for differences between the two time points for each experimental group.

B. MEMBRANE:

1) TNF-α (*Figure 22-a*): the temporal expression of this proinflammatory cytokine was downregulated at 28 days in the cells adherent to the different membrane surfaces. Interestingly, the e-PTFE membrane significantly reduced the expression profile of TNF-α compared to d-PTFE after 28 days of healing.
2) IL-6 (*Figure 22-b*): from 6 d to 28 d, e-PTFE promoted a downregulation of the proinflammatory cytokine IL-6, while the opposite trend was detected for d-PTFE. When we compared the two membrane groups, the IL-6 gene profile was significantly lower on e-PTFE at 28 days.
3) BMP-2 (*Figure 22-c*): no major differences were found between groups at the 6-day observation time, and even the temporal expression of BMP-2 did not change on the d-PTFE. In contrast, the upregulation of BMP-2 observed in the cells adherent to the e-PTFE membrane was statistically significant when compared to the d-PTFE membrane at 28 days.
4) TGF-β (*Figure 22-d*): a downregulation over time on the e-PTFE membrane was the only statistically significant observation when we analyzed the gene expression of the growth factor TGF-β.
5) FGF-2 (*Figure 22-e*): the relative gene expression of fibroblast growth factor-2 was low and similar on both membranes after 6 days of healing. A significant increase was detected at the 28-day observation time, but only in cells associated with e-PTFE.
6) COL1A1 (*Figure 22-f*): the expression profile of bone formation factor collagen 1A1 and its temporal expression were similar to that observed for FGF-2.
7) ALP (*Figure 22-g*): a similar trend to that observed for COL1A1 was seen in the expression of the early osteogenic marker ALP and was found in the cells adherent to d-PTFE and e-PTFE, and this observed temporal upregulation was statistically significant only in cells associated with e-PTFE.
8) OC (*Figure 22-h*): a sharp and significant increase in expression from 6 d to 28 d was detected for the late

osteogenic differentiation marker osteocalcin in cells associated with both membrane types.

9) VEGF (*Figure 22-i*): although the relative gene expression in cells adherent to the d-PTFE membrane remained stable at 6 and 28 days, a significant temporal downregulation was found for the e-PTFE group. The lower expression of VEGF on e-PTFE led to a statistically significant difference between the two types of membranes at 28 days.
10) FOXO-1 (*Figure 22-j*): late and statistically significant upregulation of forkhead box-O transcription factor-1, especially in cells associated with e-PTFE, was identified.

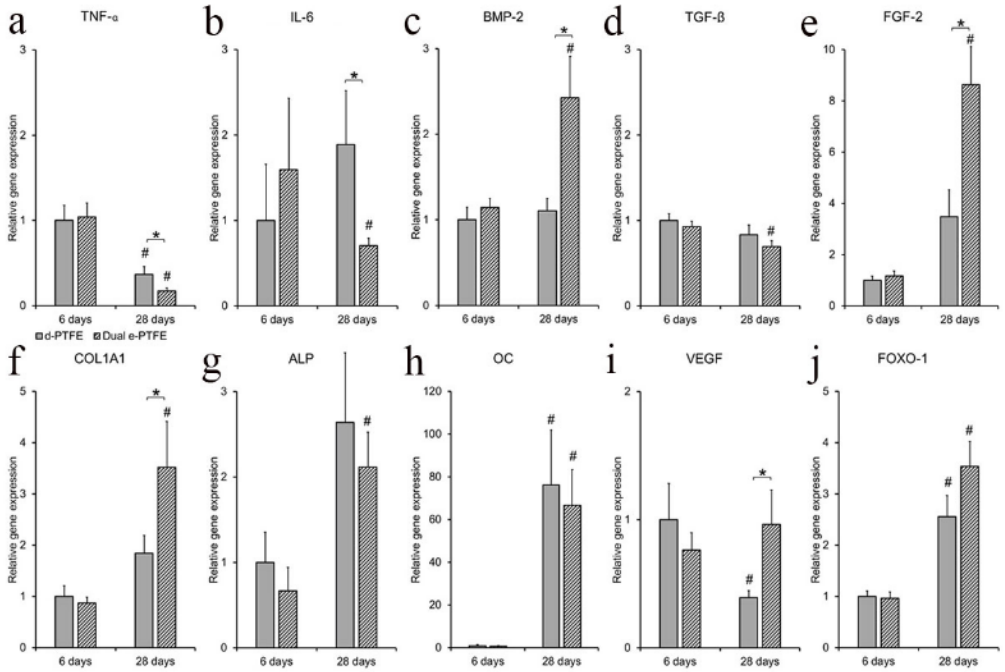

Figure 22. Gene expression profile of the selected genes in the membrane compartment. The columns in the graphs show the means and the standard error of the means. Statistically significant differences ($p < 0.05$) are indicated by bars and asterisks (*) for differences between the experimental groups or by hash signs (#) for differences between the two time points for each experimental group.

C. SOFT TISSUE:

1) TNF-α (*Figure 23-a*): at the 6-day observation, the soft tissue covering the e-PTFE membrane was characterized by a higher and statistically significant expression of the pro-inflammatory cytokine TNF-α compared with the soft tissue covering the sham defect or the d-PTFE membrane. After 28 days of healing, the opposite trend was observed, and TNF-α expression was lowest in the soft tissue covering the e-PTFE membrane.
2) IL-6 (*Figure 23-b*): a similar trend to that observed for TNF-α was observed for the relative gene expression of the proinflammatory cytokine IL-6; in this case, the only statistical significance was represented by the downregulation of IL-6 from 6 d to 28 d for all three groups.
3) BMP-2 (*Figure 23-c*): no major differences among groups were observed; a higher and statistically significant expression of BMP-2 was detected from 6 d to 28 d for all three groups.
4) FGF-2 (*Figure 23-d*): at a late stage of healing (28 d), the expression of the soft tissue proliferation marker FGF-2 was significantly upregulated in the tissue covering the e-PTFE membrane compared with the soft tissues covering either sham defects or the d-PTFE membrane; additionally, all experimental groups demonstrated an upregulation of FGF-2 in the soft tissue from 6 d to 28 d.
5) VEGF (*Figure 23-e*): the only statistically significant difference in the expression of vascular endothelial growth factor was found in the soft tissue covering the e-PTFE membrane at 28 days, which revealed a twofold increase compared to the other two groups.

6) FOXO1 (*Figure 23-f*): a similar trend to that observed for VEGF at 28 days and in the soft tissue covering the e-PTFE membrane was detected.

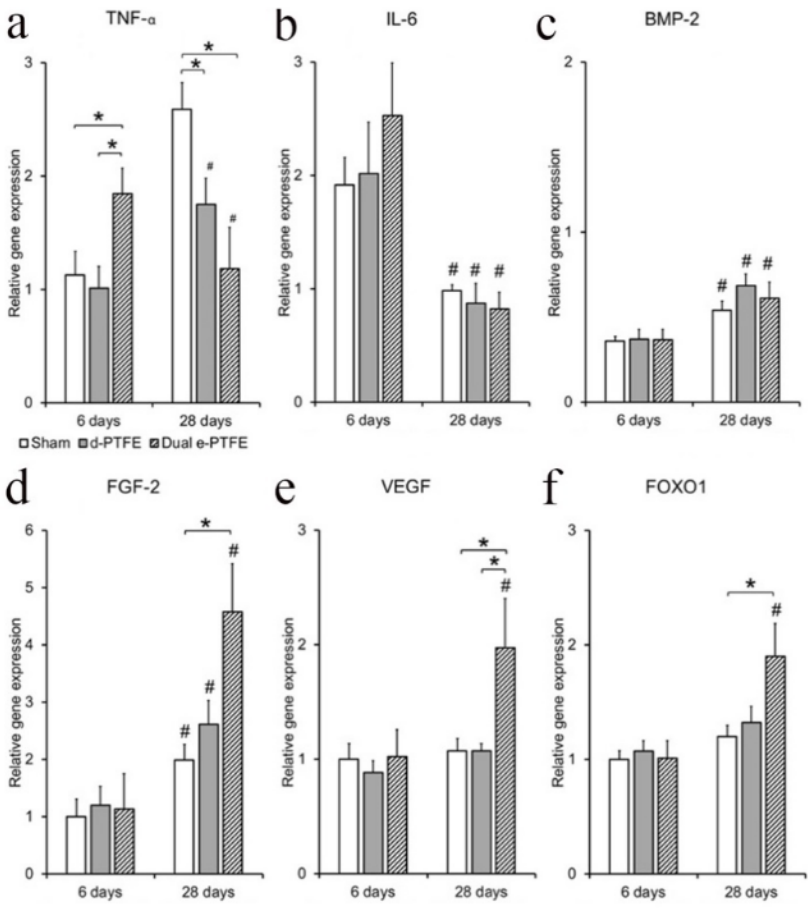

Figure 23. Gene expression profile of the selected genes in the soft tissue compartment. The column in the graphs show the mean and the standard error of the mean. Statistically significant differences ($p < 0.05$) are indicated by bars and asterisks (*) for differences between the experimental groups or by hash signs (#) for differences between the two time points for each experimental group.

By pooling data for the membrane groups and the two time points, a correlation analysis of the selected genes was utilized to evaluate the interactions among the different molecular activities during GBR in the three structural compartments of the experimental site (bone defect, membrane-associated cells, and soft tissue).

The analysis revealed that the highest number of positive and negative correlations (29) was detected between the membrane compartment and the overlying soft tissue, whereas the lowest number (3) was identified between the soft tissue above the membrane and the bone defect beneath the membrane. More distinctively, positive associations were found between the expression of growth factors (FGF- and BMP-2) and tissue regeneration markers (ALP, OC, COLL1A1) in the cells adherent to d- and e-PTFE membranes and the expression of growth and vascularization factors (FGF-2, BMP-2, VEGF) in the overlying soft tissue. Regarding the expression of proinflammatory cytokines (TNF-α and IL-6), their presence in the different compartments was often negatively associated with the expression of several genes. On the other hand, positive correlations were discovered between the expression of TNF-α and IL-6 in membrane-associated cells and the expression of the same proinflammatory cytokines in the bone defect (*Table 6*).

Table 6. Correlation analysis displaying the positive and negative correlations of gene expression between the different compartments (M = membrane; ST = soft tissue; D = bone defect) during GBR using PTFE membranes. The positive and negative correlation coefficients (r) and the significant p values (p) are provided.

Positive correlations	(r)	(p)	**Negative corr.**	(r)	(p)
BMP-2 $_{M}$ & FGF-2 $_{ST}$	0.4	0.008	FGF-2 $_{M}$ & IL-6 $_{ST}$	-0.5	0.0001
BMP-2 $_{M}$ & VEGF $_{ST}$	0.4	0.008	TGF-β $_{M}$ & FGF-2 $_{ST}$	-0.5	0.001
FGF-2 $_{M}$ & FGF-2 $_{ST}$	0.6	0.0001	TGF-β $_{M}$ & FOXO1 $_{ST}$	-0.4	0.004
FGF-2 $_{M}$ & VEGF $_{ST}$	0.5	0.002	TNF-α $_{M}$ & BMP-2 $_{ST}$	-0.5	0.002
FGF-2 $_{M}$ & FOXO1 $_{ST}$	0.4	0.006	TNF-α $_{M}$ & FGF-2 $_{ST}$	-0.7	0.0001
TGF-β $_{M}$ & IL-6 $_{ST}$	0.4	0.006	TNF-α $_{M}$ & VEGF $_{ST}$	-0.5	0.0001
TNF-α $_{M}$ & IL-6 $_{ST}$	0.7	0.0001	TNF-α $_{M}$ & FOXO1 $_{ST}$	-0.5	0.0001
ALP $_{M}$ & FGF-2 $_{ST}$	0.5	0.001	ALP $_{M}$ & IL-6 $_{ST}$	-0.4	0.006
ALP $_{M}$ & VEGF $_{ST}$	0.4	0.005	OC $_{M}$ & IL-6 $_{ST}$	-0.6	0.0001
OC $_{M}$ & BMP-2 $_{ST}$	0.5	0.002	FOXO1 $_{M}$ & IL-6 $_{ST}$	-0.5	0.0001

OC $_{M}$ & FGF-2 $_{ST}$	0.7	0.0001	COLL1A1 $_{M}$ & IL-6 $_{ST}$	-0.4	0.006
OC $_{M}$ & VEGF $_{ST}$	0.6	0.0001			
OC $_{M}$ & FOXO1 $_{ST}$	0.6	0.0001			
FOXO1 $_{M}$ & BMP-2 $_{ST}$	0.4	0.004			
FOXO1 $_{M}$ & FGF-2 $_{ST}$	0.6	0.0001			
FOXO1 $_{M}$ & VEGF $_{ST}$	0.6	0.0001			
COLL1A1 $_{M}$ & FGF-2 $_{ST}$	0.5	0.0001			
COLL1A1 $_{M}$ & VEGF $_{ST}$	0.5	0.001			
TNF-α $_{M}$ & TNF-α $_{D}$	0.4	0.007	BMP-2 $_{M}$ & HIF-1α $_{ST}$	-0.4	0.004
TNF-α $_{M}$ & IL-6 $_{D}$	0.7	0.0000001	FGF-2 $_{M}$ & TNF-α $_{D}$	-0.5	0.001
OC $_{M}$ & OC $_{D}$	0.4	0.008	FGF-2 $_{M}$ & IL-6 $_{D}$	-0.5	0.001
			ALP $_{M}$ & IL-6 $_{D}$	-0.5	0.002
			ALP $_{M}$ & HIF-1α $_{D}$	-0.5	0.001
			OC $_{M}$ & TNF-α $_{D}$	-0.5	0.003
			OC $_{M}$ & IL-6 $_{D}$	-0.7	0.00000001
			OC $_{M}$ & HIF-1α $_{D}$	-0.6	0.0001
			FOXO1 $_{M}$ & TNF-α $_{D}$	-0.5	0.001
			FOXO1 $_{M}$ & IL-6 $_{D}$	-0.7	0.000000001
			FOXO1 $_{M}$ & HIF-1α $_{D}$	-0.6	0.00001
			COLL1A1 $_{M}$ & IL-6 $_{D}$	-0.5	0.0002
IL-6 $_{D}$ & IL-6 $_{ST}$	0.5	0.001	IL-6 $_{D}$ & BMP-2 $_{ST}$	-0.6	0.00001
OC $_{D}$ & VEGF $_{ST}$	0.4	0.008			

Histology and Histomorphometry

The qualitative histological assessment of the different specimens after 28 days of healing revealed an increased amount of regeneration of the bone defects covered with either membrane type when compared to the sham defect, which conversely showed typical soft tissue downgrowth inside the top part of the experimental site. Notably, new bone formation was distinguishable at the bottom side of the membranes still covering the defects (*Figure 24*).

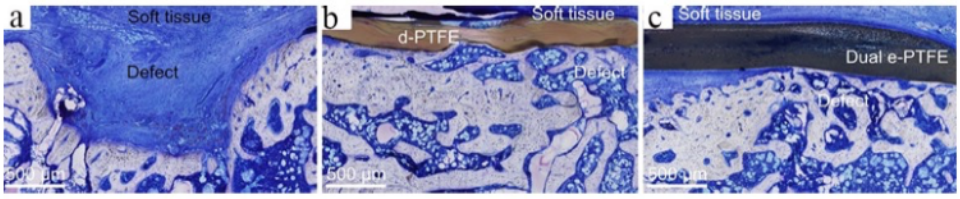

Figure 24. Histological assessment at 28 d of sham defect (a) and bone defects treated with either d-PTFE (b) or e-PTFE (c).

The histomorphometric measurements revealed significantly higher bone formation over time in both membrane groups at the central region of interest and more specifically at the top part of the central ROI. The comparative analysis of newly formed bone (%) showed that, after 28 days, only the top central ROI in the e-PTFE group had a significantly higher bone percentage than the bottom central ROI, whereas the opposite pattern was observed in the sham and d-PTFE groups after 6 days of healing (*Figure 25*).

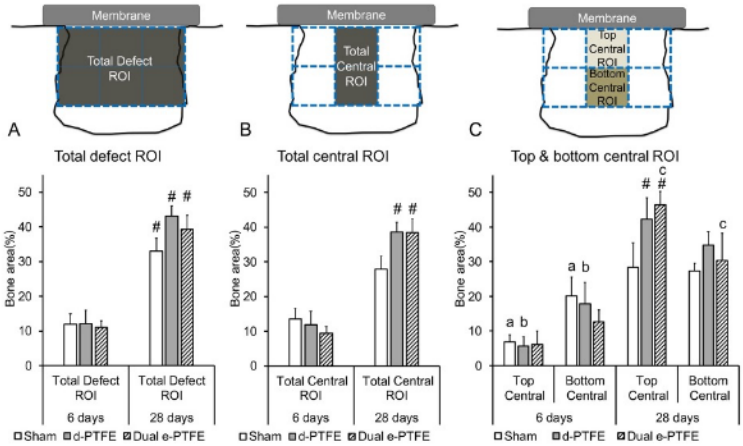

Figure 25. Histomorphometric analysis at 6 d and 28 d of experimental sites. The schematic illustrations show the region of interest (ROIs) and the corresponding histomorphometric findings. The columns in the graphs show the mean and the standard error of the mean of the percentage of new bone area formed in the ROI. Statistically significant differences ($p < 0.05$) are indicated by hash signs (#) for differences between the two time points for each experimental group or by small letters between the top and bottom ROIs for each experimental group.

5 DISCUSSION

In the current thesis, three studies (II, III & IV) explored *in vivo* and with different methodological assessments the biological mechanisms behind GBR and the potential active role of the barrier membranes.

Nonetheless, study I reported on the long-term outcome of implants placed in sites regenerated by GBR. This strategy was chosen to introduce the current clinical knowledge and background information about the topic.

5.1 GBR TREATMENT AND CLINICAL OBSERVATIONS

As aforementioned, GBR is considered as one of the most applied and best-documented bone regenerative technique to reconstruct deficient alveolar ridges and peri-implant bone deficiencies, including ridge preservation [6,93,147]. Currently, the method implies the use of a bone substitute material protected by a barrier membrane either of a biodegradable or a nonresorbable conformation prior to [148] or simultaneous with [149] implant placement.

For all patients included in study I, the GBR technique consisted of grafting with a particulate deproteinized bovine bone mineral (BioOss®, Geistlich Pharma AG, Wolhusen, Switzerland), autogenous bone or a mixture of the two, and the recipient defect was then covered with a native biodegradable collagen barrier (BioGide ®, Geistlich Pharma AG, Wolhusen, Switzerland), except for one case where no membrane was used. The cohort study was designed as a long-term retrospective evaluation of single implants placed simultaneously with, or after, GBR in the anterior area of the maxilla.

The high survival rate (100%) of implants, defined as implants remaining *in situ* at the follow-up examinations, was consistent with literature data [150-154]. Originally, 175 consecutively treated patients were identified. A total of 74 patients fulfilled the inclusion criteria including a 5-year follow-up period. The high number of dropouts could be explained by the relatively young age of the patient group. Hence, demonstrating a higher social mobility due to studies, work etc. Furthermore, the follow-up program was not mandatory for the patients, instead it was offered to the patients as part of the clinic's unique follow-up and subsequent database. Nevertheless, the main purpose of study I

was to report on the long-term stability of the regenerated bone in relation to several clinical variables.

The clinical decision regarding the optimal bone augmentation protocol was primarily based on the defect morphology [93] and, quite unexpectedly, well-contained bone defects exhibited significant marginal bone loss in comparison to larger augmented defects. In another retrospective study, implants with dehiscences and fenestrations were treated with GBR and were evaluated after 3 years [155]. The mean peri-implant marginal bone loss was slightly higher for the test implants placed in grafted bone as compared to control implants surrounded by pristine bone (0.54 ± 0.26mm for the and 0.43 ± 0.22mm, respectively), but no significance emerged between groups, and the results were in agreement with the current literature [98,156,157]. Prior research focused on the radiographical marginal bone level to estimate the outcome of the combined GBR-implant approach in dehiscence and fenestration defects. A resorbable membrane alone [158] or a combination of different barrier membranes and deproteinized bovine bone mineral [159] were used. Noteworthy, in both studies less marginal bone loss was observed at the pristine control sites than at the GBR treated defects at 24- and 59-months following loading, even though in Mayfield and co-workers [158] this difference did not reach statistical significance.

The assessment from conventional periapical radiography of bone levels around implants with reconstructed buccal defects represents a professional challenge [160,161]. Three-dimensional tomography (CBCT) has exhibited compelling advantages in the radiographical analysis of the buccal sites [162], although radiation burden does not always justify its use [163]. In one study, implants placed immediately in extraction sockets in combination with a GBR procedure were radiographically evaluated using CBCT [164]. At the 7-year follow-up, almost one-third of the implants presented with no buccal bone. This finding was confirmed by a 10-year investigation, in which one fourth of the GBR implants revealed absence of buccal bone on the CBCTs [165]. Several authors have advised on the importance of performing exceedingly horizontal augmentation with over addition of 2-4mm or more to obtain stable outcomes by supplementing the natural bone remodeling that occurs around the implants [166-168]. However, in our study like in Benic and co-workers [164], no attempt to over-augment the buccal bone plate in case of minor defects was made, and this technical detail might have been one of the factors that has jeopardized the long-term results of marginal bone levels. More specifically, when using only particulate bone and resorbable collagen membranes, compromised regeneration may occur [169,170]. Some authors have suggested that due to their poor mechanical properties [81], collagen membranes may collapse in the

presence of compressive forces from the lips, tongue and gingiva, with a subsequent downward displacement of the grafting material immediately after flap closure [171] or during the healing period [170].

Despite the paucity of research examining the long-term follow-up of implants placed with GBR procedures [149,172], it has been reported that staged and combined GBR-implant approaches in the upper anterior jaw related with high implant success and survival rates, but the level of evidence was better for the staged approach than for the combined technique [173]. In a multicenter prospective clinical trial on 19 consecutive patients with 20 dehiscences and 6 fenestrations, augmentation was performed with a combined approach using non-resorbable barrier membranes combined with either autogenous bone or bone allograft [174]. After five years, the mean marginal bone loss was 2.03 ± 0.5mm. Conversely, a prospective case series study on 20 patients reported a bone loss of 0.44 ± 0.24mm after 6 years at implants that received simultaneous GBR with autogenous chips, deproteinized bovine bone and a biodegradable barrier in post-extraction single-tooth gaps in the anterior maxilla [175]. Furthermore, the CBCT examination revealed a mean thickness of the buccal bone between 1.05 and 1.96mm at different levels. In Study I, radiographic changes in terms of crestal bone loss appeared to occur at a greater rate when the simultaneous surgical procedure was chosen. The clinical significance of this observation though is not fully understood and does not necessarily support any conclusions regarding the marginal bone level changes in the simultaneously regenerated sites as compared to defects augmented via a staged approach. In terms of reported peri-implant clinical outcomes, it has been shown that both these surgical interventions resulted in low bleeding on probing values over time and no major differences regarding probing pocket depth, plaque level changes and marginal bone level [176-179]. As opposed to relatively small, well controlled, prospective efficacy studies [172], a recent large retrospective effectiveness study on 1007 patients who were provided with 3082 implants [133], reported a correlation between grafting procedures and higher risk for early inflammation at the implants.

Nowadays, with an increasing knowledge and understanding on the onset and consequences of peri-implant diseases [134,136,138,180,181], it is essential to evaluate the influence of the various surgical techniques including augmentation procedures on the peri-implant tissue health and the incidence of biological complications at short- and long-term. Despite the difficulty in accurately reporting on the data of the clinical follow-ups due to the retrospective nature of Study I, univariable statistical analysis showed a significant association between the presence of early and late complications and marginal bone level changes at different time points. Interestingly, in the present study GBR and

single implant treatment were performed to a great extent in young adults. In contrast to older patients, the challenge with younger patient populations is that implants are expected to remain free from hard or soft tissue complications for a substantially longer period [182]. For correct data interpretation, it should be kept in mind that the included patients were treated in a specialist clinic focused on implant and prosthodontic treatments, and afterwards the referring dentist became responsible for the supportive therapy program [183]. These aspects may increase the generalizability of the reported clinical and radiographical outcomes in the clinical practice. Differently, the biological complications that occurred at sites immediately after GBR did not result in significantly more marginal bone loss over the years, although it has been shown that early events during the healing period following augmentation may have an impact on the regenerative outcome. The onset of early signs of infection following GBR resulted in only 42% to 62% bone regeneration at the treated site [184]. In two recent systematic reviews, it was shown that 27% better defect restitution was achieved when membrane was not exposed [103], and that the weighted mean incidence of soft tissue complications was not different between resorbable and non-resorbable membranes (18.3% vs. 17.6%) [118].

Limits of Study I could be related to its retrospective design. However, the advantage of the present study is that it represents a group of patients extracted from routine daily practice and hence is a good test of the robustness of the actual treatment methods. Bone augmentation procedures in relation to defect morphology were not randomly allocated but applied after clinical assessment by individual surgeons, and heterogeneity existed in terms of type and size of bone deficiencies as well as bone grafting materials used for GBR. In addition, missing data due to poor registration quality or due to variables that were not considered to be adequately registered in advance may have led to information bias. Another methodological shortcoming was that the hard tissue changes were measured only two-dimensionally using intraoral radiographs that were not standardized. These facts together with a relatively small sample population are limitations, which must be considered when translating the findings of the study.

Various lines of evidence have demonstrated that GBR has been mastered to predictably regenerate enough bone for successful implant placement [6,93,148,149,153]. Clinical variables including the amount and width of the overlying soft tissue, flap thickness, flap tension, soft tissue biotype, type and size of the underlying bone defects, membrane and bone graft material selection, and clinical experience have all been studied and enhanced over the years, but they could still represent potential factors to failures and complications [118]. Bone regeneration is a complicated physiological process, reliant upon blood supply,

inflammation, and the formation of fibrous tissue and bony callus, which are promoted by both local and recruited cells [185]. Hence, an improved knowledge of the cellular and molecular events that orchestrate the sequence of biological events when a barrier membrane is interposed between the soft and bone tissue compartments [83] is advisable to further enhance and render even more predictable GBR procedures in different clinical applications.

5.2 THE ROLE OF GBR MEMBRANES

To best determine the mechanisms that regulate guided bone neogenesis during wound repair and regeneration, the use of preclinical model studies is an important component in the process of bridging the discovery research to the clinic. The wound healing and bone regenerative principles were carefully considered by employing the rat model, where small bone defects were created in each femoral epiphysis. Historically, experimental research has been conducted using defect models comprising so called "critical size defects" which will not heal spontaneously during the lifetime of the animals. Lately this concept has been re-defined to be expressed as “will not heal spontaneously during the duration of the experiment” [186]. The advantage of this is that it offers an opportunity to use smaller size defects which from an animal ethics standpoint is beneficial. It is also convenient since mechanisms-related studies usually focus on the early healing phase.

5.2.1 RESORBABLE MEMBRANES

The results of Study II indicated that an extracellular matrix-derived collagen membrane was capable of fostering bone healing through the creation of a microenvironment that favored strong crosstalk between the immune system and the skeletal system [62,64]. To initiate a bone remodeling cycle in response to tissue damage, it has been suggested that osteocytes might recognize that a specific area of bone needs to be replaced, and subsequent signals through their canaliculi might result in the release of chemokines that attract vascular elements, osteoclast precursor and bone-forming cells [38]. In Study II, an early upregulation at 3 days in defects covered with membrane of two major cell-recruitment factors MCP-1 and CXCR4 corresponded to enhanced chemotactic cues, resulting in the recruitment of monocytes and osteoclast precursors [187,188] as well as leukocytes, mesenchymal stem cells and osteoprogenitor cells [189-192]. This assumption was based on the concomitant

early upregulation of genes encoding for inflammatory cells, osteoblastic and osteoclastic phenotypes. However, the increase in MCP-1 and CXCR4 may also be interpreted as an attempt to negatively influence the outcome of the material-tissue interaction. In fact, the histological finding of giant multinucleated and osteoclast-like cells in the area immediately underneath the membrane could be related to the degradation process of the membrane, in line with earlier studies [193,194].

The evaluation of micro-environmental changes brought about the collagen-based membrane when compared to sham defects revealed a strong upregulation of the inflammatory cytokine TNF-α, with an early peak at day 3 followed by a decrease at day 6 and a second peak at day 28. Tumor necrosis factor- α is a product of the immune system secreted by macrophages and is one of the most versatile cytokines capable to impact the recruitment of mesenchymal stem cells and osteoprogenitors [195,196] and to stimulate intra-membranous bone formation [197]. More specifically, the second spike in TNF-α expression may be linked to osteoclastic remodeling [198]. The classical mechanism of bone remodeling is that matrix-derived signals act directly on osteoclasts [199], and couple bone resorption to bone formation by activating osteoblasts [200]. Notably, the strict coordination between the bone formation component of remodeling and bone resorption is referred to as "coupling" [38]. It has been reported that various molecules that are expressed and produced by osteoclasts such as sphingosine-1-phosphate (S1P) [201], ephrinA2 [202], ephrinB2 [203], semaphorin 4D [40], Wnt10b [204], platelet-derived growth factor-BB [205], collagen triple-helix repeat-containing 1 (Chtrc1) [206], C3a [207], and CatK [208] are instrumental for the coupling mechanism. Furthermore, it has been shown that the osteoclast differentiation factor RANKL signal triggers osteoblastic bone formation [209,210]. An essential cytokine for osteoclastogenesis is RANKL, which is expressed by osteoblasts, and is recognized and bound to its receptor RANK on the surface of osteoclast precursors. The RANKL-RANK intercommunication initiates signals [20] that are responsible for the differentiation, fusion, maturation, survival, and activation of osteoclasts [45,211]. Osteoprotegerin is a regulatory receptor, mainly secreted by osteoblasts, which inhibits osteoclast formation and bone resorption by interfering with the RANKL-RANK signaling. With regard to RANK-RANKL pathway, it has been reported that TNF-α triggers osteoclastogenesis by increasing RANKL and M-CSF in marrow stromal cells [212,213] and osteoblasts [214]. More recently, it has also found that TNF-α directly affects osteocyte RANKL expression [215]. Based on the correlation analysis in Study II, the pro-osteoclastic role of TNF-α was partially supported by the positive interrelationship with the osteoclastic receptor (CR) at the initial phase of healing. In that matter, another interesting observation was the detection of early upregulation of several bone formation

and bone-remodeling genes (CR, OC, CatK, RANKL) in the defect beneath the membrane compared to the gene expression in the untreated sham defect. The present evidence at the molecular level of the coupled bone remodeling activities induced by the collagen membrane was confirmed by the histological and histomorphometrical findings that disclosed increased bone formation at the top and central regions of the membrane-covered defects as compared to the sham group. Our results agree with a considerable number of histological studies, demonstrating consistent bone regeneration in defects treated with various configurations of resorbable membranes [83,216-218].

The placement of a collagen membrane as implanted biomaterial triggers a cascade of events that starts with the competitive adsorption of proteins, blood clot formation and inflammation [62]. Although this cascade of events is unspecific and occurs at any biomaterial implantation, the final result of the material-tissue interaction depends on the physicochemical properties of the materials, which can modulate the recruitment of different immune cells [64]. Among the plethora of cells involved in this highly coordinated response, macrophages seem to exert the most influence on the tissue healing process [57]. It has been shown that the extracellular matrix (ECM)-derived collagen membrane could modulate the macrophage transition from a pro-inflammatory (macrophage M1) to an anti-inflammatory phenotype (macrophage M2), thus allowing for a functional tissue repair [219,220]. Differently, recent studies by Sun and co-workers [221-223] revealed that the bone regeneration induced by the ECM-derived collagen membrane was noticeable but poor and relatively delayed as compared to modified versions of the native membrane. In Study II, this membrane was selected due its excellent biocompatibility, inherited three-dimensional porous structure that might stimulate the binding, migration, and activation of cells with different phenotypes, and bioactivity which results from naturally retained biochemical cues such as fibronectin, glycosaminoglycans and diverse growth factors (VEGF, FGF-2, TGF-β, IGF-1) [224-227]. Generally, the different characteristics of the ECM-derived collagenous barrier made it more bio-competent and therefore more attractive than single-component gel membranes such as collagen [228]. However, its biological performance during the constitutive phases of GBR was beyond expectations since data from the different analytical techniques employed, suggested that another important growth factor, BMP-2, might also be found and preserved in the collagenous membrane after *de novo* expression by cells that were recruited in the membrane compartment. BMP-2 is a member of the TGF-β superfamily, and a potent inducer of osteogenesis [229]. FGF-2 has been recognized to elicit the migration and proliferation of endothelial cells as well as fibroblasts and osteoblasts [230,231]. Moreover, these factors trigger osteoclast activity, directly or indirectly by enhanced angiogenesis and osteogenesis [232-

[234]. The correlation analysis, performed by pooling the expression levels for all experimental time-points, revealed robust interplay between the pro-osteogenic growth factors expressed in the membrane with the bone related genes within the underlying defect. Taken together, the present results suggested an active role for this specific membrane during GBR. Its immunomodulatory actions might be the result of favorable biological and physicochemical properties that allow the inward migration of cells, which acquire specific phenotypes and rapidly trigger angiogenesis and osteogenesis in the bone defect. It is noteworthy to mention that previous research, based on histochemical evaluations, confirmed that another type of collagenous membrane could actively participate in osteogenesis serving as a scaffold for migrating cells and bone matrix proteins [235].

5.2.2 NONRESORBABLE MEMBRANES

Cellular and molecular healing events in the bone compartment:

As observed with naturally derived collagen resorbable membranes, PTFE non-resorbable membranes with different surface configurations promote an increase activity of genes associated with bone formation (OC) and bone remodeling (CTR) in trabecular bone defects. Although the expression of osteogenic genes was not significantly higher when compared to the untreated sham defects, the histological data from Study IV revealed a superior structural restitution of bone at the upper portion of the membrane-covered defects. These findings are in line with previous observations that reported higher percentage of new bone in the secluded compartment underneath a membrane than in sham defects [236]. An experimental study investigated the expression of OC, VEGF and core-binding factor alpha-1 (cbfa-1), that is known as transcriptional activator of osteoblast differentiation [15], in rat tibia defects during GBR with e-PTFE membrane in comparison to uncovered defects [237]. A higher ratio of cbfa-1 positive cells was detected in the upper portion of the defects in the experimental groups after 6 days. At a later stage of healing (8 and 10 days), the bone-related gene osteocalcin increased significantly with time in the underlying membrane-covered defect compared to its expression in the sham defect. Another study documented the expression of genes and signaling pathways modulating the healing dynamics following GBR procedure in calvarial critical size defects [238]. Despite no control group was included and no histological analysis was performed, the results indicated that several genes, that may have an important role in regulating osteogenesis, were temporally expressed at different healing stages in the defect under the PTFE

membrane. Interestingly, the immune and inflammatory responses were distinctly upregulated after 7 days, together with a positive regulation of the canonical Wnt pathway, which is known to play a crucial role in skeletal development, osteoblast differentiation and bone formation [239]. In a clinical study, where the molecular mechanisms of the periodontal wound-healing process were investigated, thirty patients with deep infrabony defects around teeth were selected and treated either by flap surgery alone (control group) or by guided tissue regeneration (GTR) with a non-resorbable e-PTFE membrane (test group) [240]. Molecular regulators of bone metabolism, including alkaline phosphatase, osteopontin, osteoprotegerin and RANKL, were upregulated in the test group at the end of the study. Furthermore, higher expressions of genes associated with the inflammatory response were reported to induce osteoclastogenesis by modulating RANKL expression [241], such as IL-1 and IL-6, and were also found in membrane-covered healing defects as compared to nonprotected surgical periodontal healing sites.

Cellular and molecular healing events in the membrane compartment:

Complexity of wound-healing response after GBR involves the interaction of distinct tissues with the interposed barrier membrane and diversity in the activities of cells. Data from Study IV investigating PTFE-associated cells revealed that the membrane surfaces became populated with cells that exhibit regenerative capability and forward inflammatory signals. Nevertheless, differences in the modulation of various genes were observed between d-PTFE and e-PTFE membranes, exclusively at a late time-point (28 days). For example, the temporal expression of TNF-α was significantly downregulated regardless of membrane type, while the downregulation of IL-6 was detected only in the cells associated with the dual e-PTFE. Notably, the expression of both pro-inflammatory cytokines was significantly lower in the cells adherent to the dual e-PTFE than to the d-PTFE membrane. The inflammatory response is a decisive step of the healing process when biomaterials are surgically inserted in the body, and the level of this response relies on the material of choice and the location of implantation [56,242]. The host-guest interaction attracts macrophages as key elements [243], which have been shown to release both pro-inflammatory and anti-inflammatory cytokines depending on the material properties such as surface topography and/or surface chemistry [244-246]. It is believed that the successful clinical application of a biomaterial is characterized by an anti-inflammatory macrophage (M2) polarization to promote tissue remodeling response, inhibit fibrous encapsulation, and improve the integration with the surrounding tissue [194,247]. It has been demonstrated that TNF-α and IL-6 persistence is detrimental for regeneration and repair, culminating in redundant and chronic inflammation [242,248-250]. More

specifically, it has been shown that the topographical features of PTFE greatly affect the type and number of cytokines released by the macrophages in a time dependent manner and can be a crucial variable for the FBGCs formation [60,68,251-253]. In a recent study, the response of macrophages to different structures of PTFE (flat, expanded, and electrospun) was investigated [246]. The electrospun PTFE with continuously running fibers and the highest surface roughness was characterized by the least adhesion and activation of macrophages, coupled with the lowest secretion level of TNF-α. The authors speculated that, since the macrophages are typically 3-20μm in size and the diameter of the fibers in the electrospun PTFE is much smaller (0.5-3μm), this would have resulted in a space-impediment for the cells to predictably adhere into the surface. Moreover, the larger interfiber distance as compared to the expanded PTFE would have prevented the macrophages from extending their cytoplasmic projections and increasing the cell-material contact area that is generally needed to allow proper cell activation [60,254]. Despite a lack of characterization of the non-resorbable membranes in Study IV, the topographical differences between the d-PTFE and the dual e-PTFE were based on previous results from our research group [255]. Hence, the molecular events of the GBR healing analyzed at the "membrane-level" of the experimental site - but only based on the different pattern of production of pro-inflammatory cytokines TNF-α and IL-6 - might indicate that the dense, fibril-free structure of the d-PTFE membrane may favor the adhesion, activation, and potential FBGC formation of the macrophages in contrast to the dual e-PTFE, which appears to act as a more attenuated inflammatory microenvironment. The collective findings on PTFE membrane-associated cells showed that other cytokines and growth factors - such as BMP-2, FGF-2, COL1A1, VEGF – were significantly upregulated in the dual e-PTFE membrane compartment as opposed to the d-PTFE. Several studies suggest the key role of BMP-2 in promoting differentiation of mesenchymal cells into osteoblasts by regulating transcription of osteogenic genes such as ALP, type I collagen, osteocalcin, and bone sialoprotein [256-259]. Additionally, it has been demonstrated that BMP signaling is important for FGF-induced osteoblast differentiation and proliferation [260-262]. Disruption of the FGF-2 gene in mice results in an impairment of BMP-2 expression with a consequent reduction of bone mass [263]. FGFs are also influential players in stimulating angiogenesis, and for the proliferation of fibroblasts in the early wound healing process [230,231,264-266]. The COL1A1 gene produces a component of type I collagen, which constitutes the main part of the bone extracellular matrix during osteoblast maturation and hence, like ALP, is considered an initial marker of osteoblast differentiation [267,268]. Further, VEGF figures prominently in proliferation, migration, and activation of endothelial cells, not only to enhance the microcirculation in soft tissue wound healing but also for bone regeneration [269,270]. Along with

endothelial cells, osteoblasts, and osteoclasts also express VEGF receptors [271,272]. Mice with deletion of VEGF receptors in osteoblasts exhibited decreased bone mass two weeks after birth and fewer osteoprogenitor cells was observed in the bone marrow [273]. It has been demonstrated that redundant VEGF recruited exuberant numbers of osteoclasts, leading to resorption of newly formed bone [274,275]. Differently, normal VEGF levels are necessary for the recruitment of osteoclasts and for maintaining regular bone remodeling. In a mouse femur fracture model, suppression of VEGF resulted in decreased callus volume at different phases of repair, including bone remodeling, whereas the addition of exogeneous VEGF elevated the amount of vascularity and mineral density in the calcified callus [276]. Although in Study IV only two time periods were considered and the outcomes interpreted in the context of histological findings and up/downregulation of genes, it was interesting to observe higher expression of several genes in cells adherent to dual e-PTFE after 28 days, while no major differences in terms of osteogenic gene expression and bone formation could be observed in the bone defects underneath both d-PTFE and e-PTFE at the same healing period. Taken together, it is evident that the diverse topographical features of PTFE (i.e., presence and size and orientation of fibers, porosity, interfiber distance) might affect the characteristics of the cells interacting with the membranes, along with the production of cytokines and growth factors, suggesting a time dependent behavior of osseous regeneration.

Cellular and molecular healing events in the soft tissue compartment:

Membrane-complications related to soft tissue dehiscence still represent a major distress in GBR [118]. Studies have shown that the soft tissue seal above a barrier membrane plays a crucial role for the successful outcome of bone regeneration. It has been shown that, in the presence of membrane exposure, there might be six times less bone formation compared to nonexposed sites [277]. If the soft tissue management during GBR [278-280] is inadequate, no tight sealing protects the underlying membrane and bone from the negative influence of the oral bacteria [107]. When a membrane is inserted into the oral cavity microorganisms and eukaryotic cells compete for the settlement on the biomaterial [281-283]. If bacteria can strongly adhere to the membrane and produce a biofilm of critical size, the successful integration of the soft tissue on the material surface by fibroblasts and endothelial cells is jeopardized [282,283]. Scaffold architecture influences cell attachment and migration [117]. A recent *in vitro* study on the soft tissue integration of dental implant abutments demonstrated a higher expression of ICAM-1 on the cell surface of human gingival fibroblasts, when microstructured surfaces were compared to flat ones

[284]. ICAM-1 is an intercellular adhesion molecule involved in stabilizing cell-to-cell interactions and signal transduction. By applying microgrooves to the abutment surfaces, a dense layer of unidirectional oriented cells could also be observed already after 8 hours of incubation, indicating an acceleration and settlement process of fibroblasts. Hence, cell adhesion influences the soft tissue healing efficacy of biomaterials. Despite the absence of detailed information on the topographical characteristics of the PTFE membranes in Study IV, it was observed a significant early upregulation of pro-inflammatory cytokines TNF-α and IL-6 and a late upregulation of genes such as FGF-2, VEGF and FOXO-1 in the soft tissue covering the dual e-PTFE compared to the overlying tissues of the sham and d-PTFE groups. *In vitro* studies have shown that FGF-2 participates in the synthesis and deposition of ECM components and stimulates fibroblasts to migrate as well as to increase collagenase production, thus activating the tissue remodeling process [285]. More evidence indicate that many growth factors exhibit synergistic effects on the cellular activities when present in the microenvironment of wound healing. It has been suggested that the vascularization process induced by acellular collagen matrices was accelerated due to the simultaneous expression of genes encoding the angiogenic factor VEGF-A and FGF-2 [286]. The crosstalk among FGFs, VEGFs and inflammatory cytokines might be important in the modulation of blood vessel growth in various physiological and pathological conditions [287]. Pro-inflammatory mediators such as TNF-α and IL-1 promote angiogenesis through increased recruitment of macrophages that subsequently secrete VEGF-A, or via induction of endothelial tip cell formation and proliferation [288,289]. Interestingly, also IL-6 can positively regulate the sprouting angiogenic function of endothelial cells via the autocrine IL-6 classic signaling [290]. Taken together, these molecular observations confirm an active role, especially of the dual e-PTFE membrane, in creating a favorable soft tissue-healing environment, and the potential contribution to achieve a successful soft tissue response during GBR is corroborated by a general evaluation of the physical characteristics of the PTFE membranes in relation to the current clinical and histological evidence. Among the numerous physico-chemical characteristics to consider, the pore size of a barrier membrane is crucial to facilitate angiogenesis and promote vascular supply [291]. The d-PTFE membrane has tiny porosity of 0.2μm [292] that would not allow proper vascularized soft tissue formation which may subsequently lead to insufficient flap adhesion and a higher risk of membrane exposure [94]. Conversely, the e-PTFE membrane facing the soft tissue compartment has a "semi-open" fibrillar structure with higher porosity (5-30μm [94,293]), more suitable for angiogenesis, soft tissue remodeling and wound stability. Previous research compared the effect of three types of e-PTFE, differing in permeability and surface microstructure, with regard to soft tissue integration and bone regeneration [85]. The clinical and histological findings revealed that the membrane

characterized by two extremely rough external layers separated by a totally occlusive internal layer increased the mechanical locking into the tissues, being firmly attached to the soft tissue and adherent to the underlying bone regenerated tissue. Additional evidence confirming the positive impact of the dual e-PTFE on soft tissue healing, comes from the significant upregulation of the forkhead box O1 transcription factor in the soft tissue compartment after 28 days. Several studies in the last decade have confirmed the important role of FOXO1 in regulating wound healing and tissue regeneration, although its exact function has not been fully elucidated [294-296]. It has been found that FOXO1 deletion resulted in a reduction of TGF-β1 expression in keratinocytes, with consequent reduced mucosal epithelial migration and defective re-epithelialization [297]. Another *in vivo* study demonstrated that FOXO1 deletion in keratinocytes caused a defective wound healing because of induced lower expression of VEGF, which might affect not only angiogenesis but also other parts of the wound healing cascade such as re-epithelialization, granulation tissue formation, and collagen deposition [298]. Furthermore, it has been shown that FOXO1 exhibited a favorable inhibitory effect on fibroblast activation and extracellular matrix production, thus mitigating the overgrowth of fibrotic tissue in numerous organs [299]. Since FOXO1 appears to function as molecular control in wound healing, its target during GBR might help rewire the process of soft tissue repair.

Microbiological observations using PTFE membranes:

The traditional view of e-PTFE behavior in GBR/GTR procedures is that the membrane contamination and/or exposure to the oral cavity during or after surgery is sometimes inevitable and is responsible for partial failure of the regenerating tissues [103]. Poor soft tissue management during GBR [80] together with the alloplastic material surface are key factors predisposing to microbial proliferation and the onset of an inflammatory response that impairs the wound healing process [300]. A series of early studies indicated that oral microorganisms could contaminate the e-PTFE surface and pass through the thickness of the open microstructure of the membranes [107,108,301], with subsequent membrane retrieval 4-6 weeks after periodontal and implant surgery [108,109,302]. Conversely, it has been claimed that high-density PTFE barriers with low porosity (< 0.3μm) provide a superior resistance to bacterial penetration [303]. The use of scanning electron microscopy to analyze d-PTFE membranes, which had been exposed for 21 days in the oral cavity, revealed colonies of bacteria and scattered fibroblast-like cells on the superior surface of the membranes, and total absence of microorganisms on the inferior surface facing the bone compartment [293]. Although the design of d-PTFE might prevent migration of

bacteria into the membrane structure thus leading to successful regeneration, controversy arises regarding the lack of fibroblast adhesion to facilitate wound stability and its limited evidence of efficacy in "open GBR procedures" [94]. A recent *in vitro* study consisting of an experimental membrane-permeability setup [255], confirmed the ability of d-PTFE membranes to impede *S. oralis* cells from moving across the barrier structure. However, this study demonstrated also that a new generation of e-PTFE membranes was effective against bacterial infiltration. While the first generation of e-PTFE membranes consisted of rectangular solid and smooth nodes linked together by a fibrillar structure facing both the soft and hard tissues with different pore size on the outer and inner portions [107], the new generation was achieved by modifying the layer thickness as well as the degree and direction of expansion of e-PTFE fibers, resulting in a dual-layer configuration.

Study III was designed to further verify the influence of different surface topography of PTFE membranes in association with bacterial colonization and biofilm formation. Among the plethora of plaque biofilm collection methods, we have selected the model system that was thought to best address our experimental questions and needs. One of the most important criterions for our *in vivo* grown plaque method, was the effect of the intraoral device on the volunteer's comfort for a valid compliance over the entire duration of the study. The barrier specimens applied on the tooth surfaces were relatively small, with the result of not being troublesome regarding esthetics and phonetics. Differently, two independent research groups in Italy [109,304] studied plaque accumulation on different barrier devices fixed to removable acrylic dentures. The model designed by these authors has the advantage of avoiding the pre-treatment of specific teeth, reducing the possible damage or demineralization process of the enamel like those observed after orthodontic treatments [305]. On the other hand, acrylic removable devices are rather bulky. The participants may not be able to eat properly and may change their diet, producing a bias in the growing biofilm or risking dropouts from the study [306-308]. Despite no self-perception questionnaire was given to the subjects participating in study III, it was observed that the biofilm-substrate membrane did not create any major wearing discomfort. A compelling finding using this model system was that no bond failure of the membranes was reported. Accidentally unsticking of samples is an important issue, not only for the accuracy of the study that will lose a specimen, but also for medical reasons due to the potential ingestion and inhalation complications that might require immediate action and, in some cases, even hospitalization [309,310]. Aspiration or ingestion of foreign materials during dental procedures is a relatively uncommon risk [311]. Despite almost 90% of the ingested foreign objects could pass the gastrointestinal tract without complications, it is reported that approximately 10% will require endoscopic removal [312]. In study III, this risk

was taken into consideration and a written medical emergency protocol was included in the informed consent form at the beginning of the trial [313]. It is well-known from the orthodontic literature that successful attachment of metal brackets on tooth surfaces requires effective bonding protocols and adequate bracket base design. More specifically, bracket base morphology has large recesses such as grooves and undercuts to provide a strong mechanical bonding to the adhesive resin. Such macro-mechanical retentive features were not present on the PTFE-membranes, thus generating a challenge in the performance and success of their direct bonding on tooth enamel. One may speculate that the absence of bonding failures is a result of the short duration of the study (24h) in relation to the underlying adhesion strategy. A cyanoacrylate adhesive (SmartBond®, Gestenco International AB) was selected for the purpose of our investigation. This is a "moisture-active" light-curing bonding system which showed shear bond strength within the accepted clinical range of 6-8 megapascals (MPa) after being exposed to 5.25% sodium hypochlorite (NaOCl) for 1 minute [314]. From a clinical perspective, this means that it is necessary that this adhesive work in a wet environment in order for the uncured monomer to be converted into the more stable and cured polymer [315]. Modeling the *in vivo* oral biofilm development was still far from being considered ideal since several limitations were encountered. The interaction between the e-PTFE specimens and muscular activity (cheek, tongue) might have partially dislodged or deflected the appliances, thus disturbing the biofilm formation, together with the mechanical removal of the specimens from the tooth surfaces by using small forceps and pliers. On the other hand, the quality of the biofilm collected from the specimens should be considered as illustrative since each volunteer acted as own control (spilt-mouth design) and because there was also a comparison with the tooth-formed biofilm (dental plaque) at all different time-points.

The results of Study III demonstrated that the configuration of the PTFE (expanded vs. dense) does not influence the degree of colonization by aerobes and anaerobes since no differences in CFU counting between membrane groups were found at the early (4h) and late time points (24h). Nevertheless, the pattern of bacterial colonization and 3D biofilm structure as measured by confocal scanning laser microscopy were different and significantly higher on d-PTFE specimens, especially 4 hours after exposure to the oral microflora. Apparently, morphological structures such as micron-range fibril network on the e-PTFE and dimples on the top surface of d-PTFE may have equally contributed to biofilm formation but could also explain the early mode of action of the two membranes regarding total biofilm biomass, average thickness of the live and dead cell populations, and ratio between the surface area and the volume of live bacteria. Previous research has been shown that microtopographic confinements can facilitate bacterial adhesion and biofilm

formation [316]. However, additional physicochemical characteristics related to biomaterials (surface roughness, hydrophilicity, surface free energy, surface wettability) and chemical properties are recognized as critical for bacterial adherence and early biofilm development [317-322]. An *in vitro* study compared the ability of *Staphylococcus epidermidis* to form biofilm at an early stage on the surface of different orthopedic implant biomaterials, ruling out the effect of surface roughness [323]. Whereas no difference was observed among the five materials after culturing for 2 and 4 hours, a significantly lower biofilm coverage rate for Co-Cr-Mo alloy was detected after culturing for 6 hours, suggesting that wettability and surface free energy might have a negative impact on the horizontal expansion of early biofilm development. Although in Study III it was not plausible to pinpoint specific effects on bacterial adhesion to one specific property of the two PTFE membranes, it was interesting to notice a more homogeneous distribution of live bacteria on the e-PTFE specimen at both time points, as revealed by the increased surface area to volume ratio. This observation agrees with data from a recent *in vitro* study on the adhesion of *Streptococcus oralis* on three e-PTFE membranes of distinct microstructure and one d-PTFE membrane [255]. The analysis and visualization of biofilm architecture at 24 hours disclosed homogeneous and evenly distributed monolayers of bacterial cells in a “carpet-like” arrangement on the different e-PTFE membranes, whereas thicker biofilm “tower formations” were observed within surface indentations of d-PTFE. Whether these early interactions of microorganisms with biomaterial surface characteristics would be of clinical relevance is unknown. Nonetheless, Study III has contributed with useful results in assessing the initial stages of biofilm formation, despite the complex phenomena that occur during GBR were not precisely reproduced. Finally, the microbiological detection of low counts for *Staphylococcus* spp. on both PTFE surfaces is not unusual, considering the polymicrobial nature and complexity of the biofilm communities. The opportunistic pathogen *S. aureus* is an asymptomatic colonizer of human nares [324], is a frequent isolate of the oral cavity [325-330] and it is well-known to be the most difficult microorganism to deal with in traumatic, surgical and burn wound infections. In Study III, its frequent identification should not be overrated since its danger in wound infection or delayed healing could be validated only in case of pure monomicrobial flora [300].

6 SUMMARY AND CONCLUSION

- The retrospective Study I on single-tooth implant rehabilitation provided an insight into the clinical arena of GBR, unveiling interesting observations. First, a favorable long-term outcome in terms of implant survival rate was found, but the initial high drop-out figure from the original cohort population must be kept in mind. Second, the registered clinical complications, especially after the first year of implant function, left open to interpretation the real effectiveness of the chosen treatments. Finally, the potential impact of certain factors on the long-term stability of marginal bone levels was disclosed. Thus, the bone defect morphology, the simultaneous approach GBR-implant placement, and the onset of early and late complications seemed to have a negative impact on the crestal bone in a relatively young patient population.

- Experimental Study II demonstrated that naturally derived collagen-based membrane promoted bone formation in bone defects. This included the migration of different cell phenotypes (e.g., monocytes/macrophages and osteoprogenitors) from the surrounding tissue into the membrane. The cells in the membrane expressed and released factors crucial for bone formation and bone remodeling (BMP-2, FGF-2, VEGF, and TGF-β). This influenced the bone regeneration process in the defect by stimulating the activity of osteoblasts and osteoclasts, the main cells of bone remodeling. The cellular and molecular activities inside the membrane strongly correlated with pro-osteogenic and bone remodeling in the defect, hence promoting a higher degree of bone regeneration and restitution of the defect.

- In Study III a clinical human model was developed, and different analytical procedures were employed to characterize the early stages of biofilm formation on nonresorbable barrier membranes. The dual e-PTFE and d-PTFE membranes were not manufactured to exert an antibacterial effect, and the short exposure to the oral cavity did not reproduce the real GBR conditions to anaerobic microorganisms and mature biofilm development. Nonetheless, a different pattern of bacterial colonization was found, most likely depending on the topographical differences between the membranes. Less biofilm biomass accumulation and biofilm thickness were detected on the surface of the dual e-PTFE in contrast to d-PTFE membranes.

Furthermore, a distinctive presence of *Staphylococcus spp.* was detected when the materials were introduced in the oral environment as compared to their original colonization of tooth surfaces.

- In experimental Study IV, the experimental platform was implemented, and the analytical techniques were also applied for studying the cellular and molecular events in the soft tissue compartment above nonresorbable PTFE membranes with distinct topographical characteristics. No difference in terms of induced-bone regeneration process could be found in the underlying bone defect between dual e-PTFE and d-PTFE membranes. Conversely, the downregulation of pro-inflammatory mediators (TNF-α, IL-6) and the upregulation of factors related to angiogenic, and proliferative responses (VEGF, FOXO-1, and FGF-2) suggest a positive and active influence of the dual e-PTFE on the soft tissue healing as compared to d-PTFE membranes.

- It is concluded that the GBR membrane, besides its known barrier properties, also acts as a bioactive compartment which affects both the overlying soft tissue and the underlying bone defect. These novel findings indicate a potential for additional and potentially improved tissue regenerative strategies.

7 FUTURE PERSPECTIVES

The market for GBR is expected to grow in response to the increasing demand for dental implants, especially amongst the population of developing countries. Despite major efforts in tissue engineering development for the optimal membrane design, the current biomaterials used for bone regenerative procedures are often selected based on their clinical manageability rather than an appropriate systematic approach to enhance the biological outcomes.

The present thesis demonstrated that different types of membranes, which are usually selected in the clinic for their "passive" barrier properties in relation to the morphology of the bone defect to be regenerated, display a more complex biological behavior, actively interacting with the surrounding injured tissues and, to a certain extent, fine-tuning the cascade of molecular and cellular events that regulate the wound healing dynamics.

Notably, the application of the q-PCR analytical technique in the *in vivo* studies might be seen as a properly standardized methodological platform that could be applied to generate consistent and reproducible gene expression data in case of new membranes and indeed bone grafting materials to be tested, where modifications of physicochemical and mechanical properties (porosity, scaffold architecture, thickness, wettability) as well as the incorporation of biological factors (e.g.; FGF, BMP-2, BMP-7, PDGF) and antibacterial agents could be evaluated in a methodical way. On this matter, it would also be of interest to increase more information and knowledge on the bacteria related to biomaterial associated complications since their role for the short- and long-term outcomes of GBR procedures remains to be elucidated

On the biological behavior of barrier membranes: implications for Guided Bone Regeneration

ACKNOWLEDGEMENT

My debts are great and widely spread.

First and foremost, to my main supervisor, Christer Dahlin, for constant guidance and assistance with my PhD journey. I am truly grateful and honored to have worked with you on this research topic. Your presence, craft and counsel are on each page of this thesis.

Peter Thomsen, for being a great source of inspiration with your incessant scientific curiosity, and your invaluable knowledge and expertise. I will always cherish our meetings where you've been uniquely open, enthusiastic and with a panoramic mind.

My co-supervisor, Omar Omar, who drew me there, with sharp wit and intellectual depth, to better understand the projects on gene expression he championed - a wish to integrate biology, medicine, and biomaterials.

I am very grateful to Margarita Trobos, for being attentive, hardworking, plainspoken, for all your help in explaining the complex universe of microorganisms, and for your great friendship.

A special thanks to Lena Emanuelsson, Birgitta Norlindh, Anna Johansson, and Maria Hoffman for your high level of professionalism and the generosity of spirit that gave me great encouragement, contributing to the accomplishment of this thesis.

I wish to express my deepest gratitude to all my co-authors, none of them should underestimate how helpful and important they have been: Ibrahim Elgali, Forugh Vazirisani, Emina Čirgić, Furqan Ali Shah, Lena Emanuelsson, Anna Johansson, and Maria Hoffman.

I thank all researchers I've met over the years at the Department of Biomaterials, for sharing with me their time, projects, and life experiences.

I also want to thank all colleagues at the Brånemark Clinic. Jan-Anders Ekelund and Pia Skyllerström for being there with your time and allowing me to work with flexible scheduling. Jan Kowar, Sargon Barkarmo, Malin Olsson Malm, and Victoria Stenport for supporting my PhD journey with interesting discussions, constructive suggestions, and moral help. I owe a huge debt of

gratitude to Annelii Malmqvist for invaluable competence, patience and help in our everyday clinical work.

I am so thankful to Bertil Friberg, who loomed large in my career, helped deepen my understanding of implant dentistry, and shared his extraordinary knowledge and skills with kindness and respect. It has been a great privilege to have worked with you.

I wish to thank all my friends in Italy, in particular Marco, Luciano, Alessandro, and Lorenzo for always being there, despite the miles between us. A special thanks to Francesco Tavani for providing every conceivable kind of professional, intellectual, and emotional support through all these years.

I am immensely grateful to my family: my mother Maria Teresa and my father Luciano, for your love and guidance in life; my brother Alessandro and his family, for being always present when needed.

Finally, to my two fantastic daughters, Silvia and Louisa, my universe!

And to "my" Jennie, love, and best friend in life, who has always believed in me and, through an unrelentingly devoted support, has made possible to reach this further and long-desired professional step. Words are not enough to say thank you. You are my everything, and I love you forever.

In studies during my PhD graduate work, funding was generously provided by the BIOMATCELL VINN Excellence Center of Biomaterials and Cell Therapy, supported by VINNOVA and the Västra Götaland Region, the Swedish Research Council (2015-09495 and 2018-02891), VINNOVA (2018-00252), Osteology Foundation, the Swedish state under the agreement between the Swedish government and the county councils, the ALF agreement (ALFGBG-725641), the CARe - Centre for Antibiotic Resistance Research at University of Gothenburg, the Doctor Felix Neubergh Foundation, the Stiftelsen Handlanden Hjalmar Svensson, the IngaBritt and Arne Lundberg Foundation and the Area of Advance Materials of Chalmers and GU Biomaterials within the Strategic Research Area initiative launched by the Swedish Government.

REFERENCES

1. Turri A, Cirgic E, Shah FA, et al. Early plaque formation on PTFE membranes with expanded or dense surface structures applied in the oral cavity of human volunteers. *Clin Exp Dent Res.* 2021;7(2):137-146.
2. Pedrero SG, Llamas-Sillero P, Serrano-Lopez J. A Multidisciplinary Journey towards Bone Tissue Engineering. *Materials (Basel).* 2021;14(17).
3. Dahlin C, Gottlow J, Linde A, Nyman S. Healing of maxillary and mandibular bone defects using a membrane technique. An experimental study in monkeys. *Scand J Plast Reconstr Surg Hand Surg.* 1990;24(1):13-19.
4. Dahlin C, Linde A, Gottlow J, Nyman S. Healing of bone defects by guided tissue regeneration. *Plast Reconstr Surg.* 1988;81(5):672-676.
5. Dahlin C, Sennerby L, Lekholm U, Linde A, Nyman S. Generation of new bone around titanium implants using a membrane technique: an experimental study in rabbits. *Int J Oral Maxillofac Implants.* 1989;4(1):19-25.
6. Jepsen S, Schwarz F, Cordaro L, et al. REGENERATION OF ALVEOLAR RIDGE DEFECTS. Consensus report of group 4 of the 15th European Workshop on Periodontology on Bone Regeneration. *J Clin Periodontol.* 2019.
7. Urban IA, Monje A. Guided Bone Regeneration in Alveolar Bone Reconstruction. *Oral Maxillofac Surg Clin North Am.* 2019;31(2):331-338.
8. Clarke B. Normal bone anatomy and physiology. *Clin J Am Soc Nephrol.* 2008;3 Suppl 3:S131-139.
9. Florencio-Silva R, Sasso GR, Sasso-Cerri E, Simoes MJ, Cerri PS. Biology of Bone Tissue: Structure, Function, and Factors That Influence Bone Cells. *Biomed Res Int.* 2015;2015:421746.
10. Buck DW, 2nd, Dumanian GA. Bone biology and physiology: Part I. The fundamentals. *Plast Reconstr Surg.* 2012;129(6):1314-1320.
11. Dwek JR. The periosteum: what is it, where is it, and what mimics it in its absence? *Skeletal Radiol.* 2010;39(4):319-323.
12. Andersen TL, Sondergaard TE, Skorzynska KE, et al. A physical mechanism for coupling bone resorption and formation in adult human bone. *Am J Pathol.* 2009;174(1):239-247.
13. Frost HM, Vilanueva AR, Jett S, Eyring E. Tetracycline-based analysis of bone remodelling in osteopetrosis. *Clin Orthop Relat Res.* 1969;65:203-217.
14. Capulli M, Paone R, Rucci N. Osteoblast and osteocyte: games without frontiers. *Arch Biochem Biophys.* 2014;561:3-12.

15. Ducy P, Zhang R, Geoffroy V, Ridall AL, Karsenty G. Osf2/Cbfa1: a transcriptional activator of osteoblast differentiation. *Cell.* 1997;89(5):747-754.
16. Fakhry M, Hamade E, Badran B, Buchet R, Magne D. Molecular mechanisms of mesenchymal stem cell differentiation towards osteoblasts. *World J Stem Cells.* 2013;5(4):136-148.
17. Grigoriadis AE, Heersche JN, Aubin JE. Differentiation of muscle, fat, cartilage, and bone from progenitor cells present in a bone-derived clonal cell population: effect of dexamethasone. *J Cell Biol.* 1988;106(6):2139-2151.
18. Crockett JC, Mellis DJ, Scott DI, Helfrich MH. New knowledge on critical osteoclast formation and activation pathways from study of rare genetic diseases of osteoclasts: focus on the RANK/RANKL axis. *Osteoporos Int.* 2011;22(1):1-20.
19. Boyce BF, Hughes DE, Wright KR, Xing L, Dai A. Recent advances in bone biology provide insight into the pathogenesis of bone diseases. *Lab Invest.* 1999;79(2):83-94.
20. Hsu H, Lacey DL, Dunstan CR, et al. Tumor necrosis factor receptor family member RANK mediates osteoclast differentiation and activation induced by osteoprotegerin ligand. *Proc Natl Acad Sci U S A.* 1999;96(7):3540-3545.
21. Yoshida H, Hayashi S, Kunisada T, et al. The murine mutation osteopetrosis is in the coding region of the macrophage colony stimulating factor gene. *Nature.* 1990;345(6274):442-444.
22. Boyce BF, Xing L. Functions of RANKL/RANK/OPG in bone modeling and remodeling. *Arch Biochem Biophys.* 2008;473(2):139-146.
23. Longhini R, de Oliveira PA, de Souza Faloni AP, Sasso-Cerri E, Cerri PS. Increased apoptosis in osteoclasts and decreased RANKL immunoexpression in periodontium of cimetidine-treated rats. *J Anat.* 2013;222(2):239-247.
24. Franz-Odendaal TA, Hall BK, Witten PE. Buried alive: how osteoblasts become osteocytes. *Dev Dyn.* 2006;235(1):176-190.
25. Dallas SL, Prideaux M, Bonewald LF. The osteocyte: an endocrine cell ... and more. *Endocr Rev.* 2013;34(5):658-690.
26. Rochefort GY, Pallu S, Benhamou CL. Osteocyte: the unrecognized side of bone tissue. *Osteoporos Int.* 2010;21(9):1457-1469.
27. Bonewald LF. The amazing osteocyte. *J Bone Miner Res.* 2011;26(2):229-238.
28. Mikuni-Takagaki Y, Kakai Y, Satoyoshi M, et al. Matrix mineralization and the differentiation of osteocyte-like cells in culture. *J Bone Miner Res.* 1995;10(2):231-242.
29. Poole KE, van Bezooijen RL, Loveridge N, et al. Sclerostin is a delayed secreted product of osteocytes that inhibits bone formation. *FASEB J.* 2005;19(13):1842-1844.

30. Miller SC, de Saint-Georges L, Bowman BM, Jee WS. Bone lining cells: structure and function. *Scanning Microsc.* 1989;3(3):953-960; discussion 960-951.
31. Marsell R, Einhorn TA. The biology of fracture healing. *Injury.* 2011;42(6):551-555.
32. Claes L, Recknagel S, Ignatius A. Fracture healing under healthy and inflammatory conditions. *Nat Rev Rheumatol.* 2012;8(3):133-143.
33. Maruyama M, Rhee C, Utsunomiya T, et al. Modulation of the Inflammatory Response and Bone Healing. *Front Endocrinol (Lausanne).* 2020;11:386.
34. Gerstenfeld LC, Cullinane DM, Barnes GL, Graves DT, Einhorn TA. Fracture healing as a post-natal developmental process: molecular, spatial, and temporal aspects of its regulation. *J Cell Biochem.* 2003;88(5):873-884.
35. Kon T, Cho TJ, Aizawa T, et al. Expression of osteoprotegerin, receptor activator of NF-kappaB ligand (osteoprotegerin ligand) and related proinflammatory cytokines during fracture healing. *J Bone Miner Res.* 2001;16(6):1004-1014.
36. Cho HH, Kyoung KM, Seo MJ, Kim YJ, Bae YC, Jung JS. Overexpression of CXCR4 increases migration and proliferation of human adipose tissue stromal cells. *Stem Cells Dev.* 2006;15(6):853-864.
37. Iyer SS, Cheng G. Role of interleukin 10 transcriptional regulation in inflammation and autoimmune disease. *Crit Rev Immunol.* 2012;32(1):23-63.
38. Sims NA, Martin TJ. Coupling the activities of bone formation and resorption: a multitude of signals within the basic multicellular unit. *Bonekey Rep.* 2014;3:481.
39. Kenkre JS, Bassett J. The bone remodelling cycle. *Ann Clin Biochem.* 2018;55(3):308-327.
40. Negishi-Koga T, Shinohara M, Komatsu N, et al. Suppression of bone formation by osteoclastic expression of semaphorin 4D. *Nat Med.* 2011;17(11):1473-1480.
41. Hayashi M, Nakashima T, Taniguchi M, Kodama T, Kumanogoh A, Takayanagi H. Osteoprotection by semaphorin 3A. *Nature.* 2012;485(7396):69-74.
42. Simonet WS, Lacey DL, Dunstan CR, et al. Osteoprotegerin: a novel secreted protein involved in the regulation of bone density. *Cell.* 1997;89(2):309-319.
43. Furuya M, Kikuta J, Fujimori S, et al. Direct cell-cell contact between mature osteoblasts and osteoclasts dynamically controls their functions in vivo. *Nat Commun.* 2018;9(1):300.
44. Linkhart TA, Mohan S, Baylink DJ. Growth factors for bone growth and repair: IGF, TGF beta and BMP. *Bone.* 1996;19(1 Suppl):1S-12S.

45. Lerner UH, Kindstedt E, Lundberg P. The critical interplay between bone resorbing and bone forming cells. *J Clin Periodontol.* 2019;46 Suppl 21:33-51.
46. Zhao C, Irie N, Takada Y, et al. Bidirectional ephrinB2-EphB4 signaling controls bone homeostasis. *Cell Metab.* 2006;4(2):111-121.
47. Jilka RL, Weinstein RS, Bellido T, Parfitt AM, Manolagas SC. Osteoblast programmed cell death (apoptosis): modulation by growth factors and cytokines. *J Bone Miner Res.* 1998;13(5):793-802.
48. Wilson CJ, Clegg RE, Leavesley DI, Pearcy MJ. Mediation of biomaterial-cell interactions by adsorbed proteins: a review. *Tissue Eng.* 2005;11(1-2):1-18.
49. Brodbeck WG, Colton E, Anderson JM. Effects of adsorbed heat labile serum proteins and fibrinogen on adhesion and apoptosis of monocytes/macrophages on biomaterials. *J Mater Sci Mater Med.* 2003;14(8):671-675.
50. Hu WJ, Eaton JW, Ugarova TP, Tang L. Molecular basis of biomaterial-mediated foreign body reactions. *Blood.* 2001;98(4):1231-1238.
51. Jenney CR, Anderson JM. Adsorbed serum proteins responsible for surface dependent human macrophage behavior. *J Biomed Mater Res.* 2000;49(4):435-447.
52. Mariani E, Lisignoli G, Borzi RM, Pulsatelli L. Biomaterials: Foreign Bodies or Tuners for the Immune Response? *Int J Mol Sci.* 2019;20(3).
53. Badylak SF, Gilbert TW. Immune response to biologic scaffold materials. *Semin Immunol.* 2008;20(2):109-116.
54. Mesure L, De Visscher G, Vranken I, Lebacq A, Flameng W. Gene expression study of monocytes/macrophages during early foreign body reaction and identification of potential precursors of myofibroblasts. *PLoS One.* 2010;5(9):e12949.
55. Wang T, He C. TNF-alpha and IL-6: The Link between Immune and Bone System. *Curr Drug Targets.* 2020;21(3):213-227.
56. Anderson JM, Rodriguez A, Chang DT. Foreign body reaction to biomaterials. *Semin Immunol.* 2008;20(2):86-100.
57. Taraballi F, Sushnitha M, Tsao C, et al. Biomimetic Tissue Engineering: Tuning the Immune and Inflammatory Response to Implantable Biomaterials. *Adv Healthc Mater.* 2018;7(17):e1800490.
58. McNally AK, Jones JA, Macewan SR, Colton E, Anderson JM. Vitronectin is a critical protein adhesion substrate for IL-4-induced foreign body giant cell formation. *J Biomed Mater Res A.* 2008;86(2):535-543.
59. Brown BN, Ratner BD, Goodman SB, Amar S, Badylak SF. Macrophage polarization: an opportunity for improved outcomes in biomaterials and regenerative medicine. *Biomaterials.* 2012;33(15):3792-3802.

60. Saino E, Focarete ML, Gualandi C, et al. Effect of electrospun fiber diameter and alignment on macrophage activation and secretion of proinflammatory cytokines and chemokines. *Biomacromolecules.* 2011;12(5):1900-1911.
61. Mosser DM, Edwards JP. Exploring the full spectrum of macrophage activation. *Nat Rev Immunol.* 2008;8(12):958-969.
62. Sadowska JM, Ginebra MP. Inflammation and biomaterials: role of the immune response in bone regeneration by inorganic scaffolds. *J Mater Chem B.* 2020;8(41):9404-9427.
63. Broughton G, 2nd, Janis JE, Attinger CE. The basic science of wound healing. *Plast Reconstr Surg.* 2006;117(7 Suppl):12S-34S.
64. Lee J, Byun H, Madhurakkat Perikamana SK, Lee S, Shin H. Current Advances in Immunomodulatory Biomaterials for Bone Regeneration. *Adv Healthc Mater.* 2019;8(4):e1801106.
65. Hovgaard MB, Rechendorff K, Chevallier J, Foss M, Besenbacher F. Fibronectin adsorption on tantalum: the influence of nanoroughness. *J Phys Chem B.* 2008;112(28):8241-8249.
66. Hulander M, Lundgren A, Berglin M, Ohrlander M, Lausmaa J, Elwing H. Immune complement activation is attenuated by surface nanotopography. *Int J Nanomedicine.* 2011;6:2653-2666.
67. Rechendorff K, Hovgaard MB, Foss M, Zhdanov VP, Besenbacher F. Enhancement of protein adsorption induced by surface roughness. *Langmuir.* 2006;22(26):10885-10888.
68. Chen S, Jones JA, Xu Y, Low HY, Anderson JM, Leong KW. Characterization of topographical effects on macrophage behavior in a foreign body response model. *Biomaterials.* 2010;31(13):3479-3491.
69. Hotchkiss KM, Reddy GB, Hyzy SL, Schwartz Z, Boyan BD, Olivares-Navarrete R. Titanium surface characteristics, including topography and wettability, alter macrophage activation. *Acta Biomater.* 2016;31:425-434.
70. Vlacic-Zischke J, Hamlet SM, Friis T, Tonetti MS, Ivanovski S. The influence of surface microroughness and hydrophilicity of titanium on the up-regulation of TGFbeta/BMP signalling in osteoblasts. *Biomaterials.* 2011;32(3):665-671.
71. Gittens RA, Olivares-Navarrete R, McLachlan T, et al. Differential responses of osteoblast lineage cells to nanotopographically-modified, microroughened titanium-aluminum-vanadium alloy surfaces. *Biomaterials.* 2012;33(35):8986-8994.
72. Spiller KL, Anfang RR, Spiller KJ, et al. The role of macrophage phenotype in vascularization of tissue engineering scaffolds. *Biomaterials.* 2014;35(15):4477-4488.
73. Loh QL, Choong C. Three-dimensional scaffolds for tissue engineering applications: role of porosity and pore size. *Tissue Eng Part B Rev.* 2013;19(6):485-502.

74. Thevenot P, Hu W, Tang L. Surface chemistry influences implant biocompatibility. *Curr Top Med Chem.* 2008;8(4):270-280.
75. Alfarsi MA, Hamlet SM, Ivanovski S. Titanium surface hydrophilicity modulates the human macrophage inflammatory cytokine response. *J Biomed Mater Res A.* 2014;102(1):60-67.
76. Bang SM, Moon HJ, Kwon YD, Yoo JY, Pae A, Kwon IK. Osteoblastic and osteoclastic differentiation on SLA and hydrophilic modified SLA titanium surfaces. *Clin Oral Implants Res.* 2014;25(7):831-837.
77. Hamlet S, Alfarsi M, George R, Ivanovski S. The effect of hydrophilic titanium surface modification on macrophage inflammatory cytokine gene expression. *Clin Oral Implants Res.* 2012;23(5):584-590.
78. Linde A, Alberius P, Dahlin C, Bjurstam K, Sundin Y. Osteopromotion: a soft-tissue exclusion principle using a membrane for bone healing and bone neogenesis. *J Periodontol.* 1993;64(11 Suppl):1116-1128.
79. Schenk RK, Buser D, Hardwick WR, Dahlin C. Healing pattern of bone regeneration in membrane-protected defects: a histologic study in the canine mandible. *Int J Oral Maxillofac Implants.* 1994;9(1):13-29.
80. Retzepi M, Donos N. Guided Bone Regeneration: biological principle and therapeutic applications. *Clin Oral Implants Res.* 2010;21(6):567-576.
81. Zellin G, Gritli-Linde A, Linde A. Healing of mandibular defects with different biodegradable and non-biodegradable membranes: an experimental study in rats. *Biomaterials.* 1995;16(8):601-609.
82. Sanz M, Dahlin C, Apatzidou D, et al. Biomaterials and regenerative technologies used in bone regeneration in the craniomaxillofacial region: Consensus report of group 2 of the 15th European Workshop on Periodontology on Bone Regeneration. *J Clin Periodontol.* 2019;46 Suppl 21:82-91.
83. Omar O, Elgali I, Dahlin C, Thomsen P. Barrier membranes: More than the barrier effect? *J Clin Periodontol.* 2019;46 Suppl 21:103-123.
84. Elgali I, Omar O, Dahlin C, Thomsen P. Guided bone regeneration: materials and biological mechanisms revisited. *Eur J Oral Sci.* 2017;125(5):315-337.
85. Simion M, Dahlin C, Blair K, Schenk RK. Effect of different microstructures of e-PTFE membranes on bone regeneration and soft tissue response: a histologic study in canine mandible. *Clin Oral Implants Res.* 1999;10(2):73-84.
86. Buser D, Bragger U, Lang NP, Nyman S. Regeneration and enlargement of jaw bone using guided tissue regeneration. *Clin Oral Implants Res.* 1990;1(1):22-32.

87. Dahlin C, Andersson L, Linde A. Bone augmentation at fenestrated implants by an osteopromotive membrane technique. A controlled clinical study. *Clin Oral Implants Res.* 1991;2(4):159-165.
88. Simion M, Dahlin C, Trisi P, Piattelli A. Qualitative and quantitative comparative study on different filling materials used in bone tissue regeneration: a controlled clinical study. *Int J Periodontics Restorative Dent.* 1994;14(3):198-215.
89. Jovanovic SA, Schenk RK, Orsini M, Kenney EB. Supracrestal bone formation around dental implants: an experimental dog study. *Int J Oral Maxillofac Implants.* 1995;10(1):23-31.
90. Dahlin C, Lekholm U, Becker W, et al. Treatment of fenestration and dehiscence bone defects around oral implants using the guided tissue regeneration technique: a prospective multicenter study. *Int J Oral Maxillofac Implants.* 1995;10(3):312-318.
91. Jovanovic SA, Spiekermann H, Richter EJ. Bone regeneration around titanium dental implants in dehisced defect sites: a clinical study. *Int J Oral Maxillofac Implants.* 1992;7(2):233-245.
92. Mattout P, Nowzari H, Mattout C. Clinical evaluation of guided bone regeneration at exposed parts of Branemark dental implants with and without bone allograft. *Clin Oral Implants Res.* 1995;6(3):189-195.
93. Benic GI, Hammerle CH. Horizontal bone augmentation by means of guided bone regeneration. *Periodontol 2000.* 2014;66(1):13-40.
94. Carbonell JM, Martin IS, Santos A, Pujol A, Sanz-Moliner JD, Nart J. High-density polytetrafluoroethylene membranes in guided bone and tissue regeneration procedures: a literature review. *Int J Oral Maxillofac Surg.* 2014;43(1):75-84.
95. Hammerle CH, Jung RE. Bone augmentation by means of barrier membranes. *Periodontol 2000.* 2003;33:36-53.
96. Rocchietta I, Fontana F, Simion M. Clinical outcomes of vertical bone augmentation to enable dental implant placement: a systematic review. *J Clin Periodontol.* 2008;35(8 Suppl):203-215.
97. Ronda M, Rebaudi A, Torelli L, Stacchi C. Expanded vs. dense polytetrafluoroethylene membranes in vertical ridge augmentation around dental implants: a prospective randomized controlled clinical trial. *Clin Oral Implants Res.* 2014;25(7):859-866.
98. Jung RE, Fenner N, Hammerle CH, Zitzmann NU. Long-term outcome of implants placed with guided bone regeneration (GBR) using resorbable and non-resorbable membranes after 12-14 years. *Clin Oral Implants Res.* 2013;24(10):1065-1073.
99. Merli M, Moscatelli M, Mariotti G, Rotundo R, Bernardelli F, Nieri M. Bone level variation after vertical ridge augmentation: resorbable barriers versus titanium-reinforced barriers. A 6-year double-blind randomized clinical trial. *Int J Oral Maxillofac Implants.* 2014;29(4):905-913.

100. Wang HL, Boyapati L. "PASS" principles for predictable bone regeneration. *Implant Dent.* 2006;15(1):8-17.
101. Chiapasco M, Zaniboni M. Clinical outcomes of GBR procedures to correct peri-implant dehiscences and fenestrations: a systematic review. *Clin Oral Implants Res.* 2009;20 Suppl 4:113-123.
102. Soldatos NK, Stylianou P, Koidou VP, Angelov N, Yukna R, Romanos GE. Limitations and options using resorbable versus nonresorbable membranes for successful guided bone regeneration. *Quintessence Int.* 2017;48(2):131-147.
103. Garcia J, Dodge A, Luepke P, Wang HL, Kapila Y, Lin GH. Effect of membrane exposure on guided bone regeneration: A systematic review and meta-analysis. *Clin Oral Implants Res.* 2018;29(3):328-338.
104. De Sanctis M, Zucchelli G, Clauser C. Bacterial colonization of barrier material and periodontal regeneration. *J Clin Periodontol.* 1996;23(11):1039-1046.
105. Nowzari H, Matian F, Slots J. Periodontal pathogens on polytetrafluoroethylene membrane for guided tissue regeneration inhibit healing. *J Clin Periodontol.* 1995;22(6):469-474.
106. Zucchelli G, De Sanctis M, Clauser C. Integrated connective tissue in bioabsorbable barrier material and periodontal regeneration. *J Periodontol.* 1997;68(10):996-1004.
107. Simion M, Trisi P, Maglione M, Piattelli A. Bacterial penetration in vitro through GTAM membrane with and without topical chlorhexidine application. A light and scanning electron microscopic study. *J Clin Periodontol.* 1995;22(4):321-331.
108. Grevstad HJ, Leknes KN. Ultrastructure of plaque associated with polytetrafluoroethylene (PTFE) membranes used for guided tissue regeneration. *J Clin Periodontol.* 1993;20(3):193-198.
109. Simion M, Baldoni M, Rossi P, Zaffe D. A comparative study of the effectiveness of e-PTFE membranes with and without early exposure during the healing period. *Int J Periodontics Restorative Dent.* 1994;14(2):166-180.
110. Proussaefs P, Lozada J. Use of titanium mesh for staged localized alveolar ridge augmentation: clinical and histologic-histomorphometric evaluation. *J Oral Implantol.* 2006;32(5):237-247.
111. Barber HD, Lignelli J, Smith BM, Bartee BK. Using a dense PTFE membrane without primary closure to achieve bone and tissue regeneration. *J Oral Maxillofac Surg.* 2007;65(4):748-752.
112. Barboza EP, Stutz B, Ferreira VF, Carvalho W. Guided bone regeneration using nonexpanded polytetrafluoroethylene membranes in preparation for dental implant placements--a report of 420 cases. *Implant Dent.* 2010;19(1):2-7.

113. Bartee BK. Extraction site reconstruction for alveolar ridge preservation. Part 2: membrane-assisted surgical technique. *J Oral Implantol.* 2001;27(4):194-197.
114. Sbricoli L, Guazzo R, Annunziata M, Gobbato L, Bressan E, Nastri L. Selection of Collagen Membranes for Bone Regeneration: A Literature Review. *Materials (Basel).* 2020;13(3).
115. Miller N, Penaud J, Foliguet B, Membre H, Ambrosini P, Plombas M. Resorption rates of 2 commercially available bioresorbable membranes. A histomorphometric study in a rabbit model. *J Clin Periodontol.* 1996;23(12):1051-1059.
116. Owens KW, Yukna RA. Collagen membrane resorption in dogs: a comparative study. *Implant Dent.* 2001;10(1):49-58.
117. Toledano-Osorio M, Manzano-Moreno FJ, Ruiz C, Toledano M, Osorio R. Testing active membranes for bone regeneration: A review. *J Dent.* 2021;105:103580.
118. Lim G, Lin GH, Monje A, Chan HL, Wang HL. Wound Healing Complications Following Guided Bone Regeneration for Ridge Augmentation: A Systematic Review and Meta-Analysis. *Int J Oral Maxillofac Implants.* 2018;33(1):41-50.
119. Toledano M, Asady S, Toledano-Osorio M, et al. Differential Biodegradation Kinetics of Collagen Membranes for Bone Regeneration. *Polymers (Basel).* 2020;12(6).
120. Zitzmann NU, Naef R, Scharer P. Resorbable versus nonresorbable membranes in combination with Bio-Oss for guided bone regeneration. *Int J Oral Maxillofac Implants.* 1997;12(6):844-852.
121. Rentsch C, Schneiders W, Manthey S, Rentsch B, Rammelt S. Comprehensive histological evaluation of bone implants. *Biomatter.* 2014;4.
122. Vidal B, Pinto A, Galvao MJ, et al. Bone histomorphometry revisited. *Acta Reumatol Port.* 2012;37(4):294-300.
123. Hammerle CH, Schmid J, Lang NP, Olah AJ. Temporal dynamics of healing in rabbit cranial defects using guided bone regeneration. *J Oral Maxillofac Surg.* 1995;53(2):167-174.
124. Bosch C, Melsen B, Vargervik K. Guided bone regeneration in calvarial bone defects using polytetrafluoroethylene membranes. *Cleft Palate Craniofac J.* 1995;32(4):311-317.
125. Schmitz JP, Hollinger JO. The critical size defect as an experimental model for craniomandibulofacial nonunions. *Clin Orthop Relat Res.* 1986(205):299-308.
126. Shanbhag S, Pandis N, Mustafa K, Nyengaard JR, Stavropoulos A. Alveolar bone tissue engineering in critical-size defects of experimental animal models: a systematic review and meta-analysis. *J Tissue Eng Regen Med.* 2017;11(10):2935-2949.
127. Donos N, Graziani F, Mardas N, Kostopoulos L. The use of human hypertrophic chondrocytes-derived extracellular matrix for the

treatment of critical-size calvarial defects. *Clin Oral Implants Res.* 2011;22(12):1346-1353.

128. Jardini MA, De Marco AC, Lima LA. Early healing pattern of autogenous bone grafts with and without e-PTFE membranes: a histomorphometric study in rats. *Oral Surg Oral Med Oral Pathol Oral Radiol Endod.* 2005;100(6):666-673.
129. Lundgren D, Lundgren AK, Sennerby L, Nyman S. Augmentation of intramembraneous bone beyond the skeletal envelope using an occlusive titanium barrier. An experimental study in the rabbit. *Clin Oral Implants Res.* 1995;6(2):67-72.
130. Schwarz F, Mihatovic I, Golubovic V, Hegewald A, Becker J. Influence of two barrier membranes on staged guided bone regeneration and osseointegration of titanium implants in dogs: part 1. Augmentation using bone graft substitutes and autogenous bone. *Clin Oral Implants Res.* 2012;23(1):83-89.
131. Higuchi R, Fockler C, Dollinger G, Watson R. Kinetic PCR analysis: real-time monitoring of DNA amplification reactions. *Biotechnology (N Y).* 1993;11(9):1026-1030.
132. Jemt T, Sunden Pikner S, Grondahl K. Changes of Marginal Bone Level in Patients with "Progressive Bone Loss" at Branemark System(R) Implants: A Radiographic Follow-Up Study over an Average of 9 Years. *Clin Implant Dent Relat Res.* 2015;17(4):619-628.
133. Antoun H, Karouni M, Abitbol J, Zouiten O, Jemt T. A retrospective study on 1592 consecutively performed operations in one private referral clinic. Part I: Early inflammation and early implant failures. *Clin Implant Dent Relat Res.* 2017;19(3):404-412.
134. Renvert S, Persson GR, Pirih FQ, Camargo PM. Peri-implant health, peri-implant mucositis, and peri-implantitis: Case definitions and diagnostic considerations. *J Periodontol.* 2018;89 Suppl 1:S304-S312.
135. Karlsson K, Derks J, Hakansson J, Wennstrom JL, Petzold M, Berglundh T. Interventions for peri-implantitis and their effects on further bone loss: A retrospective analysis of a registry-based cohort. *J Clin Periodontol.* 2019;46(8):872-879.
136. Berglundh T, Armitage G, Araujo MG, et al. Peri-implant diseases and conditions: Consensus report of workgroup 4 of the 2017 World Workshop on the Classification of Periodontal and Peri-Implant Diseases and Conditions. *J Clin Periodontol.* 2018;45 Suppl 20:S286-S291.
137. Heitz-Mayfield LJA, Salvi GE. Peri-implant mucositis. *J Clin Periodontol.* 2018;45 Suppl 20:S237-S245.
138. Schwarz F, Derks J, Monje A, Wang HL. Peri-implantitis. *J Periodontol.* 2018;89 Suppl 1:S267-S290.
139. Trobos M, Johansson ML, Jonhede S, et al. The clinical outcome and microbiological profile of bone-anchored hearing systems (BAHS)

with different abutment topographies: a prospective pilot study. *Eur Arch Otorhinolaryngol.* 2018;275(6):1395-1408.

140. Heydorn A, Nielsen AT, Hentzer M, et al. Quantification of biofilm structures by the novel computer program COMSTAT. *Microbiology (Reading).* 2000;146 (Pt 10):2395-2407.
141. Elgali I, Turri A, Xia W, et al. Guided bone regeneration using resorbable membrane and different bone substitutes: Early histological and molecular events. *Acta Biomater.* 2016;29:409-423.
142. Tan SC, Yiap BC. DNA, RNA, and protein extraction: the past and the present. *J Biomed Biotechnol.* 2009;2009:574398.
143. Vandesompele J, De Preter K, Pattyn F, et al. Accurate normalization of real-time quantitative RT-PCR data by geometric averaging of multiple internal control genes. *Genome Biol.* 2002;3(7):RESEARCH0034.
144. Andersen CL, Jensen JL, Orntoft TF. Normalization of real-time quantitative reverse transcription-PCR data: a model-based variance estimation approach to identify genes suited for normalization, applied to bladder and colon cancer data sets. *Cancer Res.* 2004;64(15):5245-5250.
145. Pfaffl MW. A new mathematical model for relative quantification in real-time RT-PCR. *Nucleic Acids Res.* 2001;29(9):e45.
146. Donath K, Breuner G. A method for the study of undecalcified bones and teeth with attached soft tissues. The Sage-Schliff (sawing and grinding) technique. *J Oral Pathol.* 1982;11(4):318-326.
147. MacBeth N, Trullenque-Eriksson A, Donos N, Mardas N. Hard and soft tissue changes following alveolar ridge preservation: a systematic review. *Clin Oral Implants Res.* 2017;28(8):982-1004.
148. Naenni N, Lim HC, Papageorgiou SN, Hammerle CHF. Efficacy of lateral bone augmentation prior to implant placement: A systematic review and meta-analysis. *J Clin Periodontol.* 2019;46 Suppl 21:287-306.
149. Thoma DS, Bienz SP, Figuero E, Jung RE, Sanz-Martin I. Efficacy of lateral bone augmentation performed simultaneously with dental implant placement: A systematic review and meta-analysis. *J Clin Periodontol.* 2019;46 Suppl 21:257-276.
150. Donos N, Mardas N, Chadha V. Clinical outcomes of implants following lateral bone augmentation: systematic assessment of available options (barrier membranes, bone grafts, split osteotomy). *J Clin Periodontol.* 2008;35(8 Suppl):173-202.
151. Jensen SS, Terheyden H. Bone augmentation procedures in localized defects in the alveolar ridge: clinical results with different bone grafts and bone-substitute materials. *Int J Oral Maxillofac Implants.* 2009;24 Suppl:218-236.
152. Merli M, Merli I, Raffaelli E, Pagliaro U, Nastri L, Nieri M. Bone augmentation at implant dehiscences and fenestrations. A systematic

review of randomised controlled trials. *Eur J Oral Implantol.* 2016;9(1):11-32.

153. Jung RE, Brugger LV, Bienz SP, Husler J, Hammerle CHF, Zitzmann NU. Clinical and radiographical performance of implants placed with simultaneous guided bone regeneration using resorbable and nonresorbable membranes after 22-24 years, a prospective, controlled clinical trial. *Clin Oral Implants Res.* 2021.
154. Hammerle CH, Jung RE, Feloutzis A. A systematic review of the survival of implants in bone sites augmented with barrier membranes (guided bone regeneration) in partially edentulous patients. *J Clin Periodontol.* 2002;29 Suppl 3:226-231; discussion 232-223.
155. Aloy-Prosper A, Penarrocha-Oltra D, Penarrocha-Diago M, Penarrocha-Diago M. Dental implants with versus without peri-implant bone defects treated with guided bone regeneration. *J Clin Exp Dent.* 2015;7(3):e361-368.
156. Benic GI, Bernasconi M, Jung RE, Hammerle CH. Clinical and radiographic intra-subject comparison of implants placed with or without guided bone regeneration: 15-year results. *J Clin Periodontol.* 2017;44(3):315-325.
157. Zumstein T, Schutz S, Sahlin H, Sennerby L. Factors influencing marginal bone loss at a hydrophilic implant design placed with or without GBR procedures: A 5-year retrospective study. *Clin Implant Dent Relat Res.* 2019;21(5):817-826.
158. Mayfield L, Skoglund A, Nobreus N, Attstrom R. Clinical and radiographic evaluation, following delivery of fixed reconstructions, at GBR treated titanium fixtures. *Clin Oral Implants Res.* 1998;9(5):292-302.
159. Zitzmann NU, Scharer P, Marinello CP. Long-term results of implants treated with guided bone regeneration: a 5-year prospective study. *Int J Oral Maxillofac Implants.* 2001;16(3):355-366.
160. Ritter L, Elger MC, Rothamel D, et al. Accuracy of peri-implant bone evaluation using cone beam CT, digital intra-oral radiographs and histology. *Dentomaxillofac Radiol.* 2014;43(6):20130088.
161. Schliephake H, Wichmann M, Donnerstag F, Vogt S. Imaging of periimplant bone levels of implants with buccal bone defects. *Clin Oral Implants Res.* 2003;14(2):193-200.
162. Benic GI, Elmasry M, Hammerle CH. Novel digital imaging techniques to assess the outcome in oral rehabilitation with dental implants: a narrative review. *Clin Oral Implants Res.* 2015;26 Suppl 11:86-96.
163. Harris D, Horner K, Grondahl K, et al. E.A.O. guidelines for the use of diagnostic imaging in implant dentistry 2011. A consensus workshop organized by the European Association for Osseointegration at the Medical University of Warsaw. *Clin Oral Implants Res.* 2012;23(11):1243-1253.

164. Benic GI, Mokti M, Chen CJ, Weber HP, Hammerle CH, Gallucci GO. Dimensions of buccal bone and mucosa at immediately placed implants after 7 years: a clinical and cone beam computed tomography study. *Clin Oral Implants Res.* 2012;23(5):560-566.
165. Kuchler U, Chappuis V, Gruber R, Lang NP, Salvi GE. Immediate implant placement with simultaneous guided bone regeneration in the esthetic zone: 10-year clinical and radiographic outcomes. *Clin Oral Implants Res.* 2016;27(2):253-257.
166. Hammerle CH, Chen ST, Wilson TG, Jr. Consensus statements and recommended clinical procedures regarding the placement of implants in extraction sockets. *Int J Oral Maxillofac Implants.* 2004;19 Suppl:26-28.
167. Merheb J, Quirynen M, Teughels W. Critical buccal bone dimensions along implants. *Periodontol 2000.* 2014;66(1):97-105.
168. Qahash M, Susin C, Polimeni G, Hall J, Wikesjo UM. Bone healing dynamics at buccal peri-implant sites. *Clin Oral Implants Res.* 2008;19(2):166-172.
169. Benic GI, Thoma DS, Munoz F, Sanz Martin I, Jung RE, Hammerle CH. Guided bone regeneration of peri-implant defects with particulated and block xenogenic bone substitutes. *Clin Oral Implants Res.* 2016;27(5):567-576.
170. Jiang X, Zhang Y, Di P, Lin Y. Hard tissue volume stability of guided bone regeneration during the healing stage in the anterior maxilla: A clinical and radiographic study. *Clin Implant Dent Relat Res.* 2018;20(1):68-75.
171. Mir-Mari J, Wui H, Jung RE, Hammerle CH, Benic GI. Influence of blinded wound closure on the volume stability of different GBR materials: an in vitro cone-beam computed tomographic examination. *Clin Oral Implants Res.* 2016;27(2):258-265.
172. Sanz-Sanchez I, Carrillo de Albornoz A, Figuero E, et al. Effects of lateral bone augmentation procedures on peri-implant health or disease: A systematic review and meta-analysis. *Clin Oral Implants Res.* 2018;29 Suppl 15:18-31.
173. Kuchler U, von Arx T. Horizontal ridge augmentation in conjunction with or prior to implant placement in the anterior maxilla: a systematic review. *Int J Oral Maxillofac Implants.* 2014;29 Suppl:14-24.
174. Blanco J, Alonso A, Sanz M. Long-term results and survival rate of implants treated with guided bone regeneration: a 5-year case series prospective study. *Clin Oral Implants Res.* 2005;16(3):294-301.
175. Buser D, Chappuis V, Kuchler U, et al. Long-term stability of early implant placement with contour augmentation. *J Dent Res.* 2013;92(12 Suppl):176S-182S.
176. Amorfini L, Migliorati M, Signori A, Silvestrini-Biavati A, Benedicenti S. Block allograft technique versus standard guided bone

regeneration: a randomized clinical trial. *Clin Implant Dent Relat Res.* 2014;16(5):655-667.

177. Jung RE, Benic GI, Scherrer D, Hammerle CH. Cone beam computed tomography evaluation of regenerated buccal bone 5 years after simultaneous implant placement and guided bone regeneration procedures--a randomized, controlled clinical trial. *Clin Oral Implants Res.* 2015;26(1):28-34.
178. Jung RE, Herzog M, Wolleb K, Ramel CF, Thoma DS, Hammerle CH. A randomized controlled clinical trial comparing small buccal dehiscence defects around dental implants treated with guided bone regeneration or left for spontaneous healing. *Clin Oral Implants Res.* 2017;28(3):348-354.
179. Meijndert CM, Raghoebar GM, Meijndert L, Stellingsma K, Vissink A, Meijer HJ. Single implants in the aesthetic region preceded by local ridge augmentation; a 10-year randomized controlled trial. *Clin Oral Implants Res.* 2017;28(4):388-395.
180. Figuero E, Graziani F, Sanz I, Herrera D, Sanz M. Management of peri-implant mucositis and peri-implantitis. *Periodontol 2000.* 2014;66(1):255-273.
181. Heitz-Mayfield LJ, Aaboe M, Araujo M, et al. Group 4 ITI Consensus Report: Risks and biologic complications associated with implant dentistry. *Clin Oral Implants Res.* 2018;29 Suppl 16:351-358.
182. Winitsky N, Olgart K, Jemt T, Smedberg JI. A retro-prospective long-term follow-up of Branemark single implants in the anterior maxilla in young adults. Part 1: Clinical and radiographic parameters. *Clin Implant Dent Relat Res.* 2018;20(6):937-944.
183. Jemt T, Stenport V, Friberg B. Implant treatment with fixed prostheses in the edentulous maxilla. Part 1: implants and biologic response in two patient cohorts restored between 1986 and 1987 and 15 years later. *Int J Prosthodont.* 2011;24(4):345-355.
184. Lang NP, Hammerle CH, Bragger U, Lehmann B, Nyman SR. Guided tissue regeneration in jawbone defects prior to implant placement. *Clin Oral Implants Res.* 1994;5(2):92-97.
185. Huang X, Liu X, Shang Y, Qiao F, Chen G. Current Trends in Research on Bone Regeneration: A Bibliometric Analysis. *Biomed Res Int.* 2020;2020:8787394.
186. Gosain AK, Song L, Yu P, et al. Osteogenesis in cranial defects: reassessment of the concept of critical size and the expression of TGF-beta isoforms. *Plast Reconstr Surg.* 2000;106(2):360-371; discussion 372.
187. Rahimi P, Wang CY, Stashenko P, Lee SK, Lorenzo JA, Graves DT. Monocyte chemoattractant protein-1 expression and monocyte recruitment in osseous inflammation in the mouse. *Endocrinology.* 1995;136(6):2752-2759.

188. Yoshimura T, Robinson EA, Tanaka S, Appella E, Leonard EJ. Purification and amino acid analysis of two human monocyte chemoattractants produced by phytohemagglutinin-stimulated human blood mononuclear leukocytes. *J Immunol.* 1989;142(6):1956-1962.
189. Kucia M, Ratajczak J, Reca R, Janowska-Wieczorek A, Ratajczak MZ. Tissue-specific muscle, neural and liver stem/progenitor cells reside in the bone marrow, respond to an SDF-1 gradient and are mobilized into peripheral blood during stress and tissue injury. *Blood Cells Mol Dis.* 2004;32(1):52-57.
190. Martin C, Burdon PC, Bridger G, Gutierrez-Ramos JC, Williams TJ, Rankin SM. Chemokines acting via CXCR2 and CXCR4 control the release of neutrophils from the bone marrow and their return following senescence. *Immunity.* 2003;19(4):583-593.
191. Wright LM, Maloney W, Yu X, Kindle L, Collin-Osdoby P, Osdoby P. Stromal cell-derived factor-1 binding to its chemokine receptor CXCR4 on precursor cells promotes the chemotactic recruitment, development and survival of human osteoclasts. *Bone.* 2005;36(5):840-853.
192. Zhu W, Liang G, Huang Z, Doty SB, Boskey AL. Conditional inactivation of the CXCR4 receptor in osteoprecursors reduces postnatal bone formation due to impaired osteoblast development. *J Biol Chem.* 2011;286(30):26794-26805.
193. Aachoui Y, Ghosh SK. Extracellular matrix from porcine small intestinal submucosa (SIS) as immune adjuvants. *PLoS One.* 2011;6(11):e27083.
194. Badylak SF, Valentin JE, Ravindra AK, McCabe GP, Stewart-Akers AM. Macrophage phenotype as a determinant of biologic scaffold remodeling. *Tissue Eng Part A.* 2008;14(11):1835-1842.
195. Bocker W, Docheva D, Prall WC, et al. IKK-2 is required for TNF-alpha-induced invasion and proliferation of human mesenchymal stem cells. *J Mol Med (Berl).* 2008;86(10):1183-1192.
196. Fu X, Han B, Cai S, Lei Y, Sun T, Sheng Z. Migration of bone marrow-derived mesenchymal stem cells induced by tumor necrosis factor-alpha and its possible role in wound healing. *Wound Repair Regen.* 2009;17(2):185-191.
197. Gerstenfeld LC, Cho TJ, Kon T, et al. Impaired intramembranous bone formation during bone repair in the absence of tumor necrosis factor-alpha signaling. *Cells Tissues Organs.* 2001;169(3):285-294.
198. Hess K, Ushmorov A, Fiedler J, Brenner RE, Wirth T. TNFalpha promotes osteogenic differentiation of human mesenchymal stem cells by triggering the NF-kappaB signaling pathway. *Bone.* 2009;45(2):367-376.
199. Howard GA, Bottemiller BL, Turner RT, Rader JI, Baylink DJ. Parathyroid hormone stimulates bone formation and resorption in

organ culture: evidence for a coupling mechanism. *Proc Natl Acad Sci U S A.* 1981;78(5):3204-3208.

200. Weivoda MM, Ruan M, Pederson L, et al. Osteoclast TGF-beta Receptor Signaling Induces Wnt1 Secretion and Couples Bone Resorption to Bone Formation. *J Bone Miner Res.* 2016;31(1):76-85.
201. Pederson L, Ruan M, Westendorf JJ, Khosla S, Oursler MJ. Regulation of bone formation by osteoclasts involves Wnt/BMP signaling and the chemokine sphingosine-1-phosphate. *Proc Natl Acad Sci U S A.* 2008;105(52):20764-20769.
202. Irie N, Takada Y, Watanabe Y, et al. Bidirectional signaling through ephrinA2-EphA2 enhances osteoclastogenesis and suppresses osteoblastogenesis. *J Biol Chem.* 2009;284(21):14637-14644.
203. Takyar FM, Tonna S, Ho PW, et al. EphrinB2/EphB4 inhibition in the osteoblast lineage modifies the anabolic response to parathyroid hormone. *J Bone Miner Res.* 2013;28(4):912-925.
204. Ota K, Quint P, Ruan M, et al. TGF-beta induces Wnt10b in osteoclasts from female mice to enhance coupling to osteoblasts. *Endocrinology.* 2013;154(10):3745-3752.
205. Xie H, Cui Z, Wang L, et al. PDGF-BB secreted by preosteoclasts induces angiogenesis during coupling with osteogenesis. *Nat Med.* 2014;20(11):1270-1278.
206. Takeshita S, Fumoto T, Matsuoka K, et al. Osteoclast-secreted CTHRC1 in the coupling of bone resorption to formation. *J Clin Invest.* 2013;123(9):3914-3924.
207. Matsuoka K, Park KA, Ito M, Ikeda K, Takeshita S. Osteoclast-derived complement component 3a stimulates osteoblast differentiation. *J Bone Miner Res.* 2014;29(7):1522-1530.
208. Lotinun S, Kiviranta R, Matsubara T, et al. Osteoclast-specific cathepsin K deletion stimulates S1P-dependent bone formation. *J Clin Invest.* 2013;123(2):666-681.
209. Ikebuchi Y, Aoki S, Honma M, et al. Coupling of bone resorption and formation by RANKL reverse signalling. *Nature.* 2018;561(7722):195-200.
210. Udagawa N, Koide M, Nakamura M, et al. Osteoclast differentiation by RANKL and OPG signaling pathways. *J Bone Miner Metab.* 2021;39(1):19-26.
211. Levaot N, Ottolenghi A, Mann M, Guterman-Ram G, Kam Z, Geiger B. Osteoclast fusion is initiated by a small subset of RANKL-stimulated monocyte progenitors, which can fuse to RANKL-unstimulated progenitors. *Bone.* 2015;79:21-28.
212. Kitaura H, Sands MS, Aya K, et al. Marrow stromal cells and osteoclast precursors differentially contribute to TNF-alpha-induced osteoclastogenesis in vivo. *J Immunol.* 2004;173(8):4838-4846.

213. Kitaura H, Zhou P, Kim HJ, Novack DV, Ross FP, Teitelbaum SL. M-CSF mediates TNF-induced inflammatory osteolysis. *J Clin Invest.* 2005;115(12):3418-3427.
214. Hofbauer LC, Lacey DL, Dunstan CR, Spelsberg TC, Riggs BL, Khosla S. Interleukin-1beta and tumor necrosis factor-alpha, but not interleukin-6, stimulate osteoprotegerin ligand gene expression in human osteoblastic cells. *Bone.* 1999;25(3):255-259.
215. Marahleh A, Kitaura H, Ohori F, et al. TNF-alpha Directly Enhances Osteocyte RANKL Expression and Promotes Osteoclast Formation. *Front Immunol.* 2019;10:2925.
216. Colangelo P, Piattelli A, Barrucci S, Trisi P, Formisano G, Caiazza S. Bone regeneration guided by resorbable collagen membranes in rabbits: a pilot study. *Implant Dent.* 1993;2(2):101-105.
217. He H, Huang J, Chen G, Dong Y. Application of a new bioresorbable film to guided bone regeneration in tibia defect model of the rabbits. *J Biomed Mater Res A.* 2007;82(1):256-262.
218. Kim JY, Yang BE, Ahn JH, Park SO, Shim HW. Comparable efficacy of silk fibroin with the collagen membranes for guided bone regeneration in rat calvarial defects. *J Adv Prosthodont.* 2014;6(6):539-546.
219. Huleihel L, Dziki JL, Bartolacci JG, et al. Macrophage phenotype in response to ECM bioscaffolds. *Semin Immunol.* 2017;29:2-13.
220. Sicari BM, Dziki JL, Siu BF, Medberry CJ, Dearth CL, Badylak SF. The promotion of a constructive macrophage phenotype by solubilized extracellular matrix. *Biomaterials.* 2014;35(30):8605-8612.
221. Sun T, Liu M, Yao S, et al. Guided osteoporotic bone regeneration with composite scaffolds of mineralized ECM/heparin membrane loaded with BMP2-related peptide. *Int J Nanomedicine.* 2018;13:791-804.
222. Sun T, Liu M, Yao S, et al. Biomimetic Composite Scaffold Containing Small Intestinal Submucosa and Mesoporous Bioactive Glass Exhibits High Osteogenic and Angiogenic Capacity. *Tissue Eng Part A.* 2018;24(13-14):1044-1056.
223. Sun T, Yao S, Liu M, et al. Composite Scaffolds of Mineralized Natural Extracellular Matrix on True Bone Ceramic Induce Bone Regeneration Through Smad1/5/8 and ERK1/2 Pathways. *Tissue Eng Part A.* 2018;24(5-6):502-515.
224. Pu LL, Plastic Surgery Educational Foundation DC. Small intestinal submucosa (Surgisis) as a bioactive prosthetic material for repair of abdominal wall fascial defect. *Plast Reconstr Surg.* 2005;115(7):2127-2131.
225. Hodde JP, Record RD, Liang HA, Badylak SF. Vascular endothelial growth factor in porcine-derived extracellular matrix. *Endothelium.* 2001;8(1):11-24.

226. Voytik-Harbin SL, Brightman AO, Kraine MR, Waisner B, Badylak SF. Identification of extractable growth factors from small intestinal submucosa. *J Cell Biochem.* 1997;67(4):478-491.
227. Nihsen ES, Johnson CE, Hiles MC. Bioactivity of small intestinal submucosa and oxidized regenerated cellulose/collagen. *Adv Skin Wound Care.* 2008;21(10):479-486.
228. Yang L, Zhou J, Yu K, et al. Surface modified small intestinal submucosa membrane manipulates sequential immunomodulation coupled with enhanced angio- and osteogenesis towards ameliorative guided bone regeneration. *Mater Sci Eng C Mater Biol Appl.* 2021;119:111641.
229. Xiao YT, Xiang LX, Shao JZ. Bone morphogenetic protein. *Biochem Biophys Res Commun.* 2007;362(3):550-553.
230. Lieberman JR, Daluiski A, Einhorn TA. The role of growth factors in the repair of bone. Biology and clinical applications. *J Bone Joint Surg Am.* 2002;84(6):1032-1044.
231. Saadeh PB, Mehrara BJ, Steinbrech DS, et al. Mechanisms of fibroblast growth factor-2 modulation of vascular endothelial growth factor expression by osteoblastic cells. *Endocrinology.* 2000;141(6):2075-2083.
232. Collin-Osdoby P, Rothe L, Bekker S, Anderson F, Huang Y, Osdoby P. Basic fibroblast growth factor stimulates osteoclast recruitment, development, and bone pit resorption in association with angiogenesis in vivo on the chick chorioallantoic membrane and activates isolated avian osteoclast resorption in vitro. *J Bone Miner Res.* 2002;17(10):1859-1871.
233. Cowan CM, Aalami OO, Shi YY, et al. Bone morphogenetic protein 2 and retinoic acid accelerate in vivo bone formation, osteoclast recruitment, and bone turnover. *Tissue Eng.* 2005;11(3-4):645-658.
234. Irie K, Alpaslan C, Takahashi K, et al. Osteoclast differentiation in ectopic bone formation induced by recombinant human bone morphogenetic protein 2 (rhBMP-2). *J Bone Miner Metab.* 2003;21(6):363-369.
235. Taguchi Y, Amizuka N, Nakadate M, et al. A histological evaluation for guided bone regeneration induced by a collagenous membrane. *Biomaterials.* 2005;26(31):6158-6166.
236. Matsuzaka K, Shimono M, Inoue T. Characteristics of newly formed bone during guided bone regeneration: observations by immunohistochemistry and confocal laser scanning microscopy. *Bull Tokyo Dent Coll.* 2001;42(4):225-234.
237. Tanaka S, Matsuzaka K, Sato D, Inoue T. Characteristics of newly formed bone during guided bone regeneration: analysis of cbfa-1, osteocalcin, and VEGF expression. *J Oral Implantol.* 2007;33(6):321-326.

238. Al-Kattan R, Retzepi M, Calciolari E, Donos N. Microarray gene expression during early healing of GBR-treated calvarial critical size defects. *Clin Oral Implants Res.* 2017;28(10):1248-1257.
239. Logan CY, Nusse R. The Wnt signaling pathway in development and disease. *Annu Rev Cell Dev Biol.* 2004;20:781-810.
240. Lima LL, Goncalves PF, Sallum EA, Casati MZ, Nociti FH, Jr. Guided tissue regeneration may modulate gene expression in periodontal intrabony defects: a human study. *J Periodontal Res.* 2008;43(4):459-464.
241. Takayanagi H. Inflammatory bone destruction and osteoimmunology. *J Periodontal Res.* 2005;40(4):287-293.
242. Browne S, Pandit A. Biomaterial-mediated modification of the local inflammatory environment. *Front Bioeng Biotechnol.* 2015;3:67.
243. Anderson JM, Defife K, McNally A, Collier T, Jenney C. Monocyte, macrophage and foreign body giant cell interactions with molecularly engineered surfaces. *J Mater Sci Mater Med.* 1999;10(10/11):579-588.
244. Brodbeck WG, Nakayama Y, Matsuda T, Colton E, Ziats NP, Anderson JM. Biomaterial surface chemistry dictates adherent monocyte/macrophage cytokine expression in vitro. *Cytokine.* 2002;18(6):311-319.
245. Jones JA, Chang DT, Meyerson H, et al. Proteomic analysis and quantification of cytokines and chemokines from biomaterial surface-adherent macrophages and foreign body giant cells. *J Biomed Mater Res A.* 2007;83(3):585-596.
246. Lamichhane S, Anderson JA, Vierhout T, Remund T, Sun H, Kelly P. Polytetrafluoroethylene topographies determine the adhesion, activation, and foreign body giant cell formation of macrophages. *J Biomed Mater Res A.* 2017;105(9):2441-2450.
247. Brown BN, Valentin JE, Stewart-Akers AM, McCabe GP, Badylak SF. Macrophage phenotype and remodeling outcomes in response to biologic scaffolds with and without a cellular component. *Biomaterials.* 2009;30(8):1482-1491.
248. Tanaka T, Narazaki M, Kishimoto T. IL-6 in inflammation, immunity, and disease. *Cold Spring Harb Perspect Biol.* 2014;6(10):a016295.
249. Suska F, Emanuelsson L, Johansson A, Tengvall P, Thomsen P. Fibrous capsule formation around titanium and copper. *J Biomed Mater Res A.* 2008;85(4):888-896.
250. Suska F, Gretzer C, Esposito M, et al. In vivo cytokine secretion and NF-kappaB activation around titanium and copper implants. *Biomaterials.* 2005;26(5):519-527.
251. Anderson JA, Lamichhane S, Mani G. Macrophage responses to 316L stainless steel and cobalt chromium alloys with different surface topographies. *J Biomed Mater Res A.* 2016;104(11):2658-2672.

252. Bota PC, Collie AM, Puolakkainen P, et al. Biomaterial topography alters healing in vivo and monocyte/macrophage activation in vitro. *J Biomed Mater Res A.* 2010;95(2):649-657.
253. Refai AK, Textor M, Brunette DM, Waterfield JD. Effect of titanium surface topography on macrophage activation and secretion of proinflammatory cytokines and chemokines. *J Biomed Mater Res A.* 2004;70(2):194-205.
254. Blakney AK, Swartzlander MD, Bryant SJ. The effects of substrate stiffness on the in vitro activation of macrophages and in vivo host response to poly(ethylene glycol)-based hydrogels. *J Biomed Mater Res A.* 2012;100(6):1375-1386.
255. Trobos M, Juhlin A, Shah FA, Hoffman M, Sahlin H, Dahlin C. In vitro evaluation of barrier function against oral bacteria of dense and expanded polytetrafluoroethylene (PTFE) membranes for guided bone regeneration. *Clin Implant Dent Relat Res.* 2018;20(5):738-748.
256. Chen D, Harris MA, Rossini G, et al. Bone morphogenetic protein 2 (BMP-2) enhances BMP-3, BMP-4, and bone cell differentiation marker gene expression during the induction of mineralized bone matrix formation in cultures of fetal rat calvarial osteoblasts. *Calcif Tissue Int.* 1997;60(3):283-290.
257. Matsubara T, Kida K, Yamaguchi A, et al. BMP2 regulates Osterix through Msx2 and Runx2 during osteoblast differentiation. *J Biol Chem.* 2008;283(43):29119-29125.
258. Wu M, Chen G, Li YP. TGF-beta and BMP signaling in osteoblast, skeletal development, and bone formation, homeostasis and disease. *Bone Res.* 2016;4:16009.
259. Huang Z, Ren PG, Ma T, Smith RL, Goodman SB. Modulating osteogenesis of mesenchymal stem cells by modifying growth factor availability. *Cytokine.* 2010;51(3):305-310.
260. Jiang T, Ge S, Shim YH, Zhang C, Cao D. Bone morphogenetic protein is required for fibroblast growth factor 2-dependent later-stage osteoblastic differentiation in cranial suture cells. *Int J Clin Exp Pathol.* 2015;8(3):2946-2954.
261. Hughes-Fulford M, Li CF. The role of FGF-2 and BMP-2 in regulation of gene induction, cell proliferation and mineralization. *J Orthop Surg Res.* 2011;6:8.
262. Park JB. Effects of the combination of fibroblast growth factor-2 and bone morphogenetic protein-2 on the proliferation and differentiation of osteoprecursor cells. *Adv Clin Exp Med.* 2014;23(3):463-467.
263. Naganawa T, Xiao L, Coffin JD, et al. Reduced expression and function of bone morphogenetic protein-2 in bones of Fgf2 null mice. *J Cell Biochem.* 2008;103(6):1975-1988.
264. Bottcher RT, Niehrs C. Fibroblast growth factor signaling during early vertebrate development. *Endocr Rev.* 2005;26(1):63-77.

265. Fujihara C, Kanai Y, Masumoto R, et al. Fibroblast growth factor-2 inhibits CD40-mediated periodontal inflammation. *J Cell Physiol.* 2019;234(5):7149-7160.
266. Tavelli L, McGuire MK, Zucchelli G, et al. Biologics-based regenerative technologies for periodontal soft tissue engineering. *J Periodontol.* 2020;91(2):147-154.
267. Tang Y, Rajendran P, Veeraraghavan VP, et al. Osteogenic differentiation and mineralization potential of zinc oxide nanoparticles from Scutellaria baicalensis on human osteoblast-like MG-63 cells. *Mater Sci Eng C Mater Biol Appl.* 2021;119:111656.
268. Toledano-Osorio M, Manzano-Moreno FJ, Toledano M, et al. Doxycycline-Doped Polymeric Membranes Induced Growth, Differentiation and Expression of Antigenic Phenotype Markers of Osteoblasts. *Polymers (Basel).* 2021;13(7).
269. Geiger F, Bertram H, Berger I, et al. Vascular endothelial growth factor gene-activated matrix (VEGF165-GAM) enhances osteogenesis and angiogenesis in large segmental bone defects. *J Bone Miner Res.* 2005;20(11):2028-2035.
270. Kleinheinz J, Stratmann U, Joos U, Wiesmann HP. VEGF-activated angiogenesis during bone regeneration. *J Oral Maxillofac Surg.* 2005;63(9):1310-1316.
271. Yang Q, McHugh KP, Patntirapong S, Gu X, Wunderlich L, Hauschka PV. VEGF enhancement of osteoclast survival and bone resorption involves VEGF receptor-2 signaling and beta3-integrin. *Matrix Biol.* 2008;27(7):589-599.
272. Hu K, Olsen BR. The roles of vascular endothelial growth factor in bone repair and regeneration. *Bone.* 2016;91:30-38.
273. Liu Y, Berendsen AD, Jia S, et al. Intracellular VEGF regulates the balance between osteoblast and adipocyte differentiation. *J Clin Invest.* 2012;122(9):3101-3113.
274. Henriksen K, Karsdal M, Delaisse JM, Engsig MT. RANKL and vascular endothelial growth factor (VEGF) induce osteoclast chemotaxis through an ERK1/2-dependent mechanism. *J Biol Chem.* 2003;278(49):48745-48753.
275. Nakagawa M, Kaneda T, Arakawa T, et al. Vascular endothelial growth factor (VEGF) directly enhances osteoclastic bone resorption and survival of mature osteoclasts. *FEBS Lett.* 2000;473(2):161-164.
276. Street J, Bao M, deGuzman L, et al. Vascular endothelial growth factor stimulates bone repair by promoting angiogenesis and bone turnover. *Proc Natl Acad Sci U S A.* 2002;99(15):9656-9661.
277. Machtei EE. The effect of membrane exposure on the outcome of regenerative procedures in humans: a meta-analysis. *J Periodontol.* 2001;72(4):512-516.

278. Fugazzotto PA. Maintenance of soft tissue closure following guided bone regeneration: technical considerations and report of 723 cases. *J Periodontol.* 1999;70(9):1085-1097.
279. Greenstein G, Greenstein B, Cavallaro J, Elian N, Tarnow D. Flap advancement: practical techniques to attain tension-free primary closure. *J Periodontol.* 2009;80(1):4-15.
280. Park JC, Kim CS, Choi SH, Cho KS, Chai JK, Jung UW. Flap extension attained by vertical and periosteal-releasing incisions: a prospective cohort study. *Clin Oral Implants Res.* 2012;23(8):993-998.
281. Busscher HJ, van der Mei HC, Subbiahdoss G, et al. Biomaterial-associated infection: locating the finish line in the race for the surface. *Sci Transl Med.* 2012;4(153):153rv110.
282. Zhao B, van der Mei HC, Subbiahdoss G, et al. Soft tissue integration versus early biofilm formation on different dental implant materials. *Dent Mater.* 2014;30(7):716-727.
283. Martinez-Perez M, Conde A, Arenas MA, et al. The "Race for the Surface" experimentally studied: In vitro assessment of Staphylococcus spp. adhesion and preosteoblastic cells integration to doped Ti-6Al-4V alloys. *Colloids Surf B Biointerfaces.* 2019;173:876-883.
284. Doll PW, Husari A, Ahrens R, Spindler B, Guber AE, Steinberg T. Enhancing the soft-tissue integration of dental implant abutments-in vitro study to reveal an optimized microgroove surface design to maximize spreading and alignment of human gingival fibroblasts. *J Biomed Mater Res B Appl Biomater.* 2021;109(11):1768-1776.
285. Barrientos S, Stojadinovic O, Golinko MS, Brem H, Tomic-Canic M. Growth factors and cytokines in wound healing. *Wound Repair Regen.* 2008;16(5):585-601.
286. Lin Z, Nica C, Sculean A, Asparuhova MB. Enhanced Wound Healing Potential of Primary Human Oral Fibroblasts and Periodontal Ligament Cells Cultured on Four Different Porcine-Derived Collagen Matrices. *Materials (Basel).* 2020;13(17).
287. Presta M, Dell'Era P, Mitola S, Moroni E, Ronca R, Rusnati M. Fibroblast growth factor/fibroblast growth factor receptor system in angiogenesis. *Cytokine Growth Factor Rev.* 2005;16(2):159-178.
288. Fahey E, Doyle SL. IL-1 Family Cytokine Regulation of Vascular Permeability and Angiogenesis. *Front Immunol.* 2019;10:1426.
289. Sainson RC, Johnston DA, Chu HC, et al. TNF primes endothelial cells for angiogenic sprouting by inducing a tip cell phenotype. *Blood.* 2008;111(10):4997-5007.
290. Zegeye MM, Andersson B, Sirsjo A, Ljungberg LU. IL-6 trans-Signaling Impairs Sprouting Angiogenesis by Inhibiting Migration, Proliferation and Tube Formation of Human Endothelial Cells. *Cells.* 2020;9(6).

291. Liu J, Kerns DG. Mechanisms of guided bone regeneration: a review. *Open Dent J.* 2014;8:56-65.
292. Tunthasen R, Pripatnanont P, Meesane J. Fabrication and characterization of a semi-rigid shell barrier system made of polycaprolactone and biphasic calcium phosphate: A novel barrier system for bone regeneration. *J Mech Behav Biomed Mater.* 2021;124:104841.
293. Krauser JT. High-density PTFE membranes: uses with root-form implants. *Dent Implantol Update.* 1996;7(9):65-69.
294. Roupe KM, Veerla S, Olson J, et al. Transcription factor binding site analysis identifies FOXO transcription factors as regulators of the cutaneous wound healing process. *PLoS One.* 2014;9(2):e89274.
295. Shaklai S, Shefer G, Stern N. Glucose-dependent Foxo1 switch in healing wounds: a shred of hope for diabetic ulcers? *Diabetes.* 2015;64(1):6-8.
296. Zhang C, Ponugoti B, Tian C, et al. FOXO1 differentially regulates both normal and diabetic wound healing. *J Cell Biol.* 2015;209(2):289-303.
297. Xu F, Othman B, Lim J, et al. Foxo1 inhibits diabetic mucosal wound healing but enhances healing of normoglycemic wounds. *Diabetes.* 2015;64(1):243-256.
298. Jeon HH, Yu Q, Lu Y, et al. FOXO1 regulates VEGFA expression and promotes angiogenesis in healing wounds. *J Pathol.* 2018;245(3):258-264.
299. Xin Z, Ma Z, Hu W, et al. FOXO1/3: Potential suppressors of fibrosis. *Ageing Res Rev.* 2018;41:42-52.
300. Bowler PG, Duerden BI, Armstrong DG. Wound microbiology and associated approaches to wound management. *Clin Microbiol Rev.* 2001;14(2):244-269.
301. Simion M, Trisi P, Maglione M, Piattelli A. A preliminary report on a method for studying the permeability of expanded polytetrafluoroethylene membrane to bacteria in vitro: a scanning electron microscopic and histological study. *J Periodontol.* 1994;65(8):755-761.
302. Selvig KA, Nilveus RE, Fitzmorris L, Kersten B, Khorsandi SS. Scanning electron microscopic observations of cell populations and bacterial contamination of membranes used for guided periodontal tissue regeneration in humans. *J Periodontol.* 1990;61(8):515-520.
303. Bartee BK, Carr JA. Evaluation of a high-density polytetrafluoroethylene (n-PTFE) membrane as a barrier material to facilitate guided bone regeneration in the rat mandible. *J Oral Implantol.* 1995;21(2):88-95.
304. Zucchelli G, Cesari C, Clauser C, DeSanctis M. Early bacterial accumulation on guided tissue regeneration membrane materials. An in vivo study. *J Periodontol.* 1998;69(11):1193-1202.

305. Ghiz MA, Ngan P, Kao E, Martin C, Gunel E. Effects of sealant and self-etching primer on enamel decalcification. Part II: an in-vivo study. *Am J Orthod Dentofacial Orthop.* 2009;135(2):206-213.
306. Arweiler NB, Netuschil L, Beier D, et al. Action of food preservatives on 14-days dental biofilm formation, biofilm vitality and biofilm-derived enamel demineralisation in situ. *Clin Oral Investig.* 2014;18(3):829-838.
307. Brambilla E, Ionescu A, Gagliani M, Cochis A, Arciola CR, Rimondini L. Biofilm formation on composite resins for dental restorations: an in situ study on the effect of chlorhexidine mouthrinses. *Int J Artif Organs.* 2012;35(10):792-799.
308. Prada-Lopez I, Quintas V, Vilaboa C, Suarez-Quintanilla D, Tomas I. Devices for In situ Development of Non-disturbed Oral Biofilm. A Systematic Review. *Front Microbiol.* 2016;7:1055.
309. Allwork JJ, Edwards IR, Welch IM. Ingestion of a quadhelix appliance requiring surgical removal: a case report. *J Orthod.* 2007;34(3):154-157.
310. Webb WA. Management of foreign bodies of the upper gastrointestinal tract. *Gastroenterology.* 1988;94(1):204-216.
311. Hou R, Zhou H, Hu K, et al. Thorough documentation of the accidental aspiration and ingestion of foreign objects during dental procedure is necessary: review and analysis of 617 cases. *Head Face Med.* 2016;12(1):23.
312. Abusamaan M, Giannobile WV, Jhawar P, Gunaratnam NT. Swallowed and aspirated dental prostheses and instruments in clinical dental practice: a report of five cases and a proposed management algorithm. *J Am Dent Assoc.* 2014;145(5):459-463.
313. Varho R, Oksala H, Tolvanen M, Svedstrom-Oristo AL. Inhalation or ingestion of orthodontic objects in Finland. *Acta Odontol Scand.* 2015;73(6):408-413.
314. Mahmoud GA, Grawish ME, Shamaa MS, Abdelnaby YL. Characteristics of adhesive bonding with enamel deproteinization. *Dental Press J Orthod.* 2019;24(5):29 e21-29 e28.
315. Bishara SE, VonWald L, Laffoon JF, Warren JJ. Effect of using a new cyanoacrylate adhesive on the shear bond strength of orthodontic brackets. *Angle Orthod.* 2001;71(6):466-469.
316. Hou S, Gu H, Smith C, Ren D. Microtopographic patterns affect Escherichia coli biofilm formation on poly(dimethylsiloxane) surfaces. *Langmuir.* 2011;27(6):2686-2691.
317. Busscher HJ, van der Mei HC. Physico-chemical interactions in initial microbial adhesion and relevance for biofilm formation. *Adv Dent Res.* 1997;11(1):24-32.
318. Gottenbos B, Van Der Mei HC, Busscher HJ, Grijpma DW, Feijen J. Initial adhesion and surface growth of Pseudomonas aeruginosa on

negatively and positively charged poly(methacrylates). *J Mater Sci Mater Med.* 1999;10(12):853-855.

319. Katsikogianni M, Missirlis YF. Concise review of mechanisms of bacterial adhesion to biomaterials and of techniques used in estimating bacteria-material interactions. *Eur Cell Mater.* 2004;8:37-57.
320. Scheuerman TR, Camper AK, Hamilton MA. Effects of Substratum Topography on Bacterial Adhesion. *J Colloid Interface Sci.* 1998;208(1):23-33.
321. Subramani K, Jung RE, Molenberg A, Hammerle CH. Biofilm on dental implants: a review of the literature. *Int J Oral Maxillofac Implants.* 2009;24(4):616-626.
322. Teughels W, Van Assche N, Sliepen I, Quirynen M. Effect of material characteristics and/or surface topography on biofilm development. *Clin Oral Implants Res.* 2006;17 Suppl 2:68-81.
323. Koseki H, Yonekura A, Shida T, et al. Early staphylococcal biofilm formation on solid orthopaedic implant materials: in vitro study. *PLoS One.* 2014;9(10):e107588.
324. Wertheim HF, Melles DC, Vos MC, et al. The role of nasal carriage in Staphylococcus aureus infections. *Lancet Infect Dis.* 2005;5(12):751-762.
325. Honda E. Oral microbial flora and oral malodour of the institutionalised elderly in Japan. *Gerodontology.* 2001;18(2):65-72.
326. Koukos G, Sakellari D, Arsenakis M, Tsalikis L, Slini T, Konstantinidis A. Prevalence of Staphylococcus aureus and methicillin resistant Staphylococcus aureus (MRSA) in the oral cavity. *Arch Oral Biol.* 2015;60(9):1410-1415.
327. Marsh PD, Percival RS, Challacombe SJ. The influence of denture-wearing and age on the oral microflora. *J Dent Res.* 1992;71(7):1374-1381.
328. McCormack MG, Smith AJ, Akram AN, Jackson M, Robertson D, Edwards G. Staphylococcus aureus and the oral cavity: an overlooked source of carriage and infection? *Am J Infect Control.* 2015;43(1):35-37.
329. Merghni A, Bekir K, Kadmi Y, et al. Adhesiveness of opportunistic Staphylococcus aureus to materials used in dental office: In vitro study. *Microb Pathog.* 2017;103:129-134.
330. Merghni A, Ben Nejma M, Dallel I, et al. High potential of adhesion to biotic and abiotic surfaces by opportunistic Staphylococcus aureus strains isolated from orthodontic appliances. *Microb Pathog.* 2016;91:61-67.